Sequence-Stratigraphic Analysis of the Rollins and the Cozzette Sandstone Members, the Upper Cretaceous Mount Garfield Formation of the Piceance Basin, Colorado.

By

Fatma Z. Ouaichouche
B.A in Petroleum Engineering,
Algerian Petroleum Institute, Algeria

Submitted to the Department of
Geology and the Faculty of
the Graduate School at the University of
Kansas in partial fulfillment of
the requirements for the degree of
Master of Science

Dr. Diane Kamola
Diane L. Kamola (Chair)

Dr. Anthony Walton
Anthony W. Walton

Dr. Gwendolyn Macpherson
Gwendolyn L. Macpherson

Date Defended: *Wednesday, May 11th, 2011*

The Thesis Committee for Fatma Ouaichouche certifies that this is the approved

version of the following thesis:

Sequence-Stratigraphic Analysis of the Rollins and the Cozzette Sandstone Members, the Upper Cretaceous Mount Garfield Formation of the Piceance Basin, Colorado.

Advisory Committee:

Dr. Diane Kamola

Diane L. Kamola (Chair)

Dr. Anthony Walton

Anthony W. Walton

Dr. Gwendolyn Macpherson

Gwendolyn L. Macpherson

Date approved: *Wednesday, May 11th, 2011*

ABSTRACT

Sequence-stratigraphic study of the Cozzette and the Rollins Sandstone members, of the Mt. Garfield Formation of the Mesaverde Group, in the southern part of the Piceance basin (western Colorado), utilizes mainly well-log data along with limited outcrop data. Outcrop description of the Rollins Sandstone Member indicates a depositional succession that changes from complex marginal marine deposits at the base to marine wave-dominated shoreface successions at the top. The lower marginal-marine deposits are interpreted to occur within multiple incised-valley fills that nest and form a main stratigraphic element landward, particularly within the uppermost part of the Cozzette Sandstone Member. Incised-valley fills thin basinward. Sequence-stratigraphic interpretation of the subsurface data provides a stratigraphic history similar to that interpreted from the outcrop exposures across a regional realm. The subsurface analysis of the study interval distinguishes 5 depositional sequences that change in thickness throughout the study area and are listed as follows: CZ_1, CZ_2, CZ_3, R_1 and R_2. The depositional sequence R_2 is the youngest incomplete sequence within the study interval. Each depositional sequence is composed of incised-valley fills at the base and highstand deposits with marine shoreface at the top. The incomplete depositional sequence R_2 is represented by incised-valley fills alone. The vertical chronostratigraphic architecture of the sequence set (CZ_1, CZ_2, CZ_3, R_1) show a regional change in stacking pattern from retrogradational (CZ_1, CZ_2, and CZ_3) to progradational (R_1). The turnaround from retrogradational to progradational stacking is probably the stratigraphic limit between the Cozzette and the Rollins Sandstone members; its stratigraphic expression is probably gradational and complex in a landward direction. Incised valleys are superimposed landward, probably along axes between raised mires, and exhibit highly variable log patterns that reflect complex marginal-marine deposits.

LIST OF FIGURES

vi

1. Table of well-log data

2. Sheets of well-log information

3. Plates A:
   - The different electrofacies types are distributed through cross-sections (4 plates)

4. Plates B:
   - Sequence-stratigraphic correlations (4 plates)

ACKNOWLEDGEMENTS

TABLE OF CONTENTS

Chapter I: INTRODUCTION

I. Introduction

This study examines the upper part of the Upper Cretaceous Mount Garfield Formation of the Piceance basin in western Colorado. It is a subsurface sequence-stratigraphic study based mainly on well-log analyses and supplemented by a cursory examination of outcrop exposures located near Grand Junction, Colorado.

The outcrop exposures of the Rollins and the Cozzette Sandstone members are located on the western edge of the Piceance basin, and contain complex depositional settings. The complexity of these strata includes abrupt lateral facies changes, complex estuarine deposits, and multiple erosion surfaces that may be of both local and regional origin. To resolve the significance of the regional erosion surfaces, the study requires detailed stratigraphic correlation and subsurface analysis of the Rollins and the Cozzette Sandstone members. These extensive erosion surfaces may be interpreted as important sequence boundaries over the eastern part of the Piceance basin.

II. Research Problem

This study aims to analyze the complicated internal stratigraphy of the uppermost part of the Mount Garfield Formation through sequence-stratigraphic analysis, using mainly subsurface data. Well logs record regional stratigraphic boundaries and cyclical successions of the sedimentary rocks in the subsurface. The stratigraphic history of these sedimentary rocks can be understood when interpreted with reference to the time framework within which they were deposited (Van Wagoner et al., 1990). The time

framework is established through a sequence-stratigraphic study that allows sedimentary rocks to be interpreted as genetically related facies. Genetically related facies are grouped into stratal units that are bounded by unconformable surfaces and their correlative conformities, as outlined by Mitchum et al. (1977) and Van Wagoner et al. (1990). These surfaces form in relation to local and global sea-level changes and can be identified in the subsurface through interpretation of well logs. These surfaces divide sedimentary successions of both Rollins and Cozzette Sandstone members into time-stratigraphic units, including systems tracts, and hence provide a genetic significance.

In summary, this research study applies concepts of sequence stratigraphy to subsurface data (aided by outcrop study), relates lithostratigraphic packages to a time framework, identifies a hierarchy of chronostratigraphic units, and clarifies stratigraphic member-limits for both Rollins and Cozzette Sandstone members of the Mt. Garfield Formation.

III. Study area

1. Geographic Location

The study area is located in the southern half of the Piceance basin, within Garfield and Mesa Counties, Colorado. Including outcrop sections, the study area covers about 1165 km^2 of north-central Mesa County and south-central Garfield County (Figure 1).
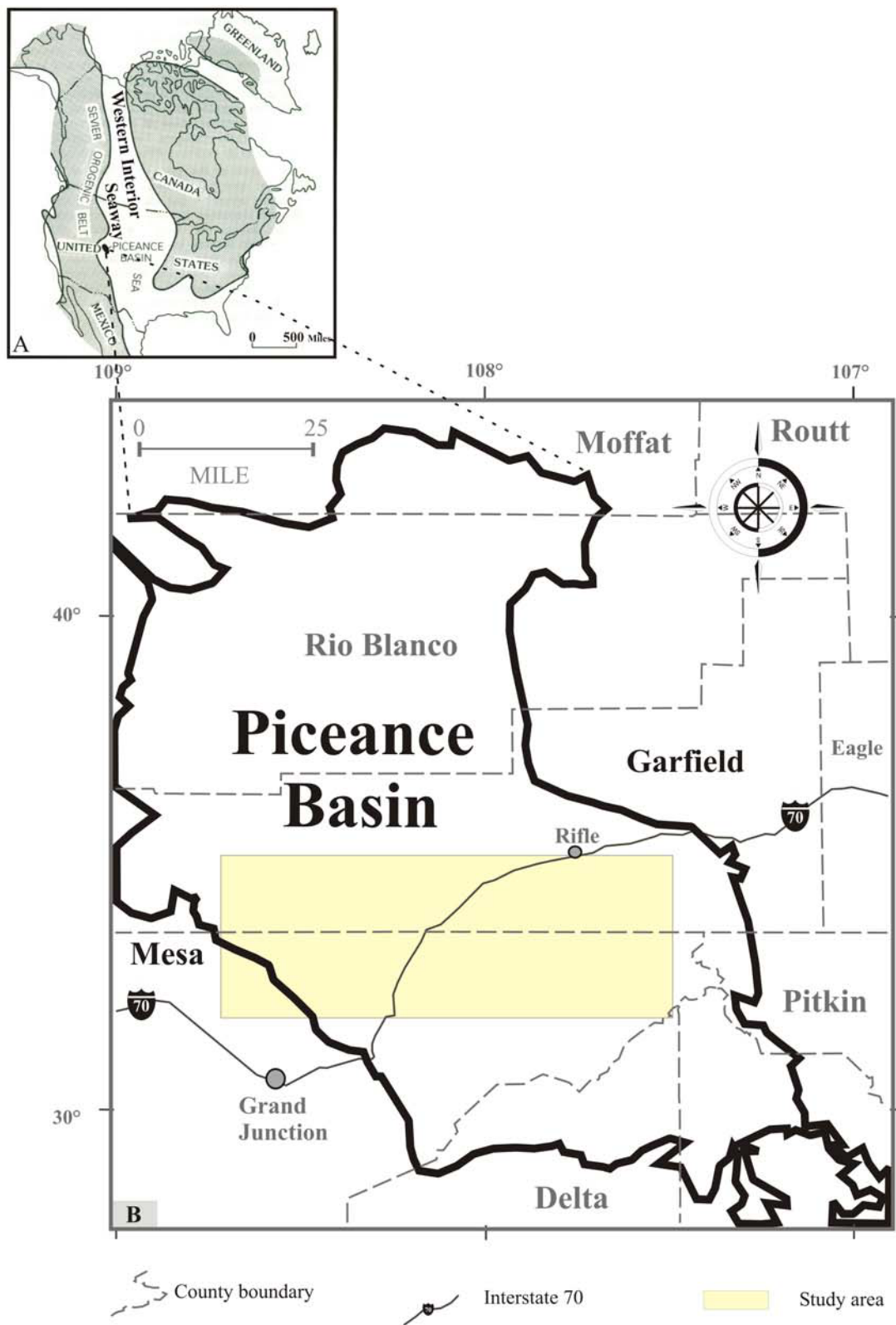
Figure 1. (A) Location map of the Piceance basin, Western Interior Seaway, and Sevier orogenic belt.
(B) Location map of the study area within the Piceance basin in Colorado (modified from Johnson, 1988).

2. Geologic Location

The Piceance basin is an asymmetrical, northwest-trending Laramide structure, and occupies an area of 15,500 km^2 (Brown et al., 1986). The Piceance basin is surrounded on the east by the White River Uplift and the Elk Mountains, on the south and southwest by the Gunnison Uplift and Upcompahgre Uplift, on the west by the Douglas Arch, and on the north by the Uinta Mountains and the Axial Basin Anticline (Figure 2). The study area contains the Rulison gas field on the northeast, the Sheep Creek and Vega gas fields on the northeast, and is bounded by the Book Cliff exposures on the west, and the Coal Basin gas field and the Grand Mesa Plateau on the south (Figure 3).
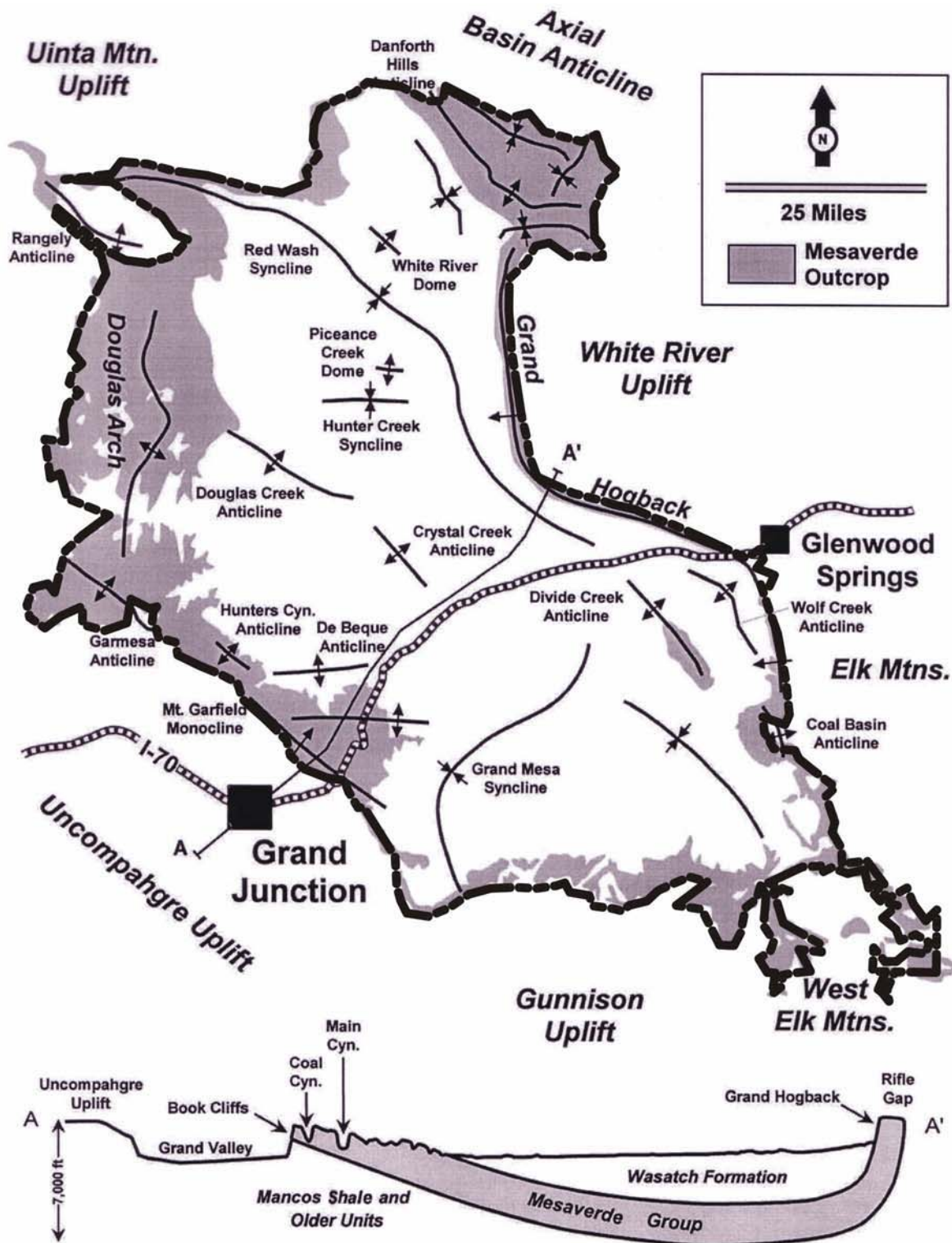
Figure 2. Structural map of the Piceance basin. Cross section AA' is a geologic structure illustrating the asymmetrical structure of the Piceance basin and the accumulated Mesaverde Group: Mesaverde Group outcrops at the edges of the Piceance basin, and is buried beneath younger sediments at the center of the basin (adapted from Cole and Cumella, 2003).

5
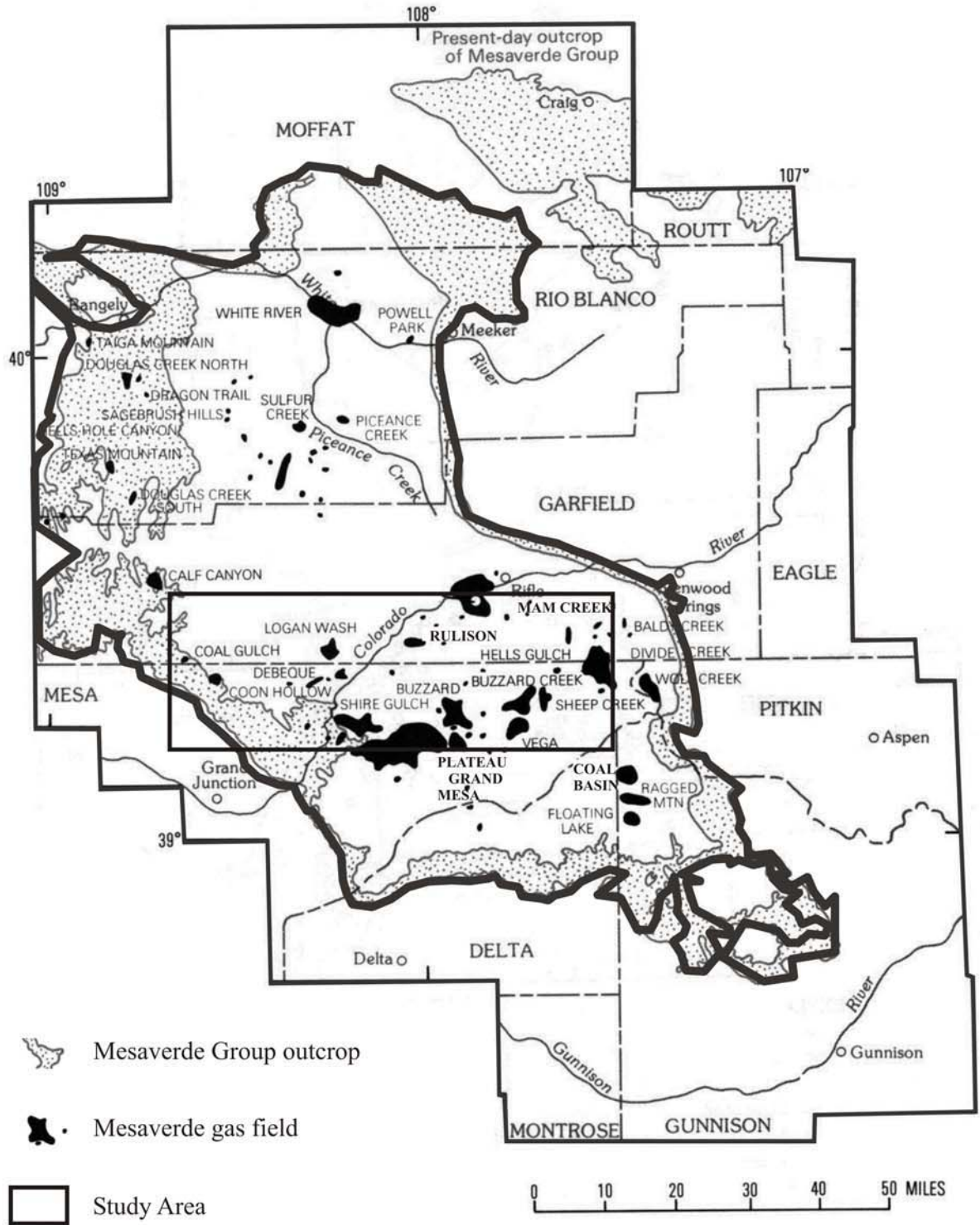
Figure 3. Well-log data of the study area contains Rulison gas field on the northeast, Sheep Creek and Vega gas fields on the east, and are bounded by Grand Mesa Plateau and Coal Basin gas field on the south, and Book Cliff exposures on the west and the northwest (modified from Johnson, 1988).

IV. Background Geology

1. Stratigraphy

In the Piceance basin, the upper part of the Mt. Garfield Formation is composed of three lithostratigraphic members. These members are, in ascending order, the Corcoran, Cozzette and Rollins Sandstone members (Young, 1955; Johnson, 1988). They are overlain by the Cameo-Wheeler coal zone of the Williams Fork Formation.

The Cameo-Wheeler coal zone is composed of multiple horizons of coal and channelized sandstone. The average thickness of the Cameo-Wheeler coal zone in the Piceance basin is about 61 m (200 feet) and approximately 70 m in the study area. Coal intervals within the Cameo-Wheeler coal zone reach a thickness of 10 m (Cole and Cumella, 2003). Presently, no correlation of the individual coal seams is published.

The Mount Garfield Formation is underlain by the Sego Sandstone to the west and by the Mancos Shale to the east (Figure 4). On a regional scale, all three lithostratigraphic members consist of marine and non-marine strata, which thin seaward (to the east) and inter-tongue with the marine Mancos Shale (Young, 1955; Johnson, 1988) (Figure 4). These formations are Campanian in age (Gill and Hail, 1975; Madden, 1989). The Rollins Sandstone Member is the youngest member of the Mt. Garfield Formation and is the most laterally extensive lithostratigraphic member in the Piceance basin (Johnson, 1988) (Figure 4).
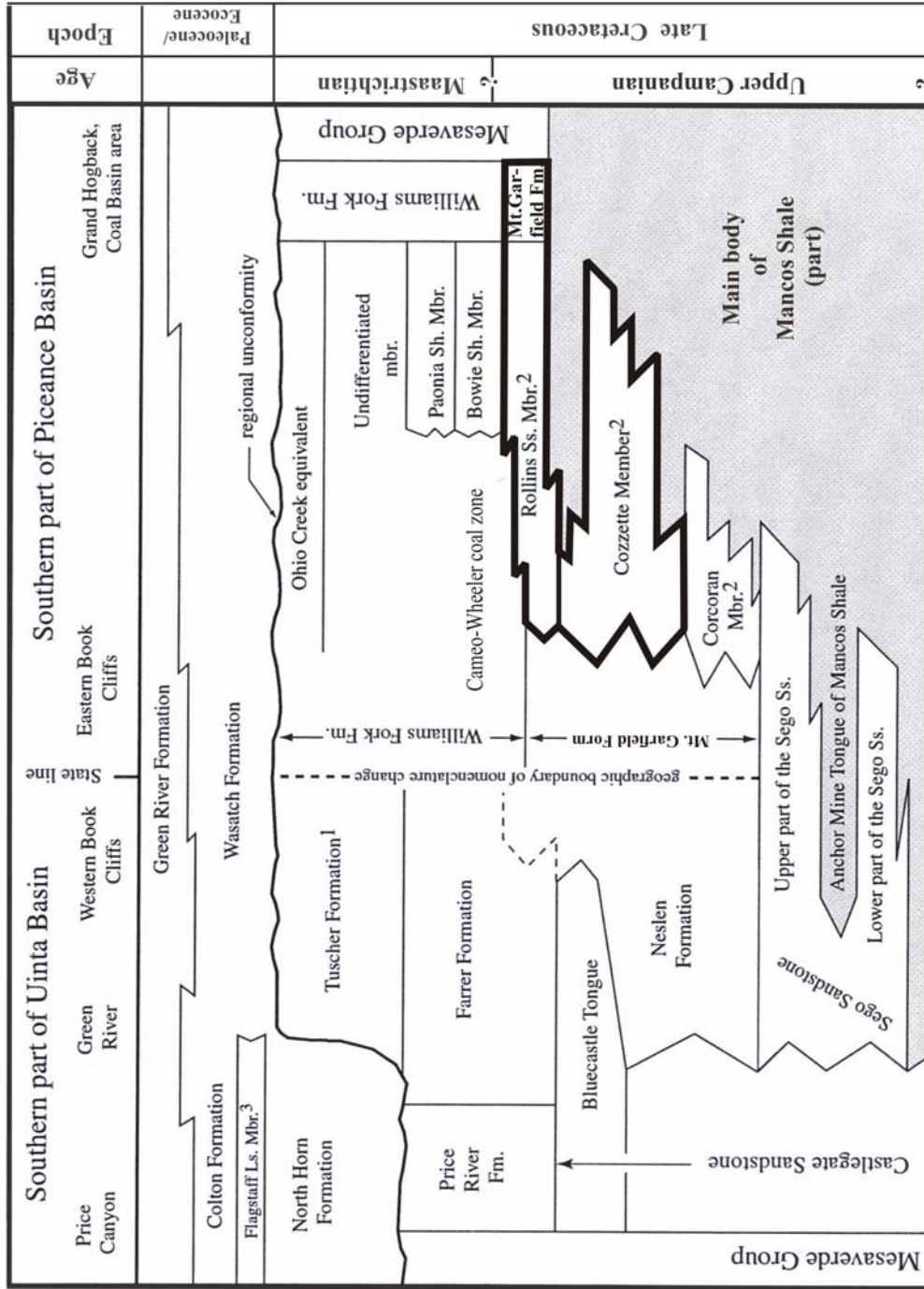
Figure 4. Schematic diagram illustrating the stratigraphy of the Upper Cretaceous and the Paleocene rocks of the Piceance basin. The Cozzette and the Rollins Sandstone members form the study interval (modified from Hettinger and Kirschbaum, 2002).

8

Using outcrop and well-log data, Hettinger and Kirshbaum (2002) placed the Sego Sandstone and the Mt. Garfield Formation within a general sequence-stratigraphic framework. A more detailed sequence-stratigraphic interpretation of parts of the Mt. Garfield Formation was completed based on outcrop study: Zater (2005) interpreted the Corcoran Sandstone Member, and Madof (2006) interpreted the Cozzette Sandstone Member. Both latter interpretations show a more complex stratigraphy than proposed earlier by Hettinger and Kirshbaum (2002).

Although a detailed sequence-stratigraphic interpretation was completed for both the Corcoran and Cozzette Sandstone members, the member boundary is still difficult to distinguish in the outcrop (personal conversation with Zater and Madof, 2005). The depositional signature of these member boundaries is not a typical depositional response of major flooding events. In some places, it is a simple flooding surface; in others, it is a more complicated expression where it is riddled with erosion surfaces. Multiple erosion surfaces locally erode into the member boundary. Some of these erosion surfaces may represent sequence boundaries and are difficult to resolve at the individual exposure alone.

2. Tectonic History

During the Cretaceous Sevier orogeny, thrusting and coeval folding gave rise to an orogenic belt in western North America, which extended from Mexico to Alaska (Jordan, 1981). The Sevier orogenic belt grew progressively through time, causing the Western Interior foreland basin to form (Jordan, 1981, 1995). The Sevier belt is proposed to be the sediment source for the Mount Garfield Formation (Armstrong, 1968;

Fouch et al., 1983; Franczyk et al., 1989). Strata of the Mt Garfield Formation were deposited along the western margin of the Western Interior foreland basin.

During the late Cretaceous to early Tertiary, the Cretaceous sedimentary strata of the foreland basin were dissected into a number of intermontane basins by basement-involved faulting of the Laramide orogeny. The Piceance basin is one of these Laramide intermontane basins (Tweto and Sims, 1963; Tweto, 1973; Taylor, 1975; Dickinson, 1978, 1987).

V. Methodology

1. Outcrop Analysis

In this study, two measured sections were described for the upper part of the Rollins Sandstone Member in the Book Cliffs exposures near the western edge of the Piceance basin. A thickness of about 26 m was described in Hunter Canyon, Section 8, Township 9 South, Range 100 West. A thickness of about 30 m was described in Corcoran Mine, Section 22, Township 9 South, Range 100 West.

Facies analysis for the Rollins Sandstone Member was achieved by recording different aspects of sedimentary facies, including lithology, texture, grain size and physical and biogenic sedimentary structures. Interpretation of the depositional environments of the Rollins Sandstone Member was carried out by examining the various aspects of sedimentary facies, listed above, as well as the lateral and vertical arrangement of facies. To interpret the sedimentary record of the study interval and to aid in well-log correlations, the measured section of the Rollins Sandstone Member in Corcoran Mine (this study) was combined with outcrop data from Madof (2005). Madof's data includes

10

measured sections from the lower part of the Rollins Sandstone Member and the upper part of the Cozzette Sandstone Member.

2. Subsurface Analysis

In the subsurface study, the stratigraphic interval was interpreted in terms of system tracts, parasequence stacking patterns and depositional sequences based on sequence stratigraphic concepts of Mitchum et al. (1977) and Van Wagoner (1995). More than one hundred well logs were initially examined to collect the database for the sequence-stratigraphic correlation. The two described measured sections along with 31 wells are used for detailed sequence-stratigraphic correlation. Well-log data were chosen based upon location and availability of gamma-ray, neutron and density (NPH-DPH) well logs. They were obtained from a State of Colorado sponsored website http://www.oil-gas.state.co.us. A high concentration of well logs exists in close proximity to outcrops, whereas well-log density decreases progressively toward the east. The dearth of well-log data toward the east limits the study area.

Four cross-sections are established to cover the southern part of the Piceance basin (Figure 5). Cross-section 3 is oriented oblique to depositional dip and oriented NNE-SSW. Cross-sections 1, 2 and 4 are depositional dip sections. Cross-sections 1 and 2 are NW-SE oriented sections, whereas cross-section 4 is a W-E oriented section.
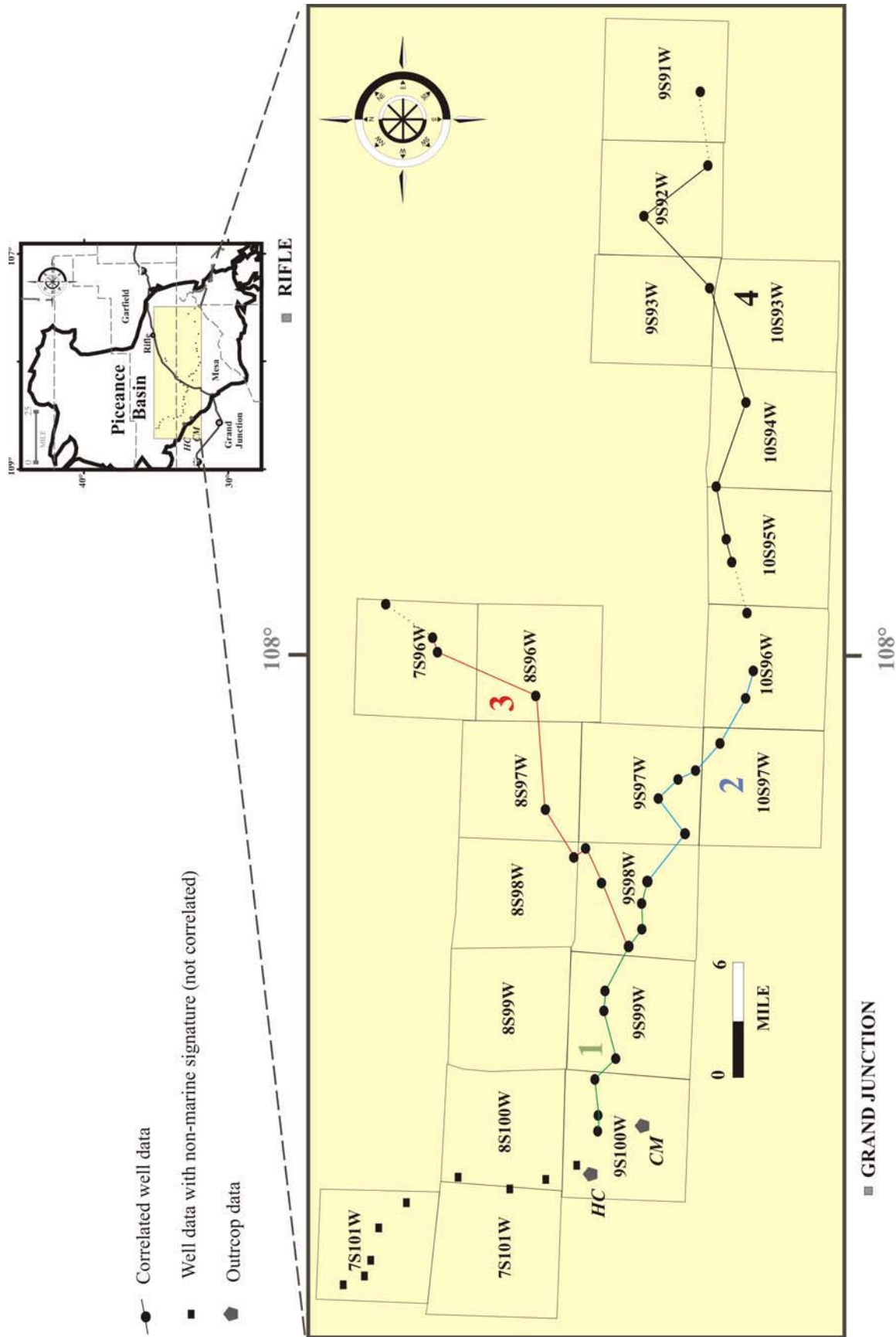
Figure 5. Location map of cross-sections in the study area. Cross-sections 1, 2 and 4 are depositional dip sections. Cross-section 3 is oblique to depositional strike. Measured sections (●) are Hunter Canyon (HC) and Corcoran Mine (CM). Well-log data (■) are non-marine deposits; they are used to help delineate the maximum landward limit of the paleoshoreline.

Sequence-Stratigraphic Correlation

The base of the Cameo-Wheeler coal zone directly overlies the top of the Rollins Sandstone Member throughout the Piceance basin (Collins, 1977; Johnson 1988). It is considered an excellent time horizon (i.e., datum) for the Piceance basin because it is the most laterally extensive and the most recognizable marker horizon (Hettinger and Kirschbaum, 2002; Cole and Cumella, 2003). It is characterized by a distinctive peak on the gamma-ray log (GR) response that separates the mud-rich intervals of the lower part of the Cameo-Wheeler coal zone from the sand-rich intervals of the Rollins Sandstone Member. Throughout the study interval, this horizon symbolizes a regional stratigraphic break.

In the eastern strata of the Piceance basin, a second datum is identified at the top of a rich-coal interval at the top of the Corcoran Sandstone Member. This is considered to be an auxiliary datum. This auxiliary datum is parallel to the principal datum in the western part of the study area. It supports the choice of the basal surface of the Cameo-Wheeler coal zone as the principal datum for cross-sections. West of the Piceance basin, beyond the study area, the upper part of the Rollins Sandstone Member contains non-marine strata (fluvial and coal bearing deposits). The auxiliary datum may form another best datum to the west.

Electrofacies Analysis

The use of an electrofacies model for the study interval standardizes the terminology of well-log curve shapes and provides a classification of log shape irregularities encountered in both the Cozzette and Rollins Sandstone members. The

electrofacies model used is derived from those of Cant (1992) and Rider (1986), and is based on geometrical considerations, such as log shape, curve characteristics, and nature of lower and upper contacts (Figure 6-a). Cylindrical (blocky), funnel, bell, irregular and "no-trend" are the main descriptions used for the overall shape of curve characteristics, specifically for GR logs; the terminology of "smooth" and "serrated" are used to describe curve characteristics (Figure 6-b).

Different electrofacies types are identified for the study interval using the GR curve characteristics, thickness, and NPH-DPH log separation. These electrofacies features are crucial for well-log correlations. The electrofacies types are different log patterns that reflect various depositional facies. In a single well log, different deflections on the GR log define significant and numerous stratigraphic breaks that may reflect the common electrofacies types that are established in the model of Cant (1992) and Rider (1986). The different electrofacies types are then traced laterally throughout the well logs indicating distinct vertical and lateral electrofacies sets that may represent a distinct spatial relationship of depositional facies. The combination of the GR log and the NPH-DPH log separations may place the depositional facies with confidence into a spatial relationship that should impart a coherent history to the sedimentary record, i.e., the NPH-DPH log is a good indicator of coal beds that are common in non-marine to marginal marine environments.
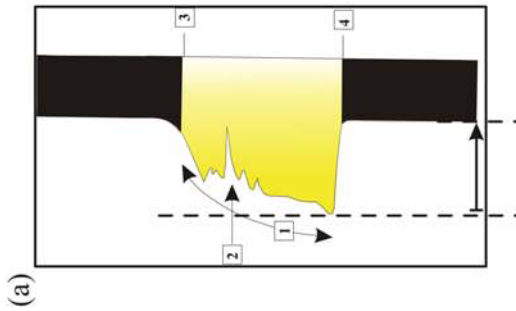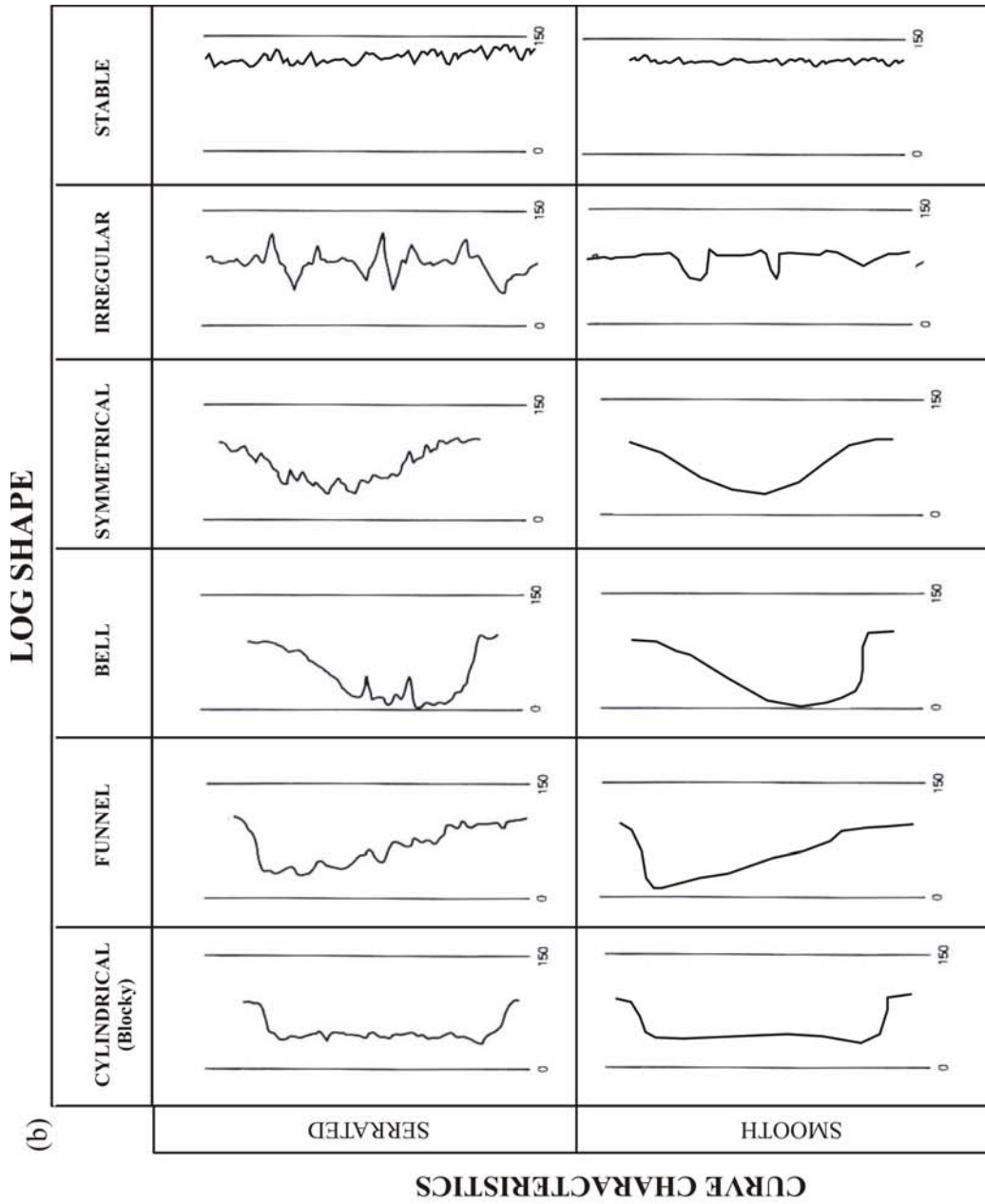
Figure 6. Electrofacies model. a): Log responses are interpreted into basic electrofacies via the following parameters: shape (1), curve characteristics (2), upper and lower contact (3 and 4). b): Basic gamma-ray log shapes and curve characteristics (modified from Cant, 1992 and Rider, 1986).

15

Correlation Process

After the regional datum was established, individual well logs are correlated. This consists of multiple steps. First, GR-electrofacies types were interpreted for individual well logs. Electrofacies were then correlated from log to log, and regional facies trends were interpreted. Through this procedure and aided by NPH-DPH curve separations, parasequence boundaries (flooding surfaces) were identified. Parasequence boundaries were traced up and down dip between well logs. The correlation of parasequence boundaries allowed the recognition of facies change from proximal to distal facies along depositional dip.

Chapter II: OUTCROP ANALYSIS

I. Introduction

Three distinct units are identified in outcrop for the Rollins Sandstone Member, based on field observations. Outcrop unit 1 occurs at the base of the Rollins Sandstone Member and consists of a heterolithic assemblage of complex small vertical trends with an overall slight upward-coarsening succession. Outcrop unit 2 occurs mostly throughout the upper outcrop exposures of the Rollins Sandstone Member and consists of an upward-coarsening succession, which is locally truncated by outcrop unit 3. This latter consists mainly of amalgamated sandstone with no typical vertical trend. Outcrop unit 2 is described in the outcrop exposures in Corcoran Mine; description of outcrop units 1 and 3 is based upon the exposures in Hunter Canyon. Outcrop analysis was completed to provide a guide in interpretation of the well-log data. Lithostratigraphy of the Mt. Garfield Formation is presented in Figure 7 as a guide in subsurface correlation.

Figure 7. The three sandstone members of the Mt. Garfield Formation, underlain by the Mancos Shale, exposed on highway 70, west of the Book Cliff Mine (Sec. 8, T.10S, R.99W).

II. Description

1. Outcrop Unit 1

Outcrop unit 1 is located in Hunter Canyon at the base of the Rollins Sandstone Member (Figure 8). It displays a heterolithic assemblage with an overall upward-coarsening trend. It contains three subunits, which are described in ascending order.

Subunit 1: The base of this subunit is covered. The first exposed interval is composed of brownish siltstone with continuous thin wavy mudstone drapes, overlain by a coal bed with enclosed siltstone layers, and is approximately 2 m thick (Figure 8). These mudstone drapes are less than 1 cm in thickness, alternate with centimeter-thick siltstone layers and together with the siltstone form an interval approximately 1 m thick. This interval is intensely burrowed. Burrows such as *Ophiomorpha* and *Planolites* are present throughout the alternating mud-siltstone interval, but most easily observed within siltstone beds where they show a random orientation. This interval is overlain by approximately 1 m of coal with siltstone partings. Siltstone partings range from 10 cm to 30 cm in thickness, are light brown to gray in color, and are well laminated. The laminations contain shale and carbonaceous material. S*lickensides* are present in the surrounding coal deposits.

Subunit 2: This subunit is 1.5 m thick (Figure 8). It displays minor intercalations of mudstone and siltstone at the base that pass into a thin bed of very fine-grained to silty sandstone at the top. Both siltstone and mudstone are locally bioturbated. Siltstone beds (~20 cm) are sharp-based, light brown to gray in color, and are interbeded with mudstone beds.
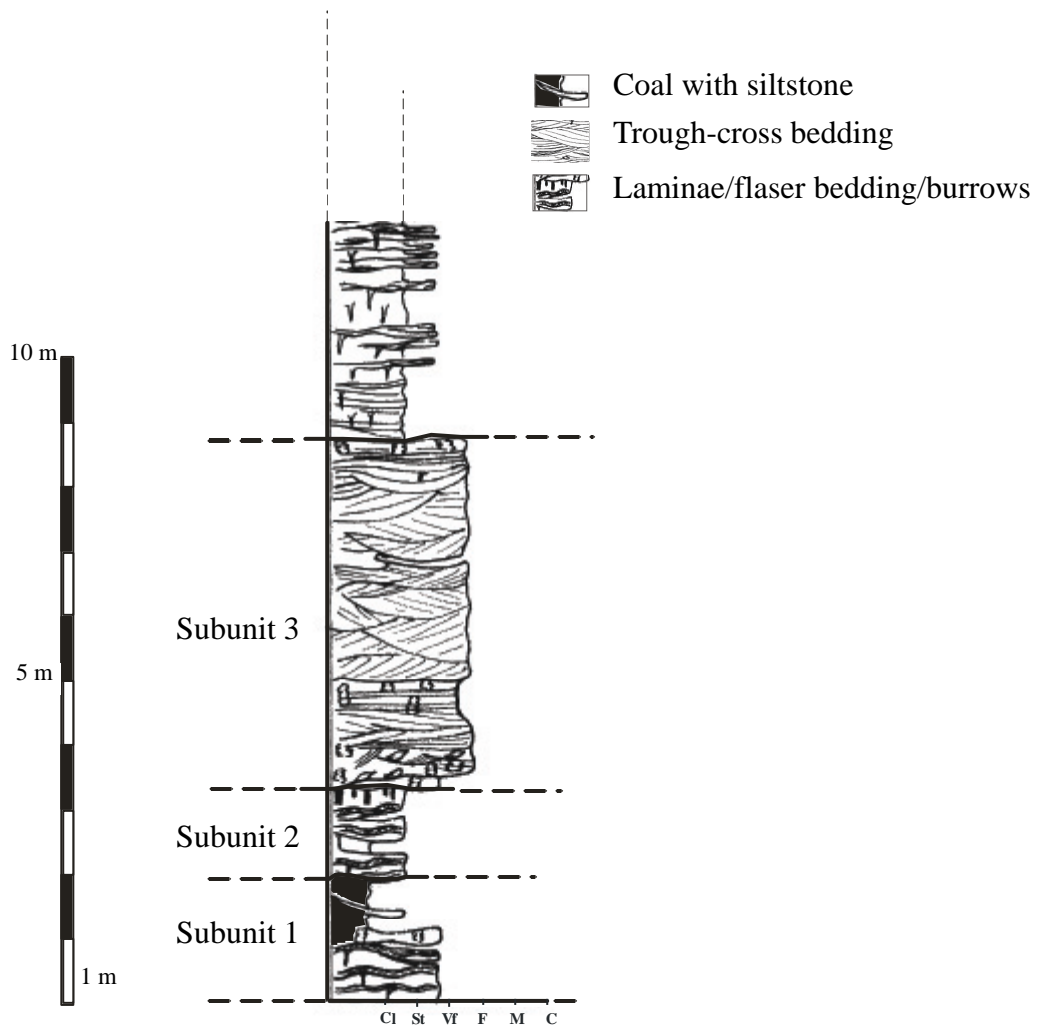
Figure 8. Illustration of outcrop unit 1 showing a complex heterolithic assemblage which is divided into 3 subunits. It exhibits a complex verical trend. It is located at the lower part of the Hunter Canyon measured section. Grain size: Cl (clay), St (silt), Vf (very fine sand), F (fine sand), M (medium sand), C (coarse sand).

The mudstone beds are black-gray in color, are thinly laminated with carbonaceous material, and exhibit a thickness that decreases gradually upward (from 20 to 5 cm or less). The overlying silty sandstone is approximately 10 to 15 cm thick, flaser bedded, with discontinuous mudstone drapes of less than 1 mm in thickness. The mudstone drapes accentuate wave-ripple cross-stratifications. Subunit 2 terminates with an intensely burrowed surface that is increasingly well-cemented, providing a cohesive and dense texture, and is yellow-brown-red in color. The color may be due to the presence of oxidized products such as hematite or magnetite that may derive from the oxidation of ferrous carbonate-siderite. This surface is marked by unidentified vertical to sub-vertical burrows.

Subunit 3: This unit is approximately 5 m thick and consists of cross-bedded sandstone that locally scours into the underlying silty sandstone layers of subunit 2 (Figure 8). The sandstone is white, very fine to fine-grained, well to moderately-well sorted with an overall slight upward decrease in grain size, and contains trough cross-stratification. The cross-bed sets are 20 to 40 cm thick, and are bioturbated with *Ophiomorpha*. *Ophiomorpha* traces are sporadically distributed across the interval and highly concentrated toward the top. The basal contact of the sandstone is sharp and undulatory. The middle is locally marked by a continuous wavy lamination (~1 mm), highlighted with very thin mudstone drapes.

2. **Outcrop Unit 2:**

Outcrop unit 2 is described in Corcoran Mine where it occurs at the top of the Rollins Sandstone Member. It is laterally continuous, distinctively white colored, and

capped with a coal bed (Figure 9). This unit is composed of six subunits arranged in an upward-coarsening trend and is described in ascending order.

The first subunit is approximately 4 m in thickness, contains carbonaceous, gray-black to gray-brown thinly laminated siltstone, interbedded with thin gray, very fine and sharp-based sandstones and contains hummocky cross-stratification. Sandstone beds thicken upward and range from 10 to 25 cm. Locally, siltstone and sandstone beds are heavily bioturbated and appear mottled. *Ophiomorpha* occurs in abundance.

The second subunit consists of approximately 10 m of white to light brown, mostly fine-grained, well sorted sandstone with amalgamated hummocky cross-stratification (maximum bed thickness ranges from 1 to approximately 3 m) (Figure 9). At the base, however, the hummocky structures are locally draped with silty shale. Burrows in this facies include *Ophiomorpha*.

The third subunit is approximately 5 m thick, contains white to light brown, well to moderately sorted, fine-grained sandstone with planar bedding (Figure 9). Locally, it is heavily bioturbated. The burrows are restricted to *Ophiomorpha* and occur abundantly throughout the entire interval. Traces of *Ophiomorpha* are also present in the bioturbated beds.

The fourth subunit is 5 m thick, and is composed of white, clean, fine to medium-grained, well to moderately sorted sandstone with low-angle troughs (Figure 9). Planar-tabular cross-stratification is local and exhibits similar cross-bed set thickness as the main low-angle troughs. Cross-bed sets of low-angle troughs are 20 to 40 cm thick, slightly bioturbated, and locally contain current-ripple laminations towards the top.

30 m

Subunit 6

Subunit 5

Subunit 4

20 m

Subunit 3

Subunit 2

10 m

Subunit 1

1 m

Covered

Covered

Cl St Vf F M C

Coal

Roots

Trough-cross bedding

Planar beddings

Hummocky bedding
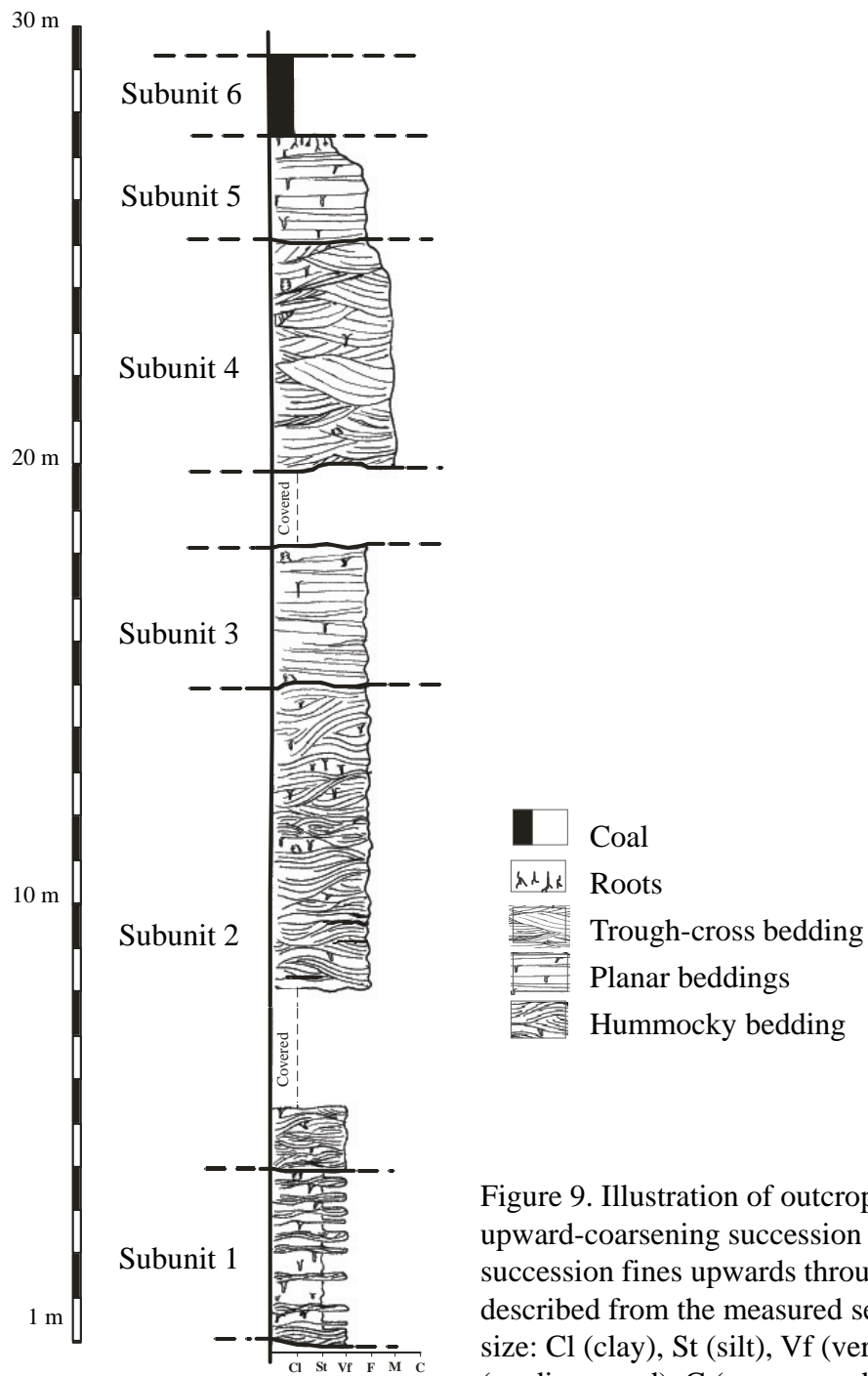
Figure 9. Illustration of outcrop unit 2 showing an overall upward-coarsening succession from subunit 1 to subunit 4. This succession fines upwards through subunit 5 to subunit 6. It is described from the measured section in Corcoran Mine. Grain size: Cl (clay), St (silt), Vf (very fine sand), F (fine sand), M (medium sand), C (coarse sand).

23

These current ripples are rare and poorly preserved. This interval is slightly bioturbated. Identifiable trace fossils are restricted to *Ophiomorpha*.

Subunit 5 is less than 3 m thick and consists of a white, moderately well-sorted, fine-grained sandstone with sub-horizontal to planar-parallel bedding. Bioturbation is rare. The top of this facies is an intensely bioturbated with root traces. Subunit 5 is overlain by 2 m of coal assigned to subunit 6 (Figure 9).

3. Outcrop Unit 3

This outcrop unit is described in Hunter Canyon where it laterally replaces the upper part of outcrop unit 2. Viewed from a distance, this facies seems to be laterally continuous and similar to that outcrop unit 2. The measured section in this area, however, reveals more complications (Figure 10).

The basal contact of this unit is sharp and planar. It truncates the underlying hummocky cross-stratified beds of outcrop unit 2, and is overlain by approximately 4 m thick interval of white to beige, fine to medium-grained sandstone, intensely bioturbated with *Thalassinoides* and *Ophiomorpha*. No distinctive physical sedimentary structures are observed. A continuous, undulatory surface occurs in the middle of this interval (Figure 10). This surface is marked by very thin shale partings. Locally, the weathering process causes the bedding plane of this structure to be exposed. The bedding plane exposure is covered with horizontal burrows of *Thalassinoides* and *Ophiomorpha* that form branched features.

Brownish channel-fill
sandstones of the
Cameo-Wheeler
Coal Seam

5 m

1 m

Cl   St   Vf   F   M   C

Outcrop Unit 3

Outcrop Unit 2
(Subunit 2)
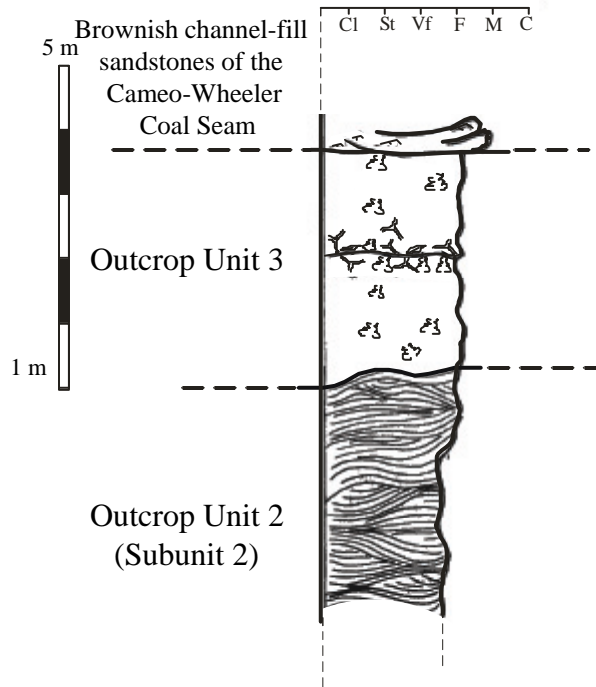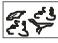
Massive sandstone intensely
bioturbated (*Thalassinoides/Ophiomorpha*)

Hummocky bedding

Figure 10. Illustration of outcrop unit 3 showing amalgamated sandstones with no typical vertical trend. It is located at the upper part of Hunter Canyon measured section. Grain size: Cl (clay), St (silt), Vf (very fine sand), F (fine sand), M (medium sand), C (coarse sand).

Diplocraterion, the U-shaped, vertical trace fossil was also detected by the presence of a multitude of paired swelling features (or paired vertices) visible on the bedding surface. *Diplocraterion* was not as abundant as *Ophiomorpha*. The interval of white massive sandstone of outcrop unit 3 extends laterally to a better stratified interval, where several beds of varying character are observed. Both intervals are truncated at the top by brown-reddish, multiple-stacked thin and low-angle trough cross-bedded sandstones. Because of the color contrast and the intense oxidation of the overlying sandstones, the brown-red sandstones were interpreted to belong in the Cameo-Wheeler coal zone, and thus it was not included in the description of outcrop unit 3.

III. Interpretation

1. Outcrop Unit 1

Subunit 1: The alternating mudstone-siltstone interval, associated with mudstone drapes, may be interpreted as a tidal deposit. These interbeds can be related to a variety of depositional settings, ranging from tidal flats to bay fill deltas, estuarine, and lagoonal settings (Masters, 1967; Van Wagoner et al., 1990; Reading and Collinson, 1996).

The existence of a coal bed with siltstone layers, toward the top of subunit 1, indicates the coexistence of two sub-environments. One is the marsh deposit that is related to coal beds, and the other is the overbank deposit that explains the siltstone partings (splits). Coal originates from vegetation in a poorly-drained setting or mire that undergo the process of coalification (McCabe, 1984; Collins, 1977). Coal beds can represent a deposition setting that developed between interdistributary channel systems and protected by natural levees. The siltstone partings within these coal settings may

26

occur during local and short-lived flood events. During periods of flood events, sporadic deposition of sand, mud and silt occurs when the levees are breached. Coal beds can also represent a depositional setting of plant roots and remains that develops within widespread mire (McCabe, 1984). The siltstone partings within these coal settings may represent both tribative and distributive channel systems (i.e., anastomosing) that develop in low-laying areas (mire and marsh) and that may be abandoned afterward. Channel abandonment results in fine-grained sediments (siltstone) that are deposited out of suspension and are trapped during the rapid compaction process of mire or marsh accumulations (coal) (McCabe, 1984).

Subunit 2: The sharp-based siltstone beds that thicken upward and the slight upward increase of the grain size from silt to silty sandstone indicate a general upward increase in energy. The increase in energy is often associated with progradational events. Subunit 2 may be interpreted as distal bay-fill deltas.

The presence of flaser bedding and mudstone drapes is interpreted as a tidal signature (Nio and Yang, 1991). The interbeds of siltstone and mudstone are interpreted to indicate a low-energy environment where silt and mud deposition periodically alternates as the energy levels fluctuate. The low energy of these depositional settings forms favorable conditions for burrowing organisms to rework sediments. The densely burrowed surface indicates a termination of sedimentation that may have been caused by either an erosional vacuity or a sudden shift in the favorable conditions of burrows. The red- and yellow-colored surface may be a result of oxidation of ferrous minerals that may be caused by a chemical weathering of sediments. For example, these sediments may contain authigenic ferrous minerals such as siderite (Lorenz, 1982; Brown et al, 1986).

Siderite ($FeCO_3$) is a ferrous carbonate mineral that forms as a diagenetic response to reducing conditions in non-marine or other iron-containing, sulfur-depleted water. Also, siderite may form during a decrease in water oxygenation that is caused by early compactional process of shallow marine deposits (Tucker, 2001). The early compactional process may cause a sudden shift in the favorable conditions for burrowing. Deposition and oxidation of siderite during the burial history of sediments may explain the yellow-brown-red color and the cohesive (resistant) texture of the surface (Tucker, 2001; Pemberton et al., 2004).

This surface may be interpreted as a significant stratigraphic boundary. The boundary is a discontinuity in the sedimentary process that is linked to either a flooding event (transgressions), a lowstand erosional event or both (Frey and Pemberton, 1984, 1985; Pemberton et al., 2002, 2004). For example, the marine flooding event that produces a parasequence boundary is associated with a significant increase in water depth and that may result in intense burrowing (Van Wagoner et al., 1990). The lowstand erosional event that produces a sequence boundary can be associated with a significant decrease in water depth (or subaerial erosional truncation), which may form subaerial exposure surface and sediment bypass landward and a rapid deposition of sediment seaward. Rapid deposition may cause early compaction of shallow marine deposits (Van Wagoner et al., 1990). Flooding events can also be accompanied by erosion (Van Wagoner et al., 1990).

Subunit 3: The sharp lower contact is interpreted as a basal scour. The overall upward decrease in grain size indicates a slight upward decrease in energy. The cross-stratification indicates the migration of megaripples. The uniformity and size of cross-

beds suggests a predominantly high-energy depositional environment. The presence of the mudstone drapes in the middle of subunit 3, however, is interpreted to indicate deposition in low-energy conditions, and a change in energy in the overall succession. Presence of O*phiomorpha* documents a marine influence. This subunit is interpreted as a channel-fill succession with marine influence.

Subunits 1, 2 and 3 show either marine or tidal influence (Figure 11). The vertical stacking of these subunits is complex and shows a vertical succession through tidal environments. This vertical stacking and the landward position of these subunits support the conclusion that these are marginal-marine deposits and may represent the complex fill of an incised valley. An incised-valley fill can include many sub-environments, including channels with marine influence (as described in subunit 3), tidal flats (lower part of subunit 1), bay-fill deltas (subunit 2), and mires and swamps (upper part of subunit 1). Each subunit is interpreted as a parasequence. Subunit 1 and 2 are separated by a parasequence boundary. The boundary between subunit 2 and subunit 3, however, is more complicated. The top of subunit 2 (bay-fill delta), which is marked by a densely burrowed surface, is overlain by sharp-based channel-fill sandstones. The overlap between the basal sharp surface of subunit 3 and the upper densely burrowed surface of subunit 1 may or may not be a parasequence boundary. The stratigraphic relationship of these subunits, to be discussed later, will help establish the significance of these boundaries.

| | DEPOSITIONAL ENVIRONMENT | SCALE (M) | DESCRIPTION |
| | | | Cl St Vf F M C |

Fluvial/Cameo-Wheeler Coal Zone

OUTCROP UNIT 3 — IVF ? — MARINE to MARGINAL-MARINE COMPLEX

25

OUTCROP UNIT 2 — TRUNCATED UPWARD SHOALING SUCCESSION

LOWER SHOREFACE (LSF)

20

15

DISTAL LSF to OFFSHORE TRANSITION

10

OUTCROP UNIT 1 — IVF ? — MARGINAL-MARINE COMPLEX

5
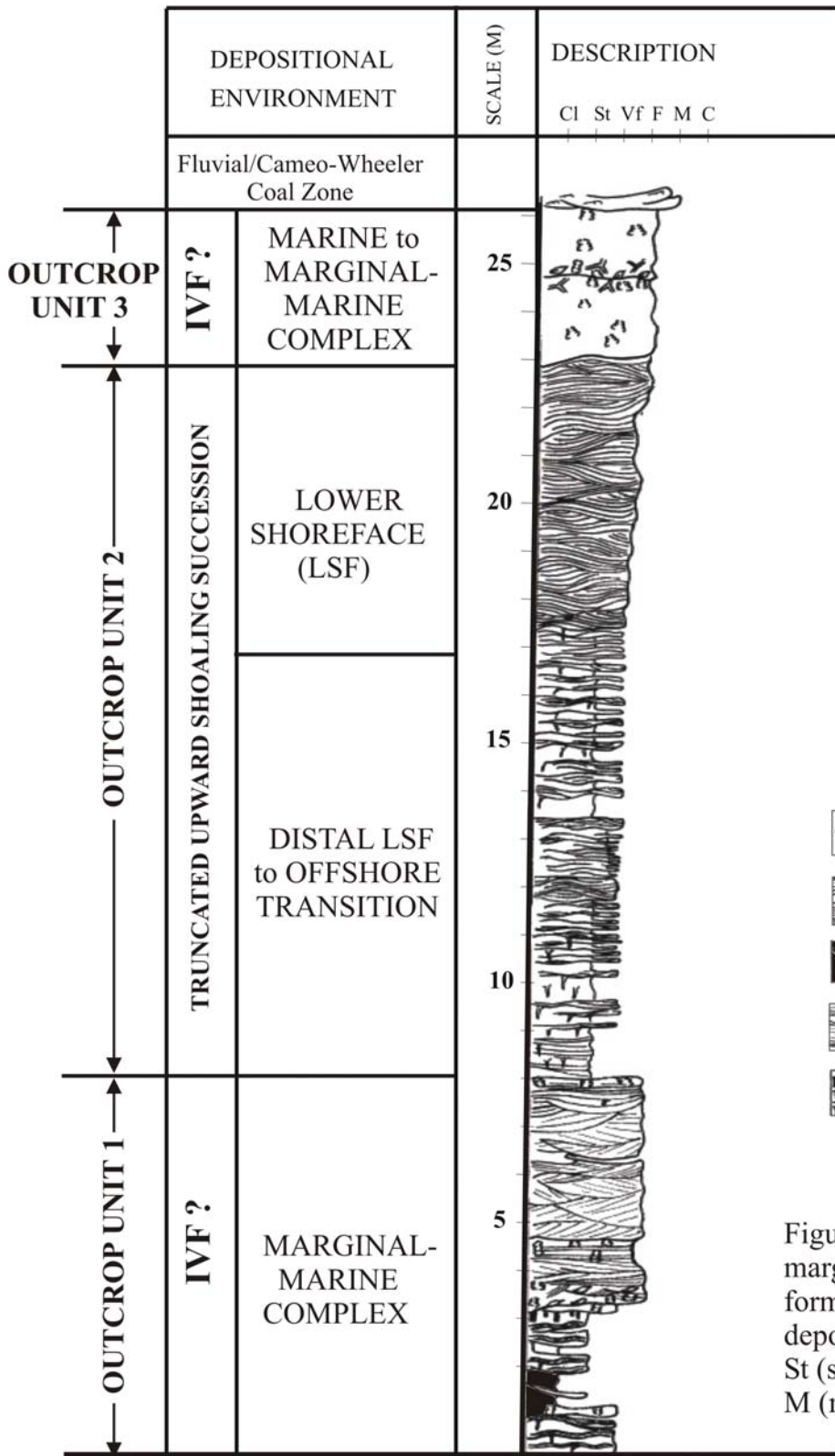
Massive sandstone intensely bioturbated (*Thalassinoides/Ophiomorpha*/wood)

Hummocky bedding

Coal with siltstone

Trough-cross bedding

Laminae/flaser bedding/burrows

Figure 11. Outcrop unit 1 and 3 are complex marginal-marine deposits, and outcrop unit 2 forms a truncated wave-dominated shoreface deposit (Hunter Canyon). Grain size: Cl (clay), St (silt), Vf (very fine sand), F (fine sand), M (medium sand), C (coarse sand).

2. Outcrop Unit 2

Outcrop 2 is an overall upward-coarsening succession; a progradational shoreface deposit. This unit is interpreted as the deposit of a wave-dominated shoreface deposit and contains a series of sub-facies (Figure 12).

The alternating sandstone and siltstone at the base of this succession indicate episodic sedimentation. The episodic sedimentation represents alternation of storm and fair-weather conditions at depth near effective storm wave base (Bourgeois, 1980; Howard and Reineck, 1981; Dott and Bourgeois, 1982; Walker, 1985; Elliot, 1986; Greenwood and Sherman, 1986). As fluctuations in energy levels occur, the erosion forms a sharp surface, peak and waning storms form sandstones beds, and slow deposition of fine particles forms beds of siltstone. Storm events are followed by a long period of quiescence allowing intensive bioturbation to develop at the top of the sharp-based sandstones (Harms, et al., 1975; Bourgeois, 1980; Pemberton et al., 1992). The environment of deposition for this facies, therefore, can be interpreted as an offshore-transition deposit.

Sandstones with hummocky cross-stratification indicate wave- and storm-dominated conditions that occur below the fair-weather wave base of the marine shelf (Harms, et al., 1975; McCubin, 1982; Walker, 1984). During storms, high-amplitude waves intensely rework the lower shoreface and probably the offshore area through a combined flow/oscillatory process (Reinson, 1984).
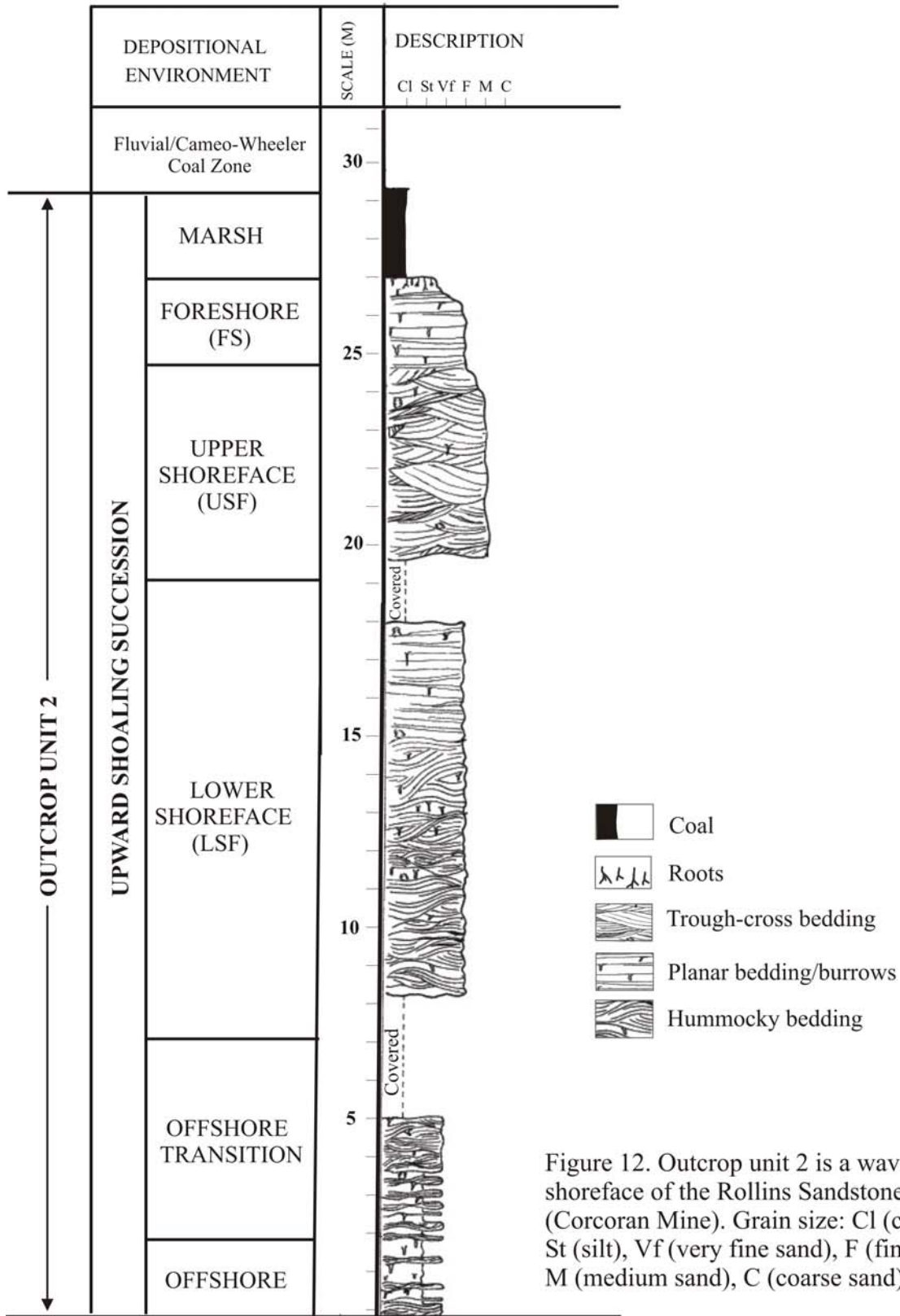
Figure 12. Outcrop unit 2 is a wave-dominated shoreface of the Rollins Sandstone Member (Corcoran Mine). Grain size: Cl (clay), St (silt), Vf (very fine sand), F (fine sand), M (medium sand), C (coarse sand).

32

The existence of interbedded siltstone with hummocky cross-stratification within the lower part of this facies may be explained by intermittent low-energy conditions associated with a decrease in storm intensity as the storm progressively moves inland or a return to fair-weather conditions (Bourgeois, 1980; Yang et al, 2005). This succession represents a lower shoreface deposit.

The planar beds of subunit 3 indicate intermittent upper flow-regime conditions, and the intense bioturbations are induced by long periods of quiescence. Reinson (1984) interpreted a similar succession in the Cretaceous strata of northeast New Brunswick, along the coastline of Canada as a middle shoreface. Planar beds similar to these are interpreted as a barred shoreface (Davidson-Arnott and Greenwood, 1974). Others have interpreted similar facies as a middle shoreface deposit (Howard and Reineck, 1981; Reinson, 1984).

Cross-bedded sandstone of subunit 4 indicates deposition under lower flow-regime conditions. The rare occurrence of current ripples and planar-tabular cross stratifications in association with the cross-bedded sandstone is probably due to a complex combination of wave-velocity fluctuation, sediment flux and water depth (Harms et al., 1975; Swift and Thorne, 1991). The cross-bedded sandstone interval is interpreted as an upper shoreface, which is found landward of the fair-weather wave base (high energy surf zone) (Howard, and Reineck, 1981; Reinson, 1984). In shoreface settings, the wave motions are brief and strong in landward-oriented flow (shallow water depth), but the seaward-directed flow return is weak (Bourgeois, 1980; Reinson, 1984). Such wave motions may cause complex hydrodynamics that may explain the occurrence of current ripples and planar-tabular cross stratifications (Carter, 1978; Howard and

Reineck, 1981). Under multidirectional wave flow and bottom conditions, the varying flow velocity and flow depth may result in migration of sinuous- and straight-crested dunes and ripples. For example, planar-tabular cross-stratifications can be associated with longshore drift currents (Reinson, 1984) whereas current-ripple structures can be associated with a gradational deceleration of flow velocity, which may occur when strong landward-oriented wave currents reverse directions and retreat, i.e., current-ripple structures are lower-low-flow regime (Reading and Collinson, 1996; Yang et al., 2005).

The fifth subunit reflects upper flow regime at shallower water depth. The rarity of trace fossils may indicate constant erosion that prevents adequate conditions for burrowing. This facies is interpreted as a foreshore deposit. The uppermost surface, characterized by abundant bioturbated root traces, is an exposure surface (Howard and Reineck, 1981). The overall white color of this facies reflects leaching of Fe-bearing minerals by acidic ground waters from the overlying coal-forming environments (Flores et al., 1984). This leaching occurred during an early diagenetic phase. The acidic ground waters are derived from the decay of organic matter in the overlying peat deposits (Flores et al., 1984; Nowak, 1991).

The final interval (coal) is interpreted to represent deposition in a marsh or swamp where concentration of carbonaceous material can occur with small silt or sand influx (McCabe, 1984). The minor silt or sand influx indicates that this facies (coal) is probably formed in a protected environment (e.g., raised mire). Coal beds are common within the study area and are associated often with thick intervals of shoreface sandstone within the Western Interior foreland basin (Fassets and Hinds, 1971; Ryer and McPhillips, 1983;

Cross, 1988). Similar coal beds within the Mt. Garfield Formation are described by Zater (2005) and Madof (2006).

3. Outcrop Unit 3

The outcrop extent and exposure of this unit is small; therefore, details of the deposition setting cannot be fully resolved (Figure 11). The lack of physical structures of this unit is explained by the abundance of trace fossils *Thalassinoides, Ophiomorpha,* and *Diplocraterion*. This ichnofacies assemblage indicates marine influence (Frey and Pemberton, 1984, 1985). The sharp base of this interval indicates a sudden truncation of the underlying shoreface succession. The prevailing sandy composition of the entire interval indicates a high-energy setting. Intense bioturbation suggests that the deposition of this succession was followed by a period of quiescence, allowing organisms to intensely rework sediments (Frey and Pemberton, 1984, 1985). The existence of a thin and continuous mud drape in the middle of this sandstone is interpreted to indicate that outcrop unit 3 was deposited as two events, separated by a period of low-energy conditions in which mud could be deposited. Sharp-based contacts of these two sandstone bodies may be erosional and may be attributed to a channel floor, but the prevailing bioturbation throughout this interval indicates marine influence. Outcrop unit 3 may represent a marine or a marginal-marine complex within an incised-valley fill (Figure 13).

Figure 13. Outcrop unit 3 overlying lower shoreface deposits of outcrop unit 2 in the Rollins Sandstone Member (Hunter Canyon). Outcrop unit 3 may represent the complex fill of an incised valley. The top of outcrop unit 3 is overlain by Hunter Canyon Formation.

Outcrop unit 3 was deposited unconformably over the lower shoreface deposit of the wave-dominated shoreface of outcrop unit 2. In a complete vertical sequence of a wave-dominated shoreface, the HCS bedforms of the lower shoreface are overlain, usually, by either trough-cross beds of the upper shoreface or planar beds of the middle shoreface. These two intervals, upper and middle shoreface, are missing and are replaced by white massive sandstone of outcrop unit 3. Also, the occurrence of a continuous, undulatory, mud-draped surface in the middle of the massive white sandstones is a facies characteristic of neither the upper shoreface nor the middle shoreface. The surface separating outcrop unit 3 from outcrop unit 2 may represent a significant break of the stratigraphic succession and may indicate that outcrop units 2 and 3 are not genetically related deposits. The undulatory mud-draped surface marking the middle part of outcrop unit 3, however, may or may not represent a significant break of the stratigraphic succession. Such mud drapes may occur during the nature reversing tidal currents of flood and ebb deltas, or they may have a post-storm origin in relation to storms that are frequent during periods of rising sea levels (Johnson and Baldwin, 1996; Yang et al, 2005; Wanless, 2011). For example, the mud-draped surface combined with the heavily bioturbated character of outcrop unit 3 may represent separate pulses of sandstone entering a partly enclosed environment, such as an inner estuary (or bay), during storms. During storms, muddy deposits of the offshore are recycled and are shifted in a landward direction to be deposited as a mud drape through river mouths (Johnson and Baldwin, 1996). Repetitive storms may fill inner estuaries episodically with pulses of sand and salty water, gradually increasing salinity of the estuary and leading marine organisms to flourish in situ during periods of quiescence (Reading and Collinson, 1996; Wanless,

2011). According to Nummedal and Molenaar (1995) *Ophiomorpha* and *Thalassinoides* can be common in estuarine mouth bars.

The uppermost surface separating the massive white sandstone of outcrop unit 3 from the overlying reddish-brown sandstone of the Hunter Canyon Formation may also indicate a significant break in the stratigraphic succession. The regional significance of these boundaries that defines stratigraphic relationships of facies can only be resolved through detailed outcrop description and correlation, and which are not part of this study. Yet the distinction between these boundaries is important to note because similar stratigraphic relationships might be encountered in the analysis of subsurface data.

Chapter III: SUBSURFACE ANALYSIS

I. Introduction

The combination of outcrop and well-log data presents an important approach for sequence stratigraphic analyses. The recognition of facies based on conventional gamma-ray models and outcrop data remains a necessary step in subsurface correlation. Subsurface analysis consists of three steps: (1) identification of well-log patterns, (2) interpretation of electrofacies lithology, and (3) interpretation of the depositional environments (Rider, 1986). The results will be used in the next chapter for stratigraphic correlations.

Well-log trends are classified following an approach based on the electrofacies model of Cant (1992) and Rider (1986). The electrofacies model is established based on the geometric features of the gamma-ray curve (GR). The overall curve shape is described as cylindrical (blocky), funnel, bell, irregular or no-trend. The curve shape can be either smooth or serrated. As the character of GR and NPH-DPH log responses was the key to mapping electrofacies in the study area, an overview log expressions and their relationship to lithologies is necessary.

1. Gamma-Ray log

The gamma ray log (GR) is the most useful log for sequence-stratigraphic interpretation (Schlumberger, 1972; Serra, 1984). In the conventional model, the GR log is primarily used as a depth reference for all running well logs, qualitatively as a

stratigraphic tool to correlate strata (log patterns), and generally as an overall clay volume evaluator.

The GR tool records natural radioactivity of a formation. Gamma rays are naturally and continuously emitted in the formation by radionuclides such as uranium (U), potassium (K) and thorium (Th). These three radioactive elements are usually more abundant in shale and dispersed clay. High pulses detected by GR log indicate a high occurrence of radioactive elements, and so, a high GR reading is used to interpret clay content. The GR log is scaled in API units. The average scale ranges from 0 to 150 or 0 to 200 API units and then wraps to record greater values. Each scale contains 10 divisions, and each division equals 15 or 20 units. Values on the scale increase to the right side of the log track. For example, the typical GR reading for sand is 20-30 API and, for shale, is 75 or 80 to 300 API (Dewan, 1983).

a. Radius of investigation and vertical resolution of GR tool

The radius of investigation of a GR tool is illustrated in Figure 15. The radius of investigation, or the sphere of influence of the GR tool, is paraphrased from Serra (1984; p100-110) as follows. The radius of investigation of the GR tool, in a homogenous formation, is a sphere centered on the detector. "R" is the radius of the sphere of investigation and corresponds to the volume of radiation absorbed by the rocks surrounding the GR tool. "R" varies from 15 cm to 30 cm and depends on formation, GR energy, and drilling-mud density. It is higher at low drilling-mud densities and lower at high drilling-mud densities. According to Dewan (1983), 90% of data is collected from the first 15 cm interval (Figure 14).
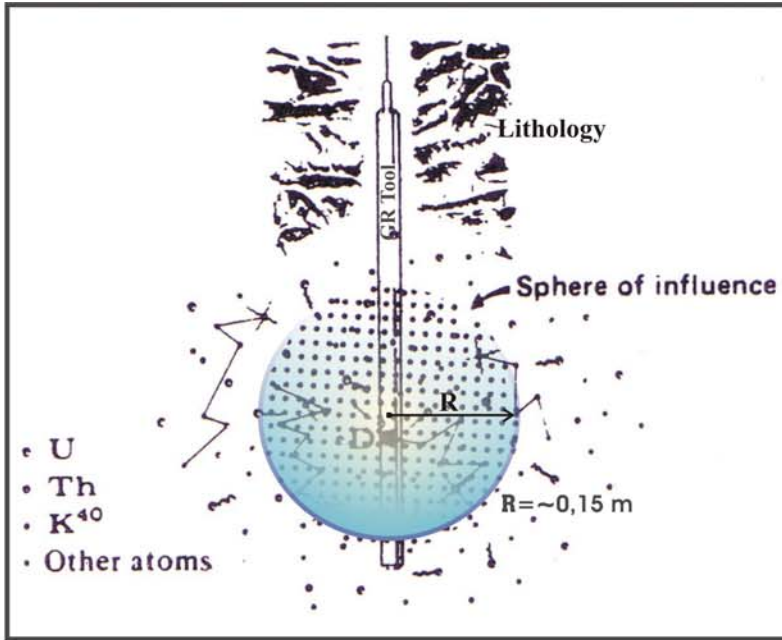
Figure 14. Sphere of investigation of gamma-ray measurements. Gamma rays are emitted in the formation by uranium (U), potassium (K) and thorium (Th). GR tool primarily records radioactivity from the first 15 cm interval (R) (modified from Serra, 1984).
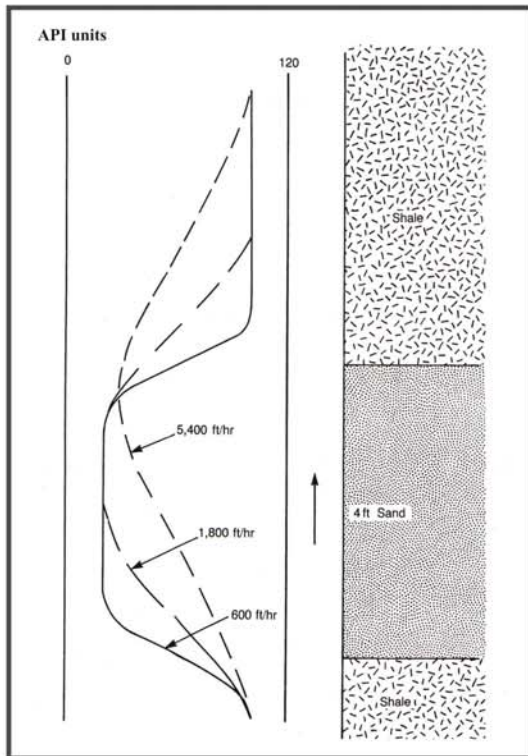
Figure 15. Logging speed of the gamma-ray tool influences the bed resolution (modified from Dewan, 1983).

41

Regarding vertical bed resolution of the GR tool, beds that are thinner than the diameter of the sphere of investigation will not be differentiated. In a succession of thin beds, the log reading will reflect the volume average of the beds within the sphere (Serra, 1984). According to Dewan (1983), the vertical bed resolution can also be affected by the speed with which the GR tool is run up the borehole (Figure 15).

b. Limitations of gamma-ray log and lithology reconstruction

High gamma-ray measurements indicate concentrations of radionuclides (thorium, potassium and uranium) that reflect clay content, but these radionuclides can occur in both clay and non-clay minerals (Serra, 1984; Rider, 1986). Therefore, both clay and non-clay minerals contribute to a high GR log response, e.g., k-feldspar-rich sand, potassium salt, apatite grains. High API measurements do not reflect directly the mean grain size in clastic deposits, e.g., clay pebbles in conglomerates will yield high API measurements (Serra, 1984; Rider, 1986). A layer of conglomerate with a high concentration of clay pebbles is classified as a high energy setting, but the high API measurements that reflect the radioactivity of clay pebbles can induce to the opposite interpretation.

Even though the GR log is used significantly in lithology identification, other lithologies cannot be resolved with the GR log alone. The combination of the GR log with other tools is, therefore, required. For example, high and low ash contents in a coal bed provide high- and low-natural radioactivity readings respectively, and thus coal beds may not be detected by GR log itself (Koczy, 1956; Schmoker and Hester, 1983; Dewan, 1983; Ellis, 1987). The combination, however, of gamma-ray log with neutron-density

logs allows for the interpretation of coal beds with confidence (Dewan, 1983; Rider, 1986). Because coal is a key reference for time boundaries in non-marine deposits, the gamma-ray and neutron-density-log combination is used to identify coal beds.

2. Neutron-Density Log (NPH-DPH)

a. Density log

The density log is used to estimate formation porosity and determine the overall formation density (Shclumberger, 1972; Serra, 1984). Formation density includes the solid matrix and the fluids enclosed in pore spaces.

The basis of the density log consists of gamma-ray bombardments that penetrate the surrounding formation. As gamma rays interact with electrons of the formation, they lose energy and return to the detector. This loss in energy is measured in electron/cm^3, and a low number of gamma rays detected indicates high electron density (the denser the rock, the higher the gamma ray loss). The values of the gamma rays detected are converted directly either to bulk density, or computed to be expressed in percentage. For bulk density, values are measured with an average scale that ranges from 2 to 3 (g/cm^3) where values increase to the right side of the log track. Measurements of the computed values, however, are expressed in percentage and form a density porosity log (DPH). DPH logs are calibrated to some rock type, commonly either quartz sandstone (density of quartz=2.65) or limestone (density of calcite=2.72). The porosity scale runs from -10% on the right to 30% on the left (with 20 divisions), and wraps to go from 30% to 70%. Neutron porosity uses the same scale.

Density logs have various limitations. In infrequent cases, the shape of the borehole will affect the density-log values (Serra, 1984; Rider, 1986). If the borehole is caved, the drilling mud will fill in the cavity, and the density log will record the petrophysical properties of the drilling mud rather than that of the surrounding lithology. The caliper log is often run with the gamma-ray log and can be used to determine if the borehole has caved and if abnormal density values need to be corrected.

b. Neutron porosity log

The neutron porosity log (NPH) is used primarily to determine the formation porosity by combining the neutron log with other tools, such as the density log. It is an excellent discriminator between oil and gas and can be used to determine lithology and fluid type (Schlumberger, 1972; Serra, 1984).

NPH tools emit neutrons into the formation, which lose energy as they collide with hydrogen atoms in the rocks around the borehole. Hydrogen atoms drastically decrease neutron energy levels because hydrogen nuclei and neutrons have a similar mass. Attenuation of neutron energy, therefore, is tightly related to the amount of hydrogen in the formation. The more abundant the hydrogen nuclei are in the formation, the faster the neutrons are absorbed. Consequently, the intensity of the neutron log response is proportional to the porosity of the rock, other things being equal. As hydrogen amounts vary with fluid types that are present in pore space, neutron readings will reflect direct measurement of the fluid in the pore space. Hydrogen is primarily present in water, oil and coal, and so high values of neutron porosity are recorded with these substances. Gas-bearing formations, however, contain less hydrogen in comparison

to oil and water, and so very low neutron porosity values occurred with gas (Dewan, 1983; Serra, 1984). Clay and other hydrogen minerals, also offer the neutron reading, appearing as anomalously high porosity. The NPH log is scaled in percentages, and it is usually recorded with the same scale and in the same well log track as DPH log.

c. NPH-DPH log versus lithology

The use of NPH-DPH log separation in lithologic interpretations is displayed in Figure 16. The figure summarizes the fundamental ideas that explain the general effect of lithology on both pore spaces and rock density, which in turn affects the neutron-density log responses. The interpretations in Figure 16 are simplified and exclude any realistic drilling complications, such as caving or chemical and physical properties of the drilling fluid (mud) that both may influence log responses.

Interpretation of NPH-DPH logs in siliciclastic sediments is complicated. The NPH log is sensitive to the hydrogen index of water in pore spaces, so it is sensitive to both free water and bound water which are primarily present in clays. The DPH log, however, is a function of the solid-matrix density of the formation (grain framework) and reflects mineralogy and intragranular water content.

An example of how mineralogy influences the DPH log response is observed when pyrite or chamosite are intercolated with coal. Coal is rich in light-weight organic matter, while pyrite and chamosite are much more dense. Pyrite and chamosite may contain high concentrations of iron and nickel, which are heavy metals. The greater the heavy metal content in chamosite, the denser the coal becomes (Dewan, 1983; Serra, 1984; Rider, 1986). As the coal density increases (g/cm^3), the DPH log measurements

(%) decrease (D of Figure 16). The DPH log response is also influenced by intragranular water content. Compacted shale beds contain less water and are more dense than under-compacted shale beds; the DPH log indicates lower apparent porosity readings with increasing shale compaction, relative to the NPH log (B_1 of Figure 16).

In compacted shale beds, the NPH log response records a relatively high hydrogen index because of the shale mineralogy and the high shale porosity (Dewan, 1983; Rider, 1986; Tuckers, 2001). Under-compacted shale beds are much less dense because the water content drastically "dilutes" the weight of the solid matrix in shale. The solid matrix of shale is composed of clay and silt-sized quartz, feldspars, and heavy minerals. Both the sand/shale ratio and distribution mode of shale within sand have an effect on both hydrogen index (NPH log) and bulk density (DPH log) (F, E, and C of Figure 16).

Unusual or complicated NPH-DPH log patterns are difficult to interpret. For example, the overall linear relationship of NPH-DPH log separations (C), when both curves increase and decrease together, is probably related to a steady and a gradual substitution of sand with shale laminae or vice versa (Rider, 1986). It is difficult to provide a detailed lithologic interpretation to this phenomenon because of the different depositional processes that deposit clay laminae in sediments (Rider, 1986). Clay laminae within sandstone are caused by different physical processes such as bioturbations (Dewan, 1983), slumps, and current fluctuations (flaser bedding, mud drapes). Therefore, one cannot tie the NPH-DPH log-separation pattern to specific environments, such as bay-head deltas, overbank deposits, tidal channel, and mouth bars.
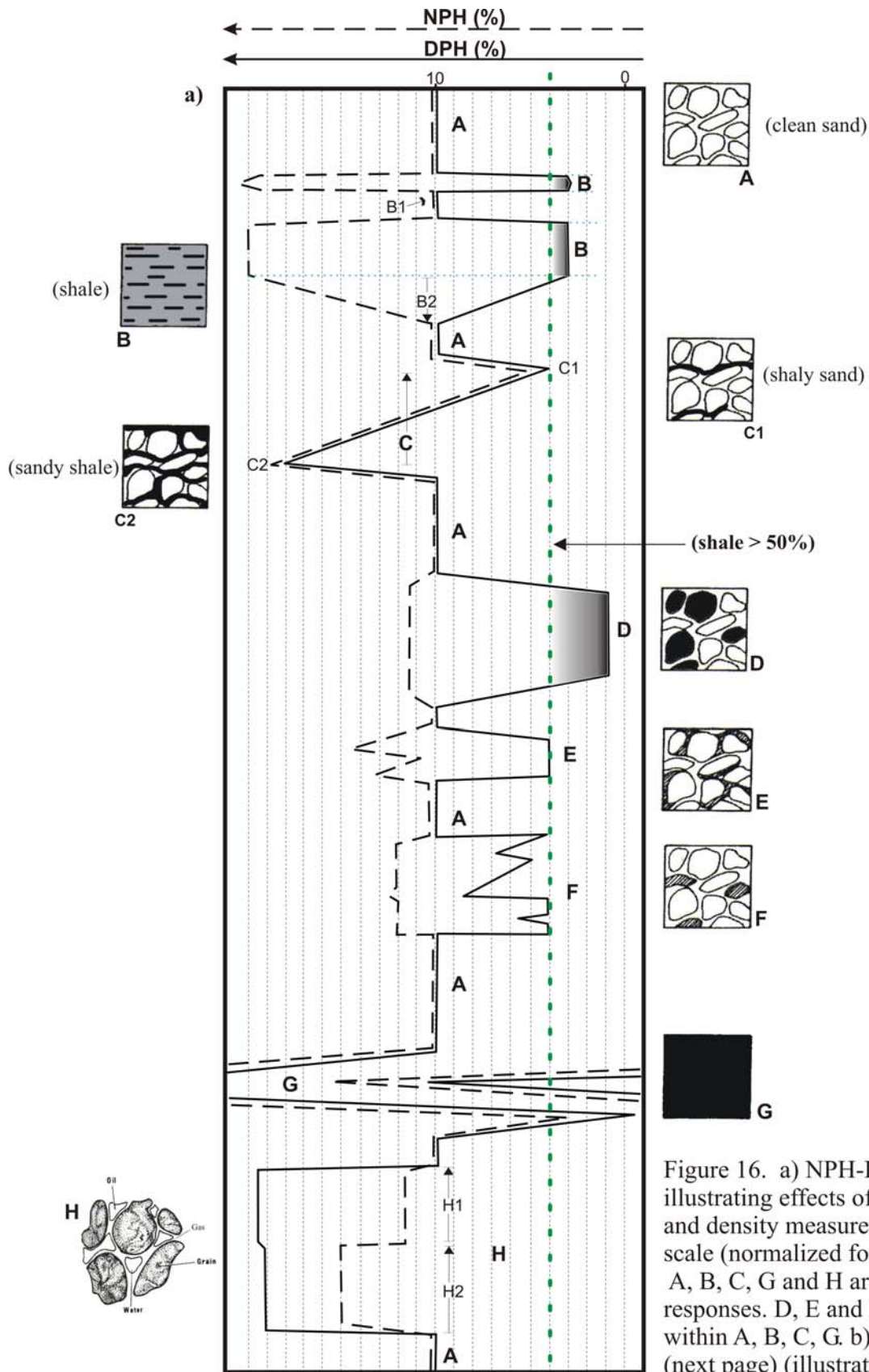
Figure 16. a) NPH-DPH log response chart illustrating effects of lithology on both neutron and density measurements for compatible sand scale (normalized for sandstone, porosity=10%). A, B, C, G and H are meter-scale log responses. D, E and F effects are of general occurence within A, B, C, G. b) Interpretation of log responses (next page) (illustrated based on published data of Serra, 1984; Dewan; 1983; Rider,1986).

Figure 16 continued.

A: PURE SAND (porosity=10%)
-NPH and DPH log curves merge and show intermediate values, ie., plot near the center of the log (Serra, 1984; Rider, 1986).

B: PURE SHALE
-In interbeded silt and shale (phyllosilicates) intervals (>1cm), the DPH log plots to the right of NPH log response, the degree of separation depends on the amount of shale present and the degree of compaction (Schlumberger, 1972; Doveton, 1994).
-The greater the shale or clay content, the greater the curve separation.
B.1-Sudden change from pure sand below to pure shale above; Simultaneous curve divergence
B.2-Gradual change from pure sand below to pure shale:
-NPH curve deflects upward to the left.
-DPH curve deflects upward to the right, and reaches a minimum value and remains stable when the overall shale amount exceeds 50% in the formation (Rider, 1986)

C: SAND WITH SHALE LAMINAE
-Shale laminae include all clays and phyllosilicates that are not altered from a framework grain.
-Laminae are defined here to include layers with burrows, slumps, flaser and wavy beds (Dewan, 1983).
-In sandstone with shale laminae (<1cm), DPH log plots to the right of, juxtaposed with NPH log response. Both curves move together in linear mode (Dewan, 1983; Rider, 1986):
C1-High sand /shale ratio, both curves exhibit low values
C2-Low sand /shale ratio, both curves exhibit high values

D: SAND WITH GRAINS OF HEAVY MINERALS
-DPH log values are at a minimum, and NPH log values plots to the left of DPH curve (Schlumberger, 1972; Rider, 1986)

E: SAND WITH CLAY CEMENT
(pore lining, filling, or bridging)
-DPH log plots right of NPH log response
-NPH log values are highly variable relative to DPH log values depending on clay type present in pore space (Serra, 1984; Dewan, 1983)
-No linear relationship between both curves
-NPH log response is more sensitive to the clay cement than DPH log response

F: SAND WITH CLAY GRAINS
- DPH log plots to the right of the NPH log response but with variable values relative to NPH log response
- No linear relationship between both curves:
- DPH log response is more sensitive to clay grains than NPH log response

G: COAL
-Generally, DPH log almost merges with the NPH log response, exhibiting abnormally high values (Serra, 1984; Dewan, 1983). Unless gas is present in the coal, both logs responses are juxtaposed.

H: SAND WITH HYDROCARBON
- DPH log plots to the left of the NPH log response
-Curve separation is more pronounced in gas-bearing interval (**H1**) than in oil-bearing intervals (**H2**) (Schlumberger, 1972). Both logs have high values of porosity.

An attempt to interpret the distinctive NPH-DPH log separations (C), however, is analyzed in the discussion chapter. Where the NPH-DPH well logs are unavailable, the resistivity well-logs are used to complete the lithologic interpretation.

II. Description

The analysis of GR well logs is used to identify numerous trends throughout the study area. Description of well-log responses is structured by using an electrofacies model that is modified from the classification of Cant (1992) and of Rider (1986), and refined using thickness, GR log variation, and NPH-DPH log separation when it is necessary. Seven different electrofacies types are described as follows.

1. Electrofacies 1

a. Description

This electrofacies is often found concentrated in the upper hundred feet of the Rollins Sandstone Member and the upper part of the Cozzette Sandstone Member. It is a funnel- to a cylinder-shaped pattern. Curve characteristics on GR log ranges from smooth to slightly serrated. The upper contact is usually sharp, whereas the lower contact ranges from sharp to gradational or rounded. The vertical scale of this log shape ranges from about 15 to 30 m. Throughout the study area, the average API values oscillate between 40 to 60 API with a minimum API of 30 and maximum API of 80. The NPH-DPH curve separation, however, progressively decreases upward. At the base, the two curves are widely separated (B1), but at the top, both curves converge to the center of the log track (A). Both curves are strongly to moderately serrated.

ELECTROFACIES TYPE	LOG CURVE SHAPE AND CHARACTERISTICS				PREVAILING LITHOLOGY	ANALOGY ELECTROFACIES VS OUTCROPS
	Gamma Ray or SP	Neutron-Density log (NPH-DPH curve separations)	Bulk density log	Resistivity (Ohm)		
Electrofacies 1 PAVLAKIS#1-5 RR	• Funnel- to cylindrical pattern • Smooth to slightly serrated • Upper contact is usually sharp. • Lower contact is sharp, gradational or rounded. • 50-100 feet (15-30 m) • 40-60 API (*30-80 API*)	• Progressively decreases upward. • Both curves are strongly to moderately serrated	*SULFUR GULCH#9-98-23#1* • Progressively increases downward	*HORSESHOE CANYON #1-21* • No trend	• Sand	• Analogous to the upper sandy part of outcrop unit 2 (wave-dominated shoreface).
Electrofacies 2 WINTER FLAT#1-10-100	• Cylindrical pattern • Smooth to slightly serrated • Upper and lower contacts are sharp • 20-35 feet (6-10,5 m) • 45-60 API (*40-75*) *API.*	• No specific trend pattern of curve separation: -decreases upward -small and stable -increases upward -cross-over (negative separation) • Both curves are strongly to moderately serrated	*not available*	*HORSESHOE CANYON #1-21* • Progressively decreases upward, the high values at the base are caused by the oil/gas effect (logs of NPH and DPH cross-over in the adjacent well)	• Sand	• Analogous to subunit 3 of outcrop unit1 (channel-fill succession).

Figure 17. Log characteristics and shapes are summarized for electrofacies 1 and 2.

This electrofacies is the thickest and the most laterally extensive electrofacies for the Rollins Sandstone Member. This electrofacies occurs in the extreme basinward expression and the lowermost part of the Cozzette Sandstone Member.

b. Interpretation

Log shape and lithology reconstruction

The funnel-shaped pattern of GR indicates an overall upward-coarsening trend in grain size from mud rich at the base to sand rich at the top. The same observation in lithology reconstruction is also identified from NPH-DPH curve separation. The upward and progressive convergence of NPH-DPH curves indicates an overall increase in sand/mud ratio with an overall change from predominantly shale at the bottom to mainly sand at the top. The strong serration or the repetitive small curve separation of NPH-DPH at the top is a pattern that can be explained by small variations in matrix mineralogy. This pattern can be explained by the mix of clean sand with negligible amounts of shale (phyllosilicate), feldspars or heavy minerals (Serra, 1984; Rider, 1986).

Depositional environment

Based on the GR models of Rider (1986) and Cant (1992), thick, upward-coarsening trends identified from the GR log are interpreted to be progradational units of marine strata. This electrofacies is analogous to the proximal expression of wave-dominated shoreface succession in the outcrop (upper sandy part of outcrop unit 2).

2. Electrofacies 2

a. Description

The GR log response of this electrofacies type is identified throughout the study area. It occurs throughout the Cozzette Sandstone Member (Figure 17). It is typically a cylindrical pattern. Curve characteristics on GR logs range from smooth to slightly serrated with sharp upper and lower contacts. The vertical scale of this electrofacies varies from 6 to 10.5 m. Throughout the study area, the average API values range from 45 to 60 API with a minimum API of 40 and a maximum API of 75. The trend of NPH-DPH curve separation is more variable. It ranges from constant (A), progressively converging, or increasing upward (B2), and locally the curves cross over each other (H), as shown in Figure 16. Both NPH and DPH log curves are strong to moderately serrated.

b. Interpretation

Log shape and lithology reconstruction

The slightly serrated cylindrical pattern of the GR log indicates a mainly sand-rich interval with minor shale (phyllosilicate) content. The varying shale content causes curve serration, but not significant to cause an upward-fining or coarsening trend in grain size. The phyllosilicates (sheet silicates which include clay minerals and micas) are either sporadically dispersed throughout the interval or form thin intervals of shale that are below GR log resolution.

The variability in NPH-DPH curve separation signifies variation in both hydrogen nuclei and bulk density of a formation, and consequently a variation in the

sand/phyllosilicate ratio; curves converge as, sand increases and diverge as phyllosilicates increase.

NPH-DPH log curves that generally exhibit a constant low separation may reflect relatively clean sandstone with the presence of shale or feldspars. Finally, DPH log curves that cross over NPH log curve indicate extremely low bulk formation density, so that the DPH log reads higher values of porosity than NPH log. Low values of the NPH log are due to low hydrogen content within intervals that enclose oil or gas, rather than water. This last log separation pattern is, therefore, the typical response of oil/gas effect which points to primarily clean sandstone with negligible amounts of shale (phyllosilicates) dispersed in an unpredictable manner. The different curve separations of NPH-DPH logs that reflect unpredictable distributions of shale or mud within electrofacies 2 may be attributed to a lateral facies change in the depositional setting. The negative separation of NPH-DPH curves, however, often indicates clean sandstone with good ability to store hydrocarbons.

Depositional environment

Based on the GR trend models of Rider (1986) and Cant (1992), this electrofacies type may represent an overall high energy channelized succession. The presence of variable clay or micas content can reflect energy fluctuation within principally high energy settings forming, for example, mud drapes in sand-rich channel successions. The sharp basal contact of GR log indicates an abrupt vertical change in lithology from coarser grains above the contact limit to finer grains below it, and may be interpreted as

an erosive surface. Combined with the outcrop study, this electrofacies may be interpreted as sand-rich channel successions, analogous to subunit 3 of outcrop unit 1.

3. Electrofacies 3

a. Description

Electrofacies 3 is an irregular pattern, with a tendency toward a gradational funnel trend, and is slightly serrated (Figure 18). The upper contact is sharp to gradational, and the lower contact is usually gradational to rarely sharp. The vertical thickness of this electrofacies ranges from about 9 to 75 m, and its average GR values are higher than those of electrofacies 1. The average API values of electrofacies 3 range from about 95 to 130 API with a minimum API of 80 and a maximum API of 150. NPH-DPH curve separation generally decreases upward (B2 of Figure 16), and both curves are slightly to moderately serrated. The DPH log often exhibits a steady trend with a very slight decrease in values towards the top. The NPH log, however, exhibits a gradational upward decrease in values. The GR log response of this electrofacies is generally identified in the lower part of both Cozzette and Rollins Sandstone members, particularly in the extreme eastern part of the Piceance basin.

b. Interpretation

Log shape and lithology reconstruction

High GR values combined with irregular-shaped pattern with funnel-shaped tendency indicates a slight decrease in clay or micas content toward the top.

54

| ELECTROFACIES TYPE | LOG CURVE SHAPE AND CHARACTERISTICS | | | | PREVAILING LITHOLOGY | ANALOGY ELECTROFACIES VS OUTCROPS |
	Gamma Ray or SP	Neutron-Density log (NPH-DPH curve separation)	Bulk density log	Resistivity (Ohm)		
Electrofacies 3 GR (API) 0—200 DPH (%) NPH (%) NICHOLS#3-7	• Irregular pattern with tendency to a gradational funnel-trend • Slightly serrated • Upper contact is sharp to gradational • Lower contact is usually gradational to rarely sharp. • 30-250 feet (9-75 m) • 95-130 API (80-150 API)	• Decreases upward: -DPH log is often steady trend with very slight decreases in values toward the top. -NPH log decrease gradationally in values toward the top.. • Both curves are slightly to moderately serrated	*not available*	 GR (API) 0—200 R (Ohm) 0—1000 HORSESHOE CANYON #1-21 • Progressively increases upward	Mud-rich	• Analogous to the offshore transition of outcrop unit 2.
Electrofacies 4 PAVLAKIS#1-5 RR	• Irregular pattern • Smooth to moderately serrated • Upper contact is sharp to gradational • Lower contact is usually sharp • 20-85 feet (6-25 m) • 90-100 API (80-200 API)	• Widely separated: -NPH curve is irregular to no-trend pattern -DPH curve is irregular-to stable trend • Both curves are strong to moderately serrated	 GR (API) 0—450 Bulk Density 2 (gm/cc) 3 SULFUR GULCH#9-98-23#1 • Irregular pattern	*not available*	• Mud-rich	• Analogous to the lowest interval of outcrop unit 2 (offshore; part of the Mancos shale).

Figure 18. Log characteristics and shapes are summarized for electrofacies 3 and 4.

The overall upward convergence of the NPH-DPH curve separation and the decreasing GR reading indicate a slight upward increase in sand content. The decrease of NPH log values toward the top indicates a gradational increase of sand at the expense of clay. The overall steady density porosity values (DPH log), however, may indicate a thick compacted shale interval. With high rate of compaction, free water is exuded from shale intervals, and dehydrated shale may form. Dehydrated shale is composed mainly of clay and silt-sized quartz, feldspars, heavy minerals, and dehydrated organic matter, which without free-water content; such shale beds may become as dense as quartz or more dense. The very slight decrease in porosity density (DPH) values toward the top may be interpreted to indicate clean and porous sandstone layers.

Depositional environment

Gamma-ray trend models of Rider (1986) and Cant (1992) suggest that this electrofacies indicates a progradational succession. The combination of a slight funnel-shaped pattern with high GR values indicates distal low-energy settings of progradational unit. Outcrop study suggests that this electrofacies is analogous to the distal mud to silt-rich deposits that interfinger with sandy intervals of the wave-dominated shoreface. This electrofacies is interpreted to be the offshore transition succession similar to that of outcrop unit 2.

4. Electrofacies 4

a. Description

The GR log presents an irregular pattern with no vertical trend, yet smooth to moderately serrated. The upper contact is sharp to gradational, and the lower contact is usually sharp (Figure 18). The average vertical scale of this electrofacies ranges from 6 to 25 m. GR values vary from 90 to 100 API with minimum and maximum API of 80-200, respectively. NPH-DPH curves are widely separated, and both curves are strong to moderately serrated. The NPH curve displays an irregular to trendless pattern and is slightly disrupted toward the top where NPH values tend to fluctuate. The DPH log, however, displays irregular to stable patterns with no major change in values. This electrofacies is concentrated basinward.

b. Interpretation

Log shape and lithology reconstruction

The irregular pattern of the GR log associated with high API values and with no specific trend indicates prominently clay-rich interval with a consistently low content of silt or sand. The wide curve separation of NPH-DPH logs reflects essentially clay-rich composition of the electrofacies. The disruption in NPH log values implies sporadic additions of sand grains. The stability of the DPH log indicates that the sporadic sand inputs, recorded by NPH log, are of negligible amounts.

Depositional environment

The GR trend models of Rider (1986) and Cant (1992) suggests that the steady, high GR values with an irregular pattern indicate interbedded mudstone and siltstone to predominantly mudstone lithology. This indicates very low-energy depositional settings. Electrofacies 4 may be attributed to pro-delta or offshore settings. Outcrop study indicates that this electrofacies is analogous to an offshore mudstone similar to the lowest interval of outcrop unit 2 and may be part of the Mancos Shale, which was not studied in the outcrop.

5. Electrofacies 5

a. Description

This electrofacies is concentrated mainly in the middle part of the study interval. The GR log response is a funnel-shaped pattern, but substantially thinner than electrofacies 1 with a vertical thickness of 6 to 10.5 m (Figure 19). It is smooth to slightly serrated. The upper and lower contacts vary from sharp to gradational. The GR values throughout the study area vary from ~120 API at the base to ~50 API at the top. Both NPH and DPH curves are strongly serrated, and they track each other simultaneously (C).
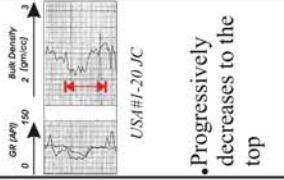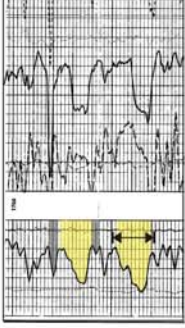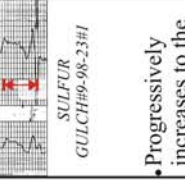
ELECTROFACIES TYPE	LOG CURVE SHAPE AND CHARACTERISTICS				PREVAILING LITHOLOGY	ANALOGY ELECTROFACIES VS OUTCROPS
GR (API) 0 – 200 / DPH (%) / NPH (%)	Gamma Ray or SP	Neutron-Density log (NPH-DPH curve separations)	Bulk density log	Resistivity (Ohm)		
Electrofacies 5 **WINTER FLAT#1-10-99**	• Thin funnel pattern • Smooth to slightly serrated • Lower and upper contacts vary from sharp to gradational • 20-35 feet (6-10,5 m) • 50-120 API	• Deflect simultaneously • Strongly serrated	*USA#1-20 JC* • Progressively decreases to the top	*not available*	• Sand and mud.	• Analogous to subunit 2 of outcrop unit1 (distal bay fill deltas)
Electrofacies 6 **SULFUR GULCH#9-98-2**	• Bell pattern • Smooth to slightly serrated • Lower and upper contacts are usually sharp • 5-20 feet (1,5-6 m) • 50-100 API	• Variable: - Gradual and simultaneous deflection with wide separation at either the top or the bottom. - Thin and sharp simultaneous deflection • Strongly serrated	*SULFUR GULCH#9-98-23#1* • Progressively increases to the top	*not available*	• Sand, mud, and coal	• Analogus to uppermost part of subunit 1of outcrop unit 1 (overbank deposit in peat swamp)

Figure 19. Log characteristics and shapes are summarized for electrofacies 5 and 6.

59

b. Interpretation

Log shape and lithology reconstruction

The small vertical scale of this electrofacies coupled with the funnel-shaped pattern of GR indicates small upward-coarsening trends in grain size. The overall trend pattern of NPH-DPH curve separation indicates either a simultaneous increase or decrease in both bulk density and hydrogen index. The NPH-DPH pattern may reflect a steady upward replacement of shale laminae with sandstone or vice versa, without affecting the overall upward-coarsening trend (Schlumberger, 1972; Dewan, 1983; Rider, 1986).

Depositional environment

Based on GR trend models of Rider (1986) and Cant (1992), thin funnel- shaped patterns indicate small progradational units with an upward increase in energy. Based on outcrop study, this electrofacies is lithologically analogous to either subunit 1 (distal bay-fill delta), subunit 2 (bay-fill delta), which exhibit a progradational character, or to the entire succession of outcrop unit 1 which exhibits a slight upward increase in grain size.

6. Electrofacies 6

a. Description

This electrofacies is encountered mainly in the center and the extreme western part of the study area. The GR log response of this electrofacies is a bell-shaped pattern. Curve characteristics range from smooth to slightly serrated, and the lower and upper contacts are usually sharp (Figure 19). The vertical scale reaches up to 6 m, and the GR

values recorded throughout the study area varies from 50 to 60 at the base to 100 API near the top.

NPH-DPH curve patterns are variable exhibiting log-separation pattern B, C and G (Figure 16). In some cases, DPH log values are low relative to NPH log values. Both NPH and DPH logs range from smooth to strongly serrated.

b. Interpretation

Log shape and lithology reconstruction

The bell-shaped pattern of the GR is an upward fining trend that indicates an upward decrease in grain size. The variable nature of NPH and DPH log separation (B and C) indicates the presence of a relatively small shale content with an overall upward increase in shale throughout the succession, and which is in agreement with the GR bell-shaped pattern. The presence of log pattern G, however, indicates coal at the top of the succession. In this case, the DPH log records low values while NPH log exhibits abnormally high values. This can be interpreted to be coal layers mixed with sand/shale input. Because coal is less dense than both shale and sand, a small amount of shale or sandstone will increase the overall density matrix of coal interval, and result in a relative decrease of DPH log values.

Depositional environment

The GR trend models of Rider (1986) and Cant (1992) suggest that the bell-shaped pattern indicates a gradational upward decrease of energy, characteristic of low-energy channel systems. Fluvial interpretation based upon log pattern and association with coal.

The sharp base of this electrofacies may be interpreted as an erosive surface with an abrupt vertical change in lithology. The NPH-DPH log pattern G that is located toward the top of this electrofacies is interpreted to indicate coal. Coal is often associated with overbank deposits, bogs and marshes. The vertical variability of clay, displayed by NPH-DPH log separation, is consistent with the low-energy depositional setting of the sinuous fluvial systems. Outcrop study suggests that the uppermost part of this electrofacies is analogous to the uppermost part of subunit 1 of outcrop unit 1, where a coal bed with silt partings indicates sporadic deposition of fine-grained sediment within a low-lying, protected area (overbank deposit in swamps). It may also be attributed to subunit 3 of outcrop unit 1, where a slight gradational decrease in grain size characterizes the channel-fill succession.

7. Electrofacies 7

a. Description

This electrofacies is generally identified in the western part of the study area. The GR log response is an irregular pattern with high fluctuations in API values and is strongly serrated (API values fluctuate up to 4 times within an interval of 3 m). The lower and upper contacts are usually sharp (Figure 20). The vertical scale of this electrofacies ranges from 3 to 15 m, and the API values range from 30 to 160 API.

NPH-DPH curve-separation is wide and the curves deflect simultaneously (C of Figure 17). In some cases, NPH values are abnormally high. Generally, both NPH and DPH logs are strongly serrated and present a sudden and rapid fluctuation in NPH and DPH log values in synchronization with the GR log values.
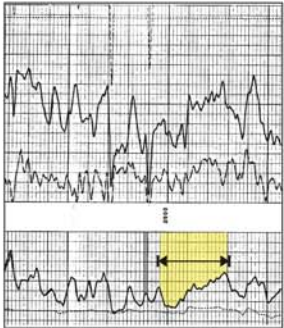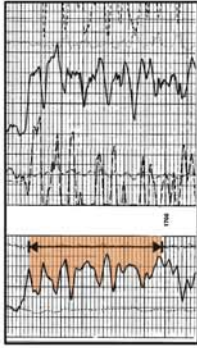
ELECTROFACIES TYPE	LOG CURVE SHAPE AND CHARCATERISTICS				PREVAILING LITHOLOGY	ANALOGY ELECTROFACIES VS OUTCROP S
GR [API] 0 — 200 — DPH [%] — NPH [%]	Gamma Ray or SP	Neutron-Density log (NPH-DPH curve separations)	Bulk density log	Resistivity (Ohm)		
Electrofacies 7 SULFUR GULCH#9-98-2	• Irregular pattern • Strongly serrated • Lower and upper contacts are normally sharp • 10-50 feet (3-15 m) • 100-160 API	• Generally wide and deflect simultaneously: -Abnormal high values of NPH log. -Sudden and rapid fluctuation in both curves. • Strongly serrated	• not available	• not available	• Coal, mud, and sand	• Analogous to the uppermost part of subunit 1 of outcrop unit 1(peat swamps with thin channel-fill sand intrusions).

Figure 20. Log characteristics and shapes are summarized for electrofacies 7.

b. Interpretation

Log shape and lithology reconstruction

The irregular pattern of the GR with strong oscillations in API units may indicate abrupt changes in lithology or a heterolithic composition of mudstone, sandstone and coal. The heterolithic composition signifies fluctuation in energy levels within the depositional environment. The repetitive wide and simultaneous curve deflection of NPH-DPH curves may indicate abrupt change in the sand to shale ratio within a primarily mud-rich interval. The rapid deflection of both curves with abnormally high values of NPH may indicate an abnormally high hydrogen index. The abnormally hydrogen index can be explained by the high hydrogen index of coal to which was added the high hydrogen index of shale, for example. The highly serrated feature of NPH-DPH log pattern with no specific trend indicates random episodic flooding events that deposit sandstone layers with probably heavy minerals into areas of low energy, mud-rich settings. Because sand is more dense than shale, and shale contains more hydrogen than sand, the NPH and the DPH logs are strongly influenced by the sand/shale inputs, which results in a rapid deflection of both logs. The overall wide log pattern C, however, indicates an overall cyclicity of energy levels where a gradational increase of sand or shale occurs throughout the depositional succession.

Depositional environment

In GR trend models of Rider (1986) and Cant (1992), a strongly serrated and irregular pattern of GR log response indicates sporadic and heterolithic deposits in either a subaqueous or subaerial depositional environment, such as distal edge of deltas or

crevasse-splay deposits. The high values of the NPH log that indicate the presence of a coal interval likely place this electrofacies in an overbank deposit rather than a distal delta. Based on outcrop study, this electrofacies is analogous to coal beds with sand or silt lenses as interpreted in outcrop unit 1.

III. Continuity of Electrofacies and NPH-DPH Log Input

1. Complications and Continuity of Electrofacies

Curve shapes of some well-log intervals can be easily identified with the defined electrofacies patterns. Some other well-log patterns, however, do not fit in the defined patterns. The indefinable electrofacies patterns may represent a variation of an idealized pattern or a distal signature of the idealized electrofacies (Figure 21). Such electrofacies are not easily interpreted.
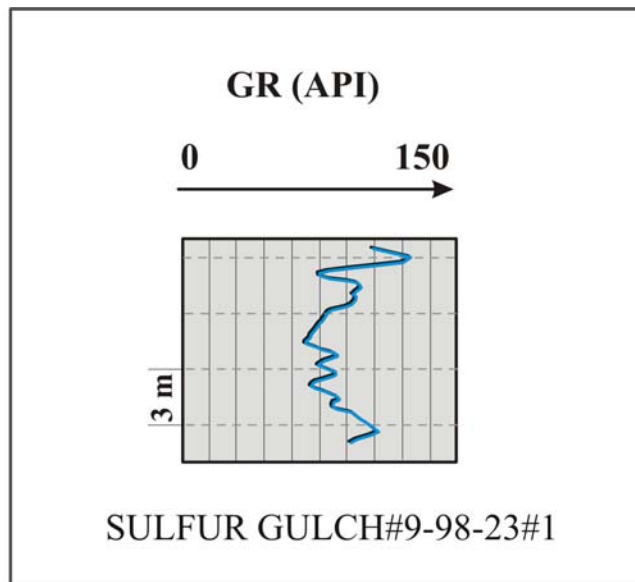
Figure 21. An example of a complicated log-shape pattern that is difficult to interpret. This log-shape pattern is probably a variation of the idealized log pattern of electrofacies 2 or 5.

The lateral continuity of each electrofacies is established through correlation of the well logs. The lateral extent can be used to help refine the depositional setting of each electrofacies type. Generally, electrofacies within continental and marginal-marine settings show abrupt lateral and vertical facies changes. Electrofacies within the marine environments, however, are not characterized by abrupt lateral changes. Marine sands are generally continuous over an area of tens of kilometers (Reinson, 1984). The lateral continuity of each electrofacies type falls into two groupings. The first grouping is composed of electrofacies 2, 5, 6, and 7 (Figures 22 and 23). These electrofacies are classified as non-marine to marginal-marine deposits. Electrofacies 2, 5, 6, and 7 cover a distance that ranges from approximately 5 km to 10 km. The second grouping is represented by electrofacies 1, 3, and 4. These electrofacies are the most laterally continuous over the study area. They are classified as open-marine deposits and cover a distance of more than 90 km (Figures 24 and 25).
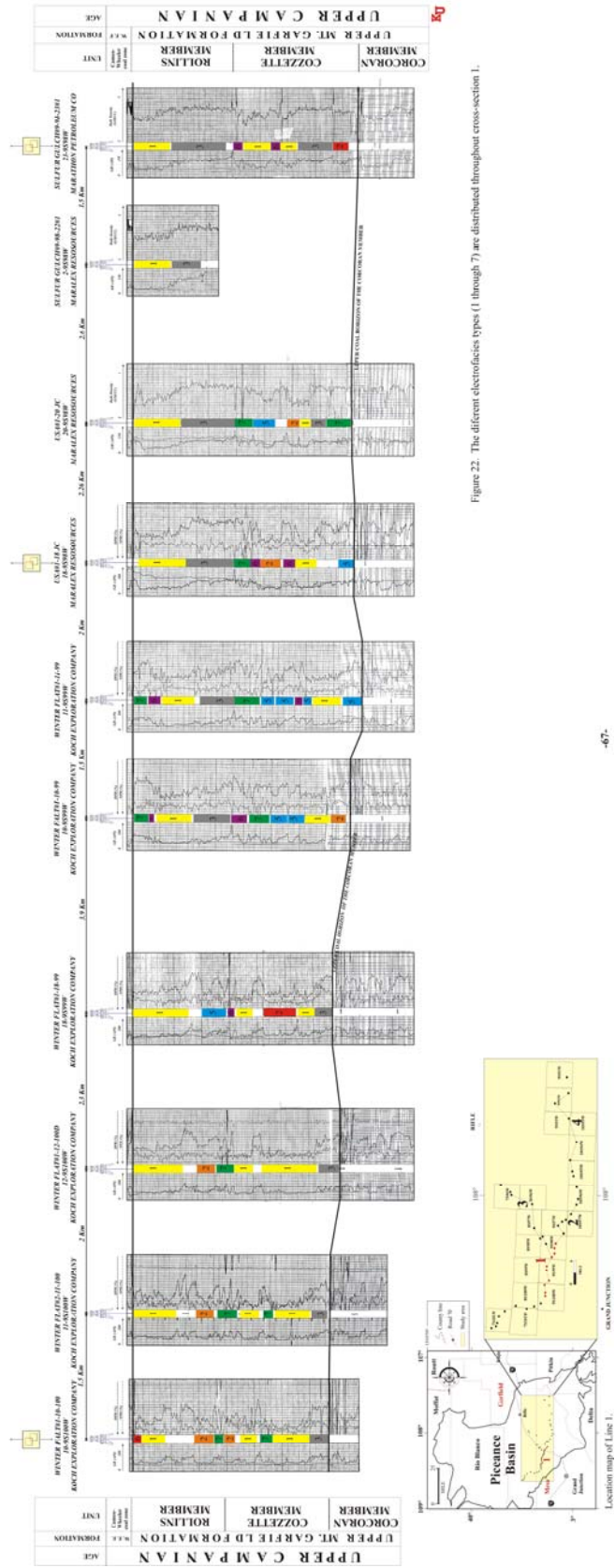
Figure 22. The different electrofacies types are distributed through cross–section 1 (see appendix).
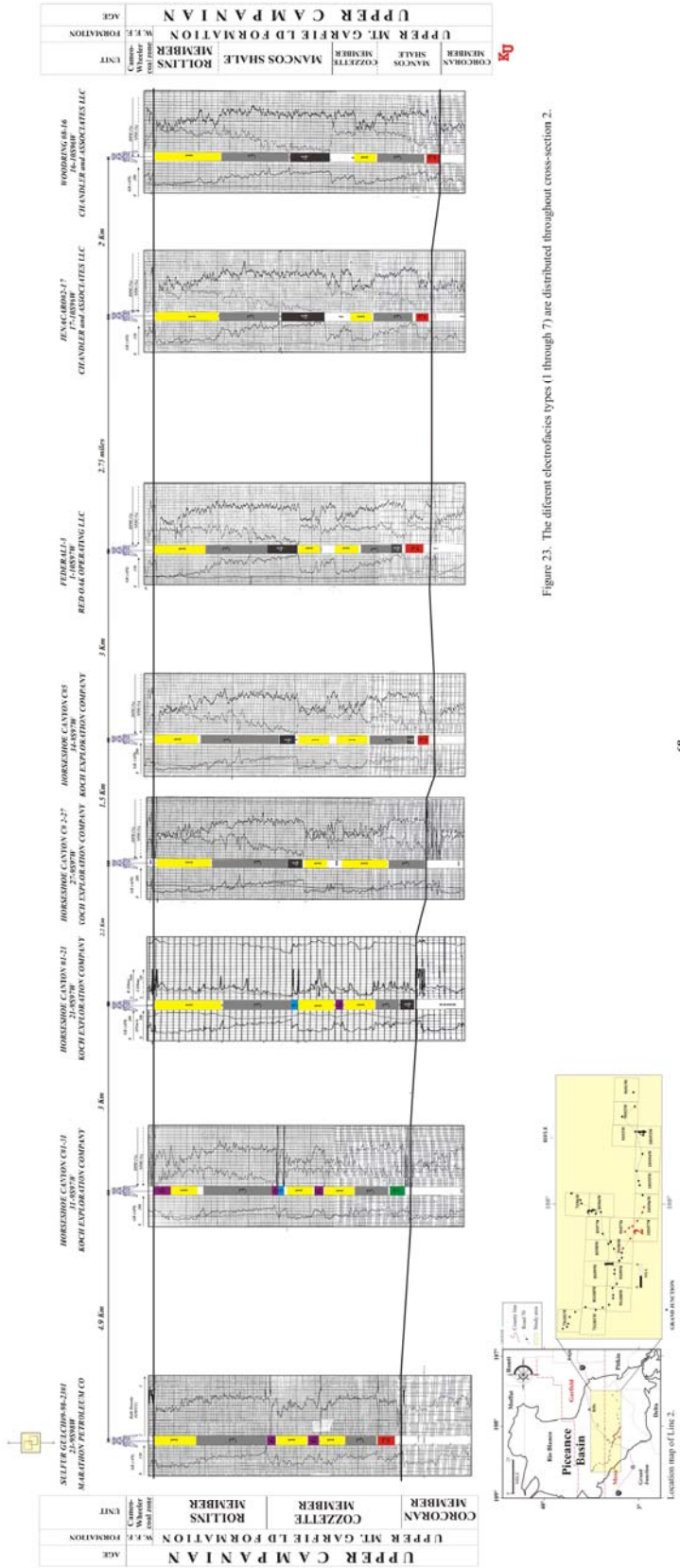
Figure 23. The different electrofacies types are distributed through cross-section2 (see appendix).

68
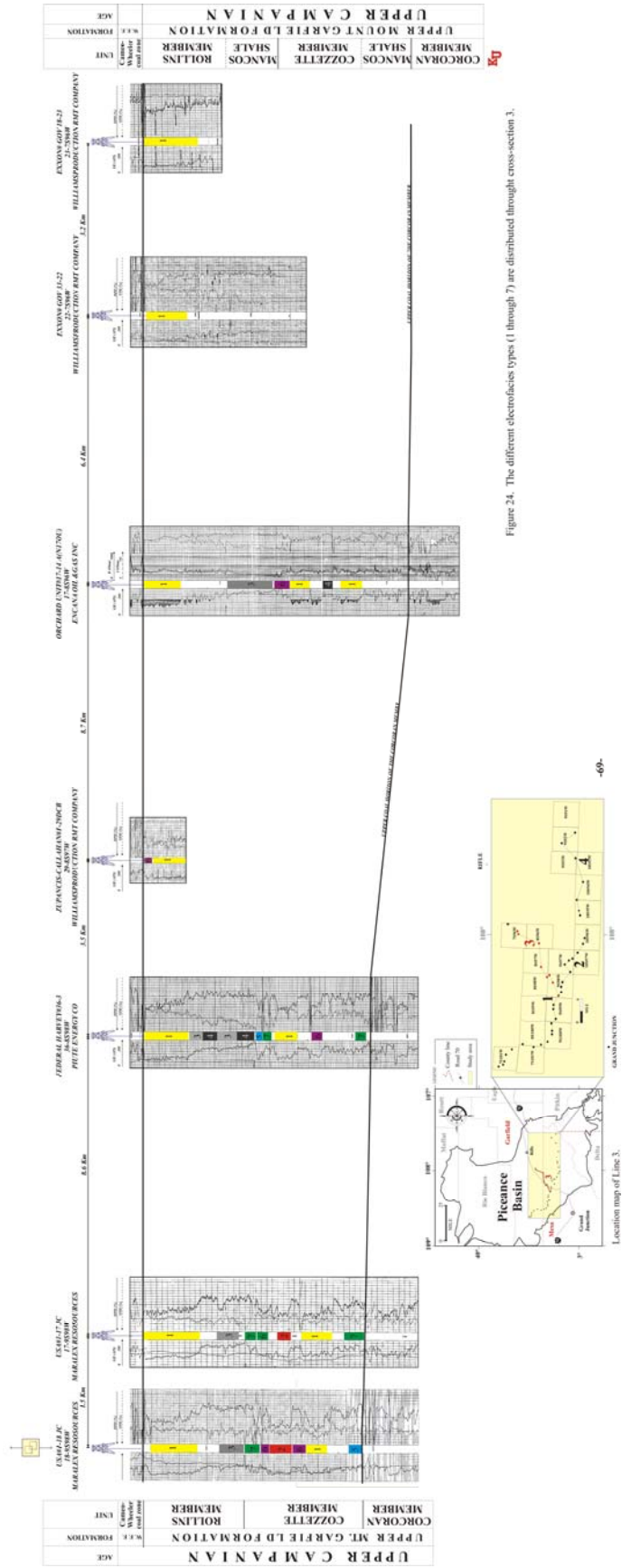
Figure 24. The different electrofacies types are distributed through cross-section 3 (see appendix).

69
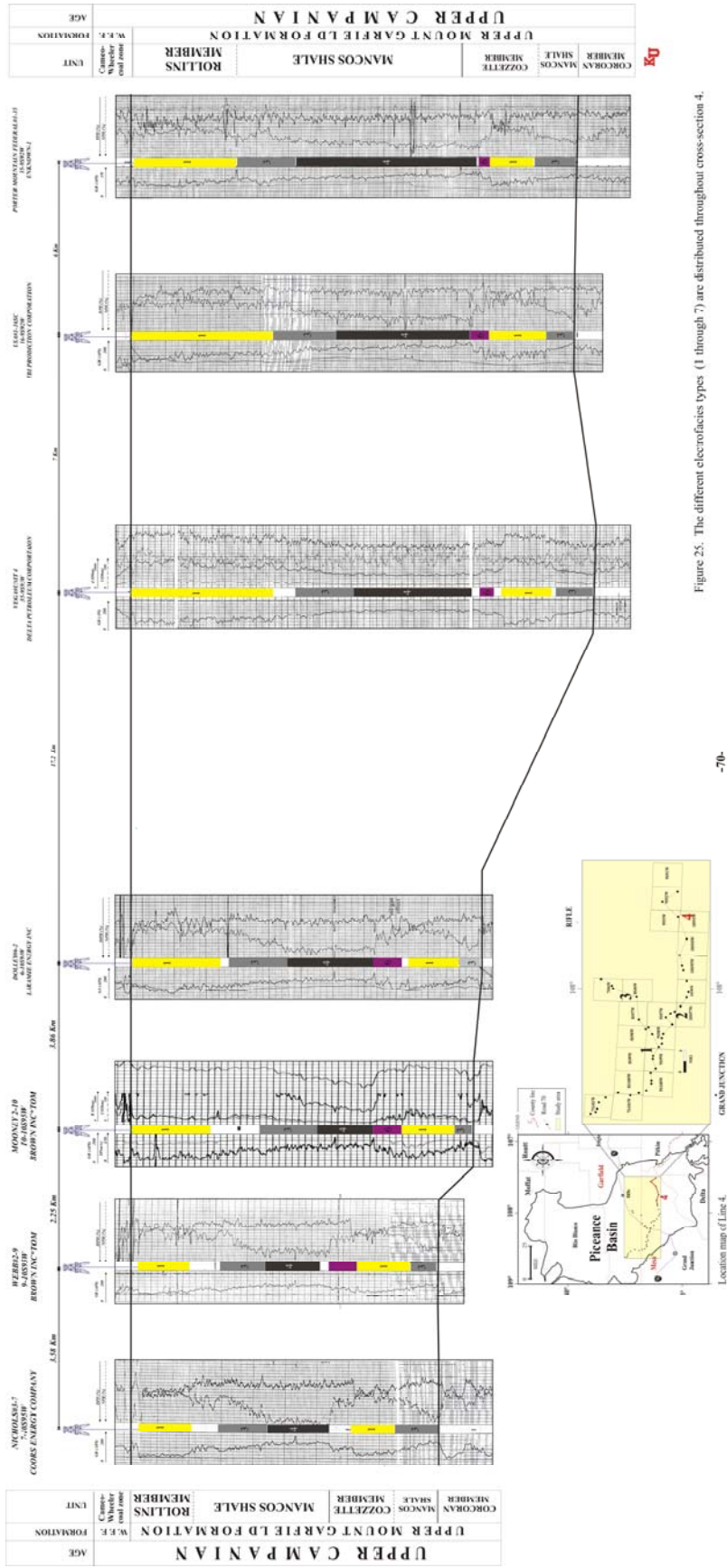
Figure 25. The different electrofacies types are distributed through cross-section 4 (see appendix).

2. NPH-DPH Logs Input

The use of NPH- DPH log separation can help refine facies interpretation that is first established based on the GR log shapes alone. NPH-DPH curve separation is the best indicator of shale distribution and amount, which reflect energy setting in a facies. NPH-DPH log separations of electrofacies 1, 3, and 4 (wave-dominated shoreface successions) are either continually wide or stable. Arbitrary and rapid log deflections, however, are observed in shallow and complicated depositional settings, such as marginal-marine deposits. These observations are typical responses in the study area and may indicate the sensitivity of the NPH-DPH log values to the prevailing energy setting. NPH-DPH logs can also distinguish some key lithologies that may define key surfaces, such as parasequence boundaries (organic-rich shale of a condensed layer or coal horizon).   In conclusion, neutron-density logs combined with GR logs provide an improved tool for interpreting the stratigraphic relationship between electrofacies and depositional environments because the combination respond differently to the various depositional settings.

Chapter IV: SEQUENCE STRATIGRAPHY

I. Introduction and Terminology

The study interval is placed in a sequence-stratigraphic framework to establish a regional stratigraphic relationship of these strata within a time framework. A sequence-stratigraphic interpretation will place the study interval into sequences and systems tracts. The sequence stratigraphic terminology used in this study is based on Van Wagoner et al. (1990).

1. Parasequence

The fundamental stratal unit is a parasequence. A parasequence is defined as "a relatively conformable succession of genetically related beds or bedsets bounded by marine flooding surfaces and their correlative surfaces" (Van Wagoner et al., 1990).

Strata within parasequences have lateral and vertical variability of facies. Within a single parasequence, strata may exhibit a gradual and down-dip transitional facies change from coastal plain to shelf. Parasequences can be traced from the non-marine realm to the marine. The down-dip change in facies within the marine environment, from shallow to deep water strata, is also recognizable in the vertical succession. In shallow marine strata, the vertical succession of a parasequence exhibits an upward shallowing succession that is arranged in an upward-coarsening trend (electrofacies 1 over electrofacies 3). The wave-dominated shoreface of the Rollins Sandstone Member is an upward shallowing succession that reveals a predictable progression from distal to proximal facies deposits. In non-marine realm, however, strata within a parasequence are less predictable (Kamola and Van Wagoner, 1995).

2. Parasequence Set

Parasequences can stack vertically to form parasequence sets. Each parasequence set is characterized by a different stacking pattern that forms under different accommodation rates. A parasequence set is "a succession of genetically related parasequences forming a distinctive stacking pattern bounded by major flooding surfaces and their correlative surfaces (Van Wagoner et al., 1990)." A genetically related set of parasequences exhibits one of three distinctive stacking patterns: progradational, retrogradational, aggradational. These three stacking patterns can represent an ideal response to a single sea-level cycle at a regional scale.

3. Depositional Sequence

A depositional sequence as defined by Vail et al. (1977) is "a stratigraphic unit composed of genetically related strata bounded at its top and base by an unconformities or their correlative surfaces." A depositional sequence can be subdivided into systems tracts based on its stratal geometry (Posamentier et al., 1988; Van Wagoner et al., 1990).

The highstand systems tract (HST) is the youngest stratal pattern within a depositional sequence. Highstand systems tracts consist of progradational or aggradational parasequence sets that are deposited during periods of stillstands in the sea level or during periods of a decreasing rate of a relative rise in the sea level (Vail et al., 1977; Posamentier et al., 1988, 1992; Mitchum et al., 1994). Highstand systems tracts are bounded by a maximum flooding surface at the base and by a sequence boundary at the top.

The transgressive systems tract (TST) is the middle systems tract of a depositional sequence and is older than the highstand systems tract (HST) (Emery and Myers, 1996). The transgressive systems tract consists of a retrogradational parasequence set deposited during the maximum rate of a relative rise in sea level (Vail et al., 1977; Posamentier et al., 1988, 1992). Transgressive systems tracts are bounded by a transgressive surface at the base and by a maximum flooding surface at the top.

The lowstand systems tract (LST) is the oldest system tract in a depositional sequence and may consist of complex depositional sets that are deposited during an early and a late phase of a relative fall in sea level. Both phases are followed by an early relative rise in sea level. Lowstand systems tracts may include the following elements in this order: basin floor fan, lowstand fan, and lowstand wedge, each of which may exhibit a different set of parasequence stacking patterns. The stacking pattern of lowstand systems tracts commonly consists of progradational parasequence sets. Lowstand systems tracts are bounded by a sequence boundary at the base and by a transgressive surface at the top (Van Wagoner et al., 1990).

4. Sequence Boundaries

A sequence boundary (SB) is a significant subaerial-erosional truncation and its correlative conformity that bounds a depositional unit. A sequence boundary is a regional surface of erosion which is often tied to a fall in sea level. This sequence boundary separates younger strata from older strata along a significant hiatal surface. Two criteria used to identify sequence boundaries are a basinward shift in facies, and a regional surface of erosion or abnormal subaerial exposure.

Generally, during a fall in sea level, river systems incise significantly into the underlying strata and form an incised valley. The plains adjacent to the valley are called interfluve areas. In interfluve areas, the sequence boundary is a flat surface and is often expressed by an abnormal subaerial exposure along which a basinward shift in facies occurs. The most common example of basinward shifts in facies is where non-marine deposits (soil horizons, flood plains, or overbank deposits) are placed directly on top of distal marine deposits (Van Wagoner et al., 1990).

The same criteria are used to recognize sequence boundaries in both outcrops and well logs. An abrupt vertical juxtaposition of different electrofacies types that marks a basinward shift in facies is used to recognize sequence boundaries (SB) in well logs. Generally, where a parasequence set with a progradational stacking pattern (HST) is overlain by a parasequence set with a retrogradational stacking pattern (TST), a sequence boundary may separate the two parasequence sets (Van Wagoner et al., 1990). In the study area, a sequence boundary is commonly placed at the base of a blocky sand-rich pattern (channel-fill sandstone of electrofacies 2), if it overlies a highly radioactive irregular pattern (open-marine mudstone of electrofacies 4). In the interfluve areas, a sequence boundary may become hard to recognize.

5. Incised-Valley Fills

Incised valleys are "…valleys formed by fluvial systems that extend their channels basinward and erode into underlying strata in response to a relative fall in sea level (Van Wagoner, 1995)." An incised valley is a local erosional event, initiated at a lowstand of base level and fills as the rate of the relative fall in sea level decreases or as the base level begins to rise (Posamentier and Allen, 1993a; Blum, 1993). Incised valleys

range in width from less than one kilometer to tens of kilometers (Van Wagoner et al., 1990).

During the relative fall in sea level that may expose steeper shelf gradient, erosion by river systems and sediment bypass must occur in order to adjust the river profile to the lower base level, thus approaching the equilibrium fluvial profile (Van Wagoner et al, 1990). The rate of fluvial incision within an incised valley depends on the previous fluvial gradient and the lowest base-level position on the shelf. Therefore, as the sea level falls, rivers incise, and sediment is carried downstream and deposited basinward as a lowstand deposit.

During the subsequent rise in sea level, variable and complex vertical successions of depositional environments are deposited within the incised valley. The most common vertical succession consists of fluvial deposits of either braided or meandering rivers, overlain by deposits with progressively more marine influence (Van Wagoner et al, 1990).

In the extreme landward extent of incised valleys, the valley fill is dominantly fluvial and characterized by vertically coalesced or nested channels. From the base to the top, fluvial deposits show a typical evolution in response to the relative rise in base level, transitioning from a higher gradient fluvial system at the base to a lower gradient fluvial system at the top. Toward the top, sediment fill ideally is a mixture of high-sinuosity fluvial systems and floodplain deposits.

In the extreme seaward extent of incised valleys, the basal fill is either fluvial or tidal, but the remaining fill is often dominated by marine to marginal marine strata. Marginal marine environments are complex by nature, and many sub-environments and

internal surfaces of erosion are observed within the valley fills (Dalrymple et al., 1992; Blum, 1993). Furthermore, additional complexity can occur if a significant surface of erosion, associated with a marine transgression, removes parts of the underlying deposits to form a transgressive surface of erosion (Van Wagoner, 1995).

II. Sequence Nomenclature

Nomenclature applied to this study follows the terminology that was initiated by Zater (2005) and followed by Madof (2006). Sequences are named according to the name of the member in which the basal sequence boundary lies. For example, if a basal sequence boundary of a sequence occurs within the Cozzette Sandstone Member, the sequence will be given the prefix of that member (for example CZ). If more than one sequence occurs within a lithostratigraphic member, they are named numerically in ascending order, starting with the prefix of that member, i.e., CZ_1, CZ_2. Parasequences are named for the sequence within which they occur: PS_1-CZ_1, and if more than one parasequence occurs within the sequence, numbers will be applied in ascending order: PS_1-CZ_1, PS_2-CZ_1. Sequence boundaries across the study interval are numbered in ascending order, i.e., SB_1, SB_2.

III. Description

Five high-frequency sequences are identified in the interval between the top of the Corcoran Member and the top of the Rollins Sandstone Member. Each depositional sequence is marked at the base by a surface of erosional truncation and a basinward shift in facies. The basal parts of these depositional sequences vary laterally across the study

area. The lateral variability can fit into one of two end-member categories. The first group is characterized by an incised-valley fill at the base of the depositional sequences and is common through the western part of the study area (cross-sections 1, 3, and western part of cross-section 2; Figure 26, 28, 27, respectively. The second group exhibits a highstand parasequence at the base of the depositional sequence and is common in the eastern part of the study area (cross-section 4, and the eastern part of cross-section 3; Figure 28 and 29).

1. Sequence 1 (CZ_1)

Sequence 1 makes up the lower part of the Cozzette Member and exhibits a constant thickness of about 40 m across all four cross-sections, except for cross-section 1. In cross-section 1, the depositional sequence is locally reduced to 18 m thick. Thickness reduction is caused by the erosional removal of strata associated with the overlying sequence boundary SB-2. The erosional removal is measured from the erosional surface SB-1 to the overlying flooding surface that seals the filling of the incised valley.

The depositional sequence in the western part of the study area (cross-sections 1, 2 and 3) is described as follows. The sequence boundary (SB-1) is generally observed as an erosional surface with interfluve expression in some locations. The maximum erosional relief of this sequence boundary is 9 m (Figure 26). Strata overlying the erosional expression of the sequence boundary SB-1 are the overbank deposits of electrofacies 7 and the sand-rich channelized succession of electrofacies 2.
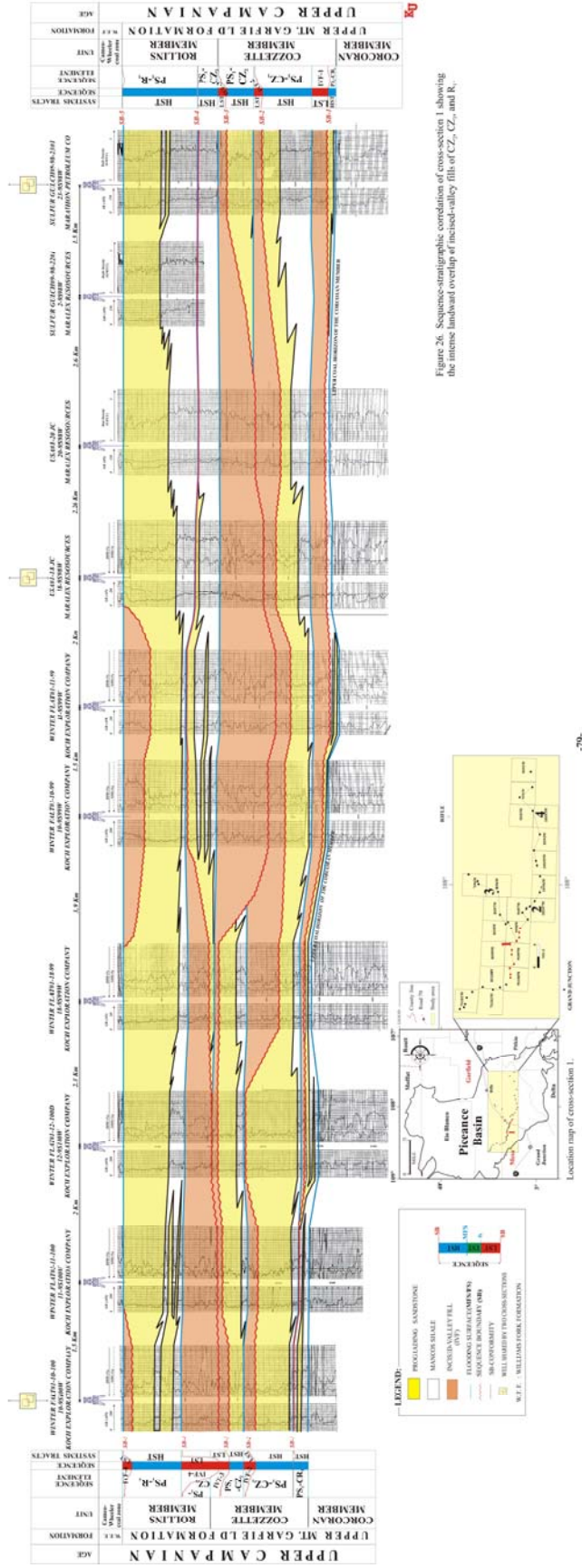
Figure 26. Sequence-stratigraphic correlation of cross-section 1 (see appendix).

These electrofacies patterns occur within an incised-valley fill (IVF-1) and are overlain by offshore transition deposits of electrofacies 3, which in turn, is overlain by the wave-dominated shoreface succession of electrofacies 1. Electrofacies 3 and 1 make up the marine deposits of parasequence PS_1-CZ_1. In some locations, electrofacies 1 is truncated at different depths by the overlying sequence boundary SB-2. Electrofacies 3 thickens basinwards.

In the eastern part of the study area, particularly in cross-section 4, the incised valley is not present and sequence boundary SB-1 is an interfluve expression. It is directly overlain by the offshore transition deposit of electrofacies 3, which in turn, is overlain by the wave-dominated shoreface of electrofacies 1 (PS_1-CZ_1).

2. Sequence 2 (CZ_2)

This sequence is located in the middle of the Cozzette Sandstone Member. Its maximum thickness is ~37 m, and it reaches a minimum thickness of less than 2 m at the extreme eastern part of cross-section 4. The minimum thickness is caused by the erosional removal of strata associated with the overlying sequence boundary SB-3 (Figure 26).

In the western part of the study area, particularly throughout cross-sections 1 and the extreme western part of both cross-sections 2 and 4 (Figure 26 and 29), the sequence boundary SB-2 is an erosional surface that rests unconformably on the underlying parasequence with a maximum erosional relief of about 11 m (cross-sections 3 and 4). There are multiple electrofacies patterns that overlie the sequence boundary SB-2.
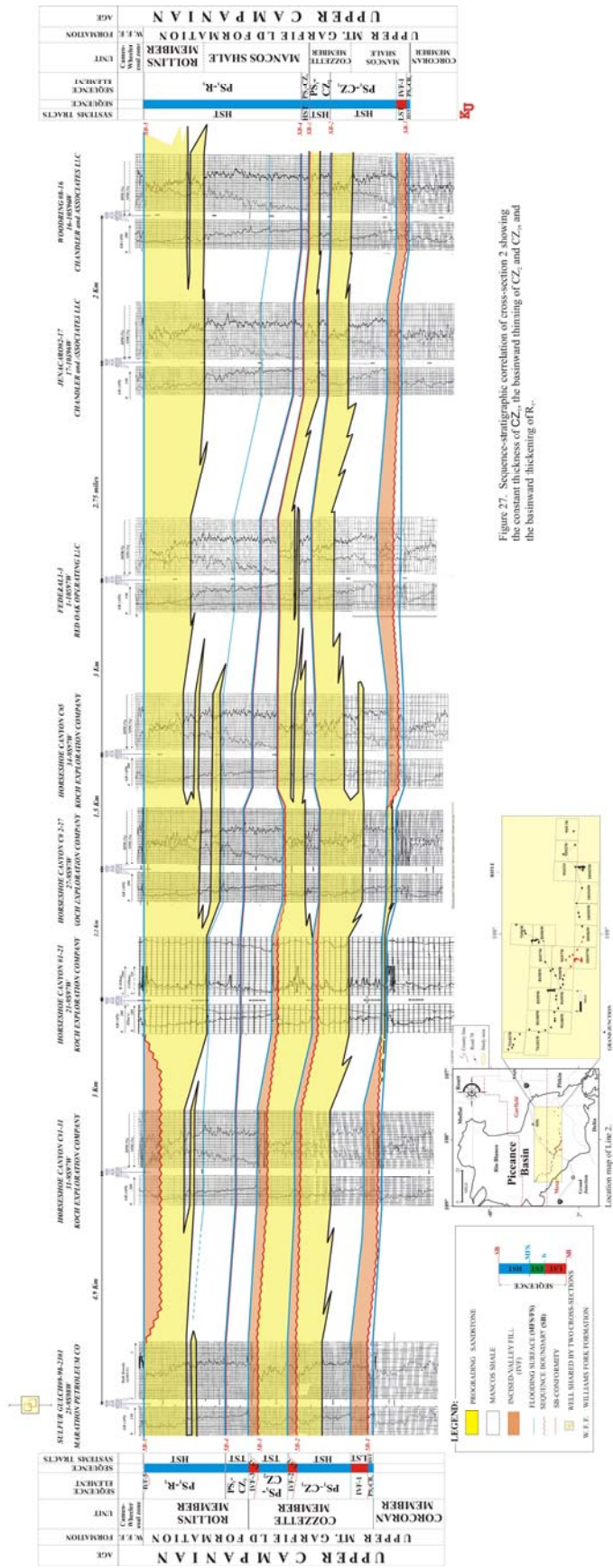
Figure 27. Sequence-stratigraphic correlation of cross-section 2 (see appendix).

These electrofacies patterns are characterized by lateral facies change and comprise sand-rich channelized successions of electrofacies 2, deltaic deposits of electrofacies 5, heterolithic channelized successions of electrofacies 6, or thin intervals of overbank deposits of electrofacies 7. These electrofacies are stacked vertically and all occur within an incised-valley fill (IVF-2). Landward, incised-valley fill (IVF-2) is overlain by very thin successions of offshore transition succession of electrofacies 3, which in turn, is followed by thicker succession of wave-dominated shoreface of electrofacies 1, or it is overlain directly by electrofacies 1 locally. In a seaward direction, the incised-valley fill is overlain by a more developed succession of the offshore transition of electrofacies 3 and electrofacies 1.

Locally, the overlying sequence boundary, SB-3, truncates both the underlying deposits, both marine (including strandplain deposits) and non-marine to marginal-marine deposits of sequence 2 (CZ_2). The marine deposits (PS_1-CZ_2) are associated with both electrofacies 1 and 3, and locally overlie the non-marine to marginal-marine deposits of IVF-2, which consists of electrofacies 2, 5, 6, and 7 (Figure 26 and 28).

The basal surface of erosion, SB-2, climbs stratigraphically eastward before it transitions into an interfluve surface expression. As this occurs, the overlying incised-valley fill gradually thins eastward.

In the extreme eastern part of cross-section 2 and throughout cross-section 4, the sequence boundary, SB-2, is an interfluve expression. It is directly overlain by the offshore transition deposits (electrofacies 3), which in turn, are overlain by a wave-dominated shoreface succession (electrofacies 1; PS_1-CZ_2).
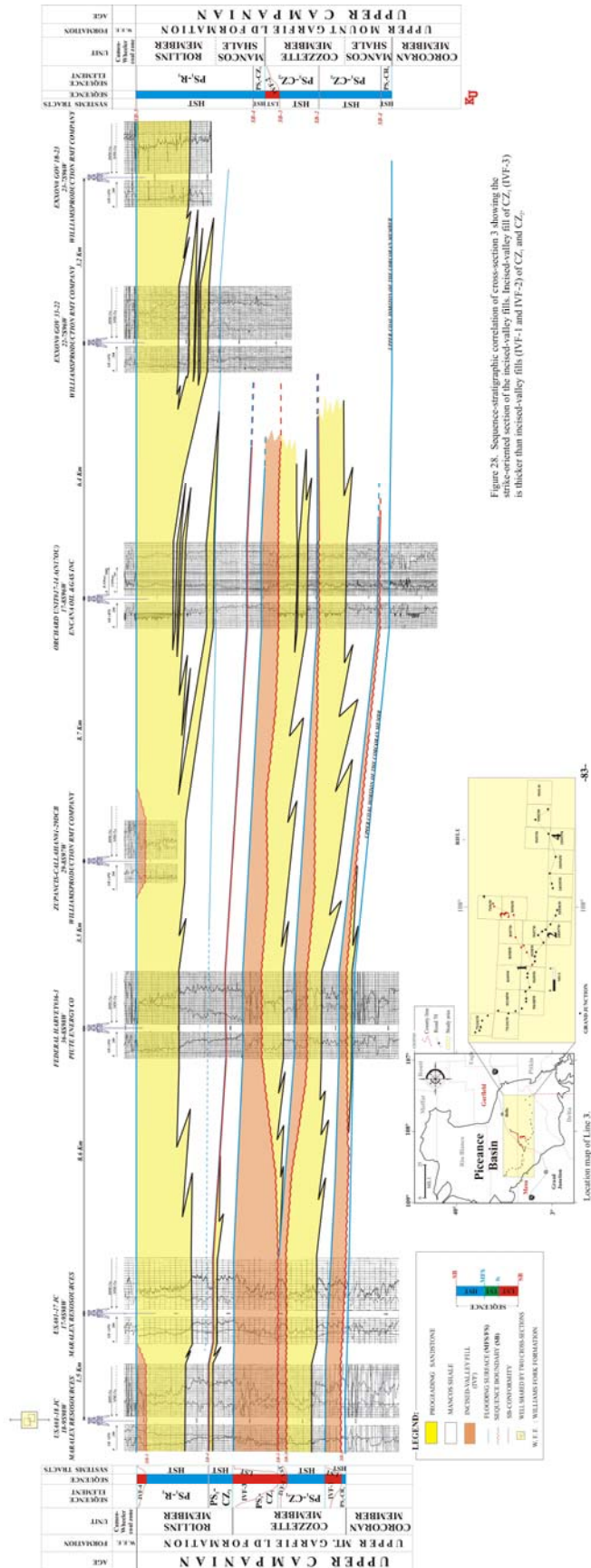
Figure 28. Sequence-stratigraphic correlation of cross-section 3 (see appendix).

In cross-section 2, electrofacies 1 thins progressively and completely disappears eastward through a downdip facies change, where it is replaced laterally by beds assigned to electrofacies 3. These beds thin significantly basinward (cross-section 4) because of the erosion associated with the overlying sequence boundary SB-3 (Figure 29).

3. Sequence 3 (CZ$_3$)

Sequence 3 extends from the upper stratigraphic limit of the Cozzette Sandstone Member to the upper stratigraphic limit of the tongue of the Mancos Shale where it underlines the Rollins Sandstone Member. Sequence 3 is 49 m thick in the western part of the study area (cross-section 1) and a minimum of 3 m to the east. Thickness reduction in the western part of the study area is caused by the erosional removal of strata associated with the overlying sequence boundary (SB-4).

Unlike the other sequence boundaries that are mainly interfluve expressions in cross-section 4 (extreme eastern part of the study area), sequence boundary SB-3 is there expressed as an erosional surface. Throughout all the four cross-sections, the erosional surface SB-3 cuts extensively into the underlying marine strata (electrofacies 1) of parasequence PS$_1$-CZ$_2$, and locally transitions to an interfluve expression in the middle part of the study area (eastern part of line 2).

In the western part of the study area, sequence boundary SB-3 has a maximum erosional relief of 36.5 m. The maximum relief is recorded when sequence boundary SB-3 incises deeply into the underlying non-marine to marginal-marine strata of sequence 2. Various electrofacies overlie the erosional expression of sequence boundary SB-3 and are characterized by a lateral facies change. These electrofacies patterns include sand-rich

channelized successions of electrofacies 2, deltaic deposits of electrofacies 5, heterolithic channelized successions of electrofacies 6, and thin intervals of overbank deposits of electrofacies 7. These electrofacies (2, 5, 6 and 7) are interpreted to fill an incised valley. The valley fill is overlain by the offshore transition succession of electrofacies 3, which is overlain by the wave-dominated shoreface succession of electrofacies 1.

In a seaward direction, the valley fill is overlain by the open-marine offshore deposits of electrofacies 4. The electrofacies patterns 4, 3, and 1 form the marine signature of parasequence PS_1-CZ_3. As with sequence 2 (CZ_2), the marine sandstone of sequence 3 (CZ_3) thins basinward. The lateral extent of the marine sandstone (PS_1-CZ_3), however, is very small. Locally, in the extreme western part of the study area, the incised-valley fill is truncated by the overlying sequence boundary (SB-4). Sequence boundary SB-4 transitions abruptly to an interfluve expression in cross-section 1, and at this location, the interfluve expression is overlain by the open-marine offshore deposits of electrofacies 4 (Figure 26).

Along the cross-sections 1, 2 and 4, the erosive surface SB-3 locally scours the underlying strata in two separate areas, crossing sections in two places. This erosive surface (SB-3) climbs stratigraphically between the incised-valley fills and transitions into an interfluve expression. As this occurs in the middle part of the study area, the incised-valley fill thins, and electrofacies patterns 2, 5, 6 and 7 lap out against the valley wall. In the extreme eastern extent of the study area, electrofacies 6 and 7 also lap out at the margins of the incised valley. The interfluve expression here is overlain directly by thin open-marine offshore deposits of electrofacies 4 (Figure 26-29).

The occurrence of incised-valley fill (IVF-3) in the extreme eastern part of the study area (cross-section 4; basinward), when compared with the other incised-valley fills, may be an artifact of the orientation of the cross-section lines. The artifact may be explained by the overall trend of incised valley (IVF-3) which may be northwest-southeast or more complicated when small and large embayments of the sea occur.
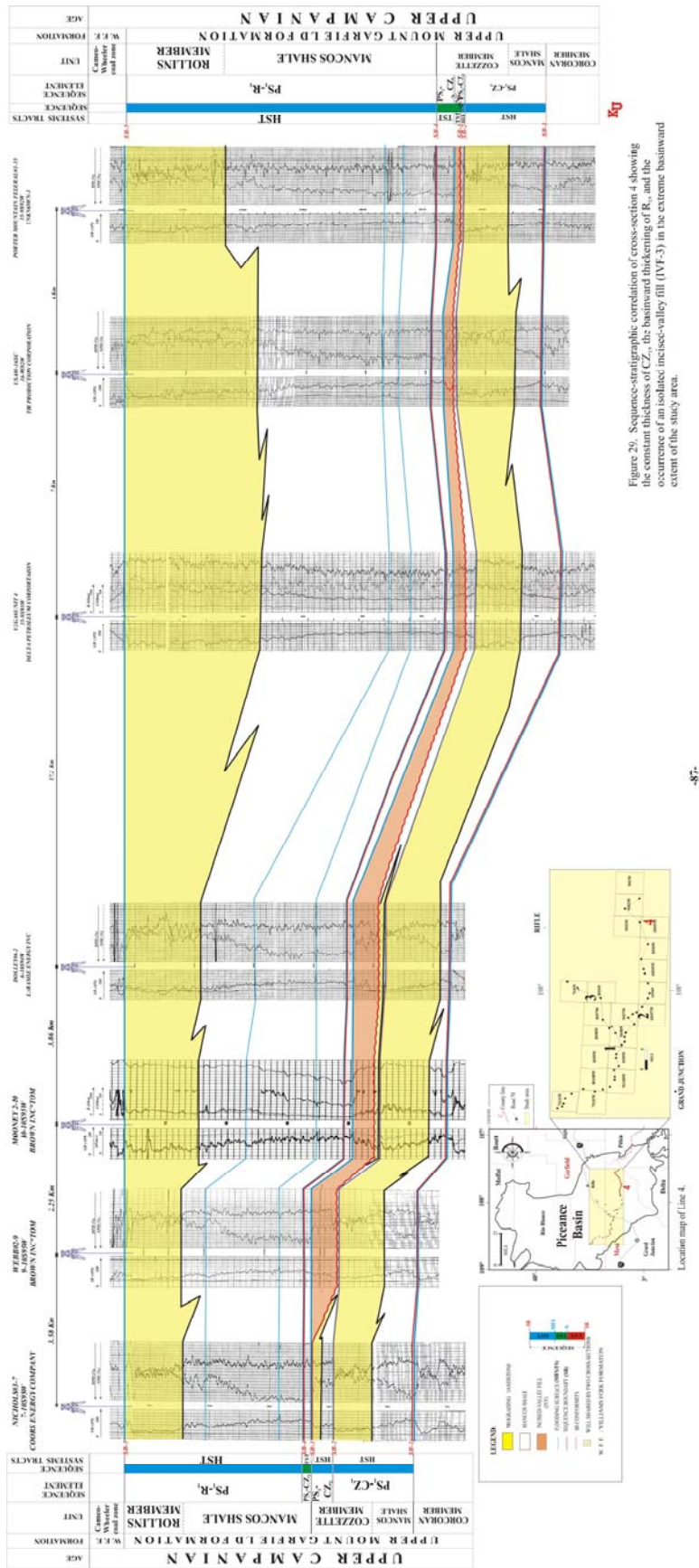
Figure 29. Sequence-stratigraphic correlation of cross-section 4 showing the constant thickness of CZ₁, the basinward thickening of R₁, and the occurrence of an isolated incised-valley fill (IVF-3) in the extreme basinward extent of the study area.

Figure 29. Sequence-stratigraphic correlation of cross-section 4 (see appendix).

4. Sequence 4 (R_1)

Sequence 4 occurs within the upper part of the Rollins Sandstone Member. Its thickness ranges from 56 to 152 m. Unlike the underlying sequences that progressively thin eastward, this sequence thickens toward the east. Sequence boundary SB-4 is usually expressed as an interfluve surface throughout the study area. The erosional expression of SB-4 is limited to the western part of cross-section 1 (extreme landward area), where it cuts into PS_1-CZ_3 and an incised-valley fill of sequence 3.

In the western part of cross-section 1, sequence boundary SB-4 is an erosional surface that becomes an interfluve expression in a seaward direction. The maximum erosional relief of SB-4 is 21 m. Rocks that overlie the erosional expression of sequence boundary SB-4 are characterized by a lateral facies change among several electrofacies and thin eastward abruptly. These rocks include sand-rich channelized successions (electrofacies 2), heterolithic channelized successions of electrofacies 6, thin intervals of overbank deposits (electrofacies 7), and deltaic deposits (electrofacies 5). The various lithologies are stacked vertically and are interpreted as part of an incised-valley fill (IVF-4). The incised-valley fill (IVF-4) is overlain by an offshore transition succession (electrofacies 3), or an open- marine offshore succession (electrofacies 4), marine rocks, which in turn, are overlain by the wave-dominated shoreface succession (electrofacies 1). This succession, overlying incised-valley fill (IVF-4), forms a marine signature of parasequence PS_1-R_1.

Erosional relief associated with SB-4 is limited to the western area of the study area. Erosion associated with sequence boundaries 1, 2 and 3 extend to the central and almost the extreme eastern part of the study area. In sequence 4, the basal surface of

erosion, SB-4, passes abruptly to an interfluve surface (cross-section 1), and rocks of electrofacies 2, 5, 6 and 7 lap out onto the edge of the incised-valley fill (IVF-4). Incised-valley fill (IVF-4) is directly overlain by thin open-marine offshore successions (electrofacies 4).

In the eastern part of the study area, sequence boundary SB-4 is an interfluve expression. It is overlain by a thick interval of open-marine offshore deposits (electrofacies 4), which is overlain by an offshore transition succession (electrofacies 3), which in turn, is overlain by the wave-dominated marine shoreface succession of electrofacies 1.

5. Sequence 5 (R_2)

Sequence 5 is located at the upper part of the Rollins Sandstone Member and at the base of the Cameo-Wheeler coal zone. It is incompletely described because it extends beyond the upper boundary of the study interval. Sequence 5 (R_2) is represented by the basal incised-valley fill (IVF-5), and is covered by the complex fluvial channel-fill succession of the Cameo-Wheeler coal zone. IVF-5 is discontinuous and ranges from 6 to 12 m in thickness; the maximum erosional relief of 12 m is recorded in the eastern part of cross-section 1. Sequence boundary SB-5 cuts into PS_1-R_1. Where sequence boundary SB-5 is an interfluve expression, it coincides with the basal stratigraphic limit of the Cameo-Wheeler coal zone.

The different rock types that overlie the erosional expression of sequence boundary SB-5 occur within an incised-valley fill and consist mainly of heterolithic channelized successions (electrofacies 6; at the base) and overbank deposits (electrofacies

7; at the top of the incised-valley fill). This lithologic assemblage extends laterally to 1.6 to 10 km. The same lithologic assemblage in other depositional sequences extends up to 37 km.

IV. Stratal Geometry

A typical vertical stratal geometry exists within these depositional sequences: marine strata (electrofacies 1, 3, and 4) overlie strata of the incised-valley fill (electrofacies 2, 5, 6, and 7) along a maximum flooding surface (parasequence boundary). The thickness of a depositional sequence and the vertical architecture within a sequence is primarily controlled by sediment supply and accommodation (Figure 30).

At the landward extent of the study area, the facies succession at the base of each depositional sequence (complex deposits of incised-valley fills) is considered the most proximal deposition observed. The proximal succession is abruptly overlain by thin intervals of a more distal succession (distal marine shale), which in turn, progressively shallows upward into thicker marine sandstone. In seaward locations, however, the proximal deposits are not present (except those in CZ_3), because the valley incision only occurred in the landward extent of the study area.
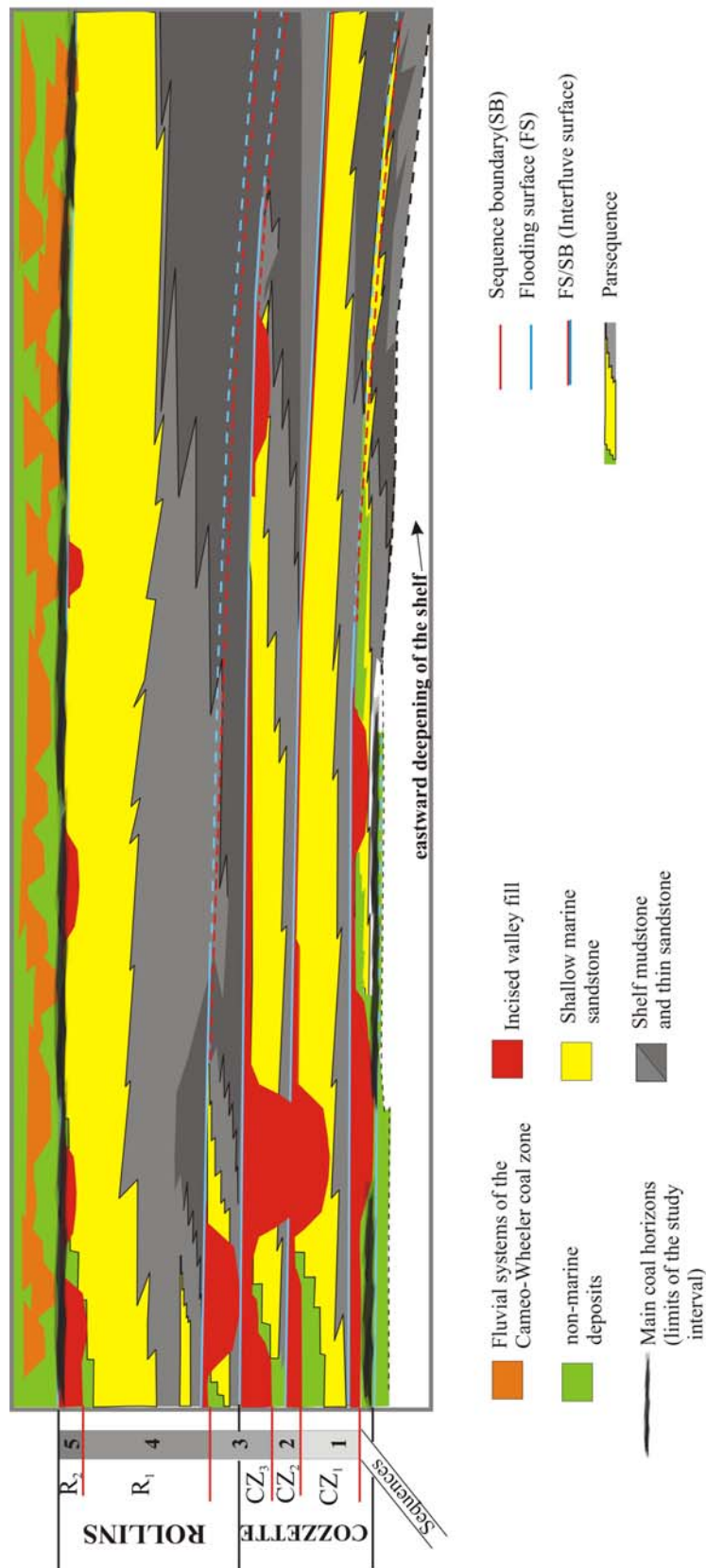
Figure 30. Stratal pattern of sequences exhibits an overall change from retrogradational to progradational. Sequence (4) marks the top of the study interval and includes marine strata that prograde and slightly thicken basinward. The lower part of the study interval is marked by the retrogradational stacking of sequences (1, 2, and 3) where the shelf is starved progressively of siliciclastics basinward prior to the extensive prograding marine parasequence of sequence (4).

91

The incised-valley fills are interpreted as deposits of the lowstand systems tract (LST) and transgressive systems tract (TST), and make up most of the depositional sequences in the western part of the study area. The LST exhibits an upward-coarsening succession where the lower part of proximal signature of non-marine to marginal marine deposits (overbanks and swamps of electrofacies 6 and 7) are overlain by the distal marginal-marine deposits (bay-head deltas or marine-influenced channels of electrofacies 5 or 2 respectively).

The transgressive systems tract comprises an upward-fining succession, where the basal part includes either a multiple stacking of beds of electrofacies 2 or 5, and ends by multiple stacking of beds of electrofacies 6 and 7. In the extreme western extent of the study area, and because of the nested feature of the incised-valley fills (Figure 31), the vertical trend within each incised-valley fill is difficult to resolve in terms of lowstand or transgressive systems tracts.

In the eastern extent of the study area, the marine strata that overlie the incised-valley fills are interpreted as highstand systems tracts (HST). The highstand systems tracts thicken basinward and form most of the depositional sequence. Highstand systems tracts (HST) exhibit an upward-coarsening succession where offshore marine or offshore-shoreface transition deposits (electrofacies 4 and 3) are overlain by rocks of the shoreface deposits (electrofacies 1).
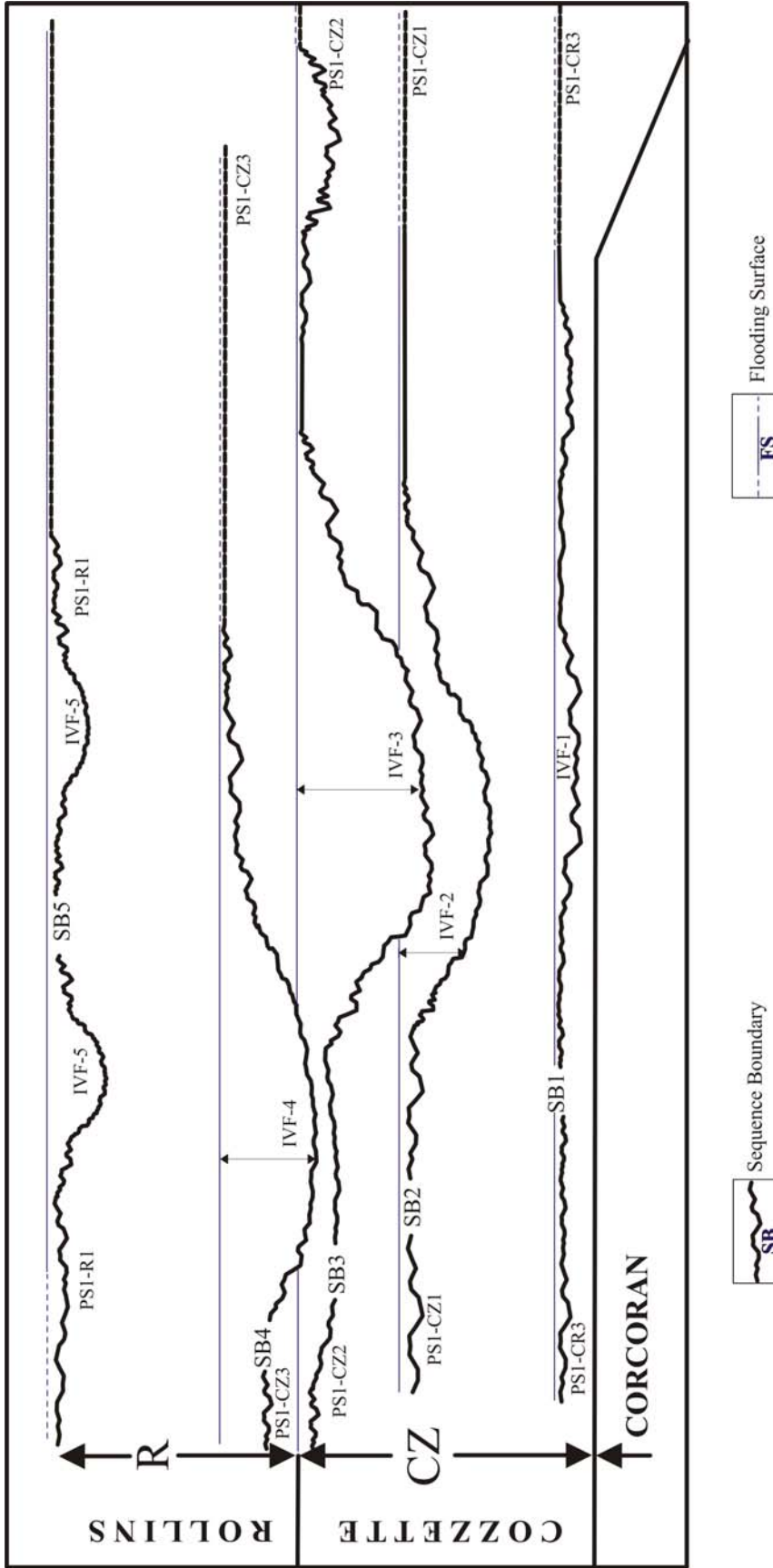
Figure 31. Schematic showing generalized regional expression of sequence boundaries. Landward, sequence boundaries are expressed as erosive surfaces that erode into former incised-valley fills; they generally transition into an interfluve expression basinward. The shallow depth of IVF-1 is probably due to an underlying peat (coal) that may prevent erosion. Erosional relief is less well-developed in the incised-valley fill IVF-5.

93

Chapter V: SEQUENCE STRATIGRAPHIC EVOLUTION

I. Sequence Evolution

The 5 stratigraphic sequences described in the Cozzette and Rollins Sandstone members are generally similar, with deposits of incised-valley fills at the proximal end and deposits of marine shelf and shoreface at the distal end. Sequence 3 (CZ_3) will be described as an example of the evolution of all five of the sequences.

Sequence 3 (CZ_3) is underlain by parasequence PS_1-CZ_2, which is the highstand phase of sequence 2 (CZ_2). PS_1-CZ_2 was deposited as the shoreface built seaward to fill the space available during the former highstand phase (Figure 32-Time A). Following progradation, river systems incised as sea level fell. The widespread stage of sea-level fall marks the end of sequence 2 (CZ_2) and the beginning stage of sequence 3 (CZ_3) (Figure 32-Time B). As this occurs, vast areas of the shelf are exposed to subaerial conditions and are incised locally by fluvial systems.   The incision surface and its correlative interfluve surface, SB-3, mark the base of depositional sequence 3 (CZ_3). SB-3 erodes a significant amount of the underlying parasequence PS_1-CZ_2 (including strandplain) to form an incised valley on the exposed shelf.

The subsequent rise of sea level results in an increase in accommodation and a gradual fill of the incised valley (IVF-3). The fill occurs in two phases, a late lowstand into early transgressive phase and a late transgressive phase. The resultant facies patterns change as the transgression progresses from the seaward to the landward extent of the incised-valley fill (IVF-3) as follows.
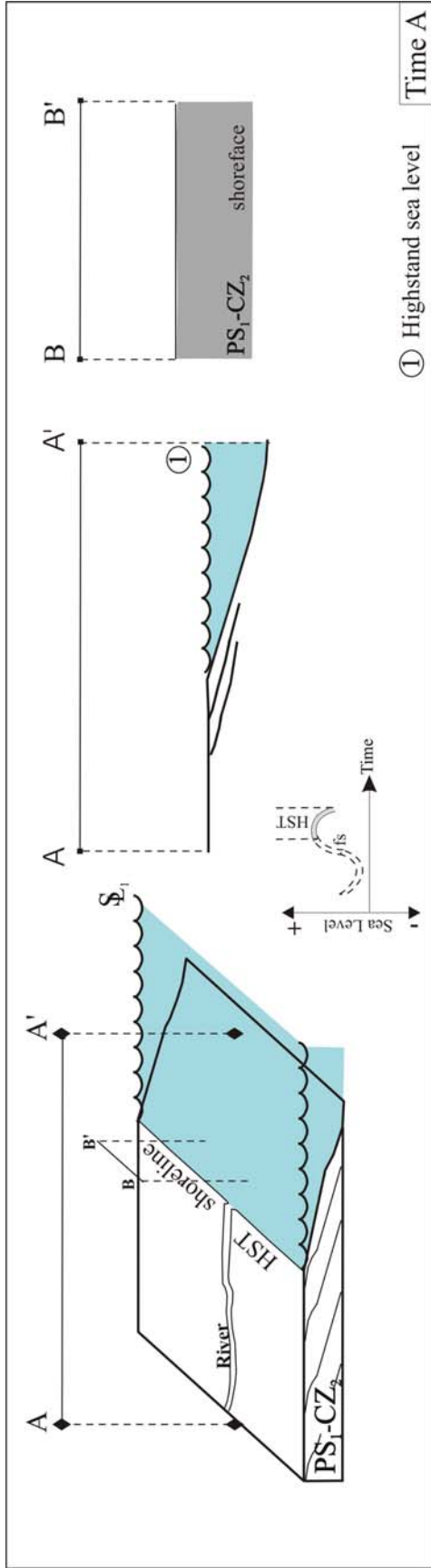
AA': Dip-oriented section, from strandplain extending into shoreface.
BB': Strike-oriented section through the shoreface deposits of CZ_2.

fs: Minor flooding surface that marks the base of the transgressive systems tract. It delineates the late-phase of relative fall in sea level from the above early-phase of relative rise in sea level.
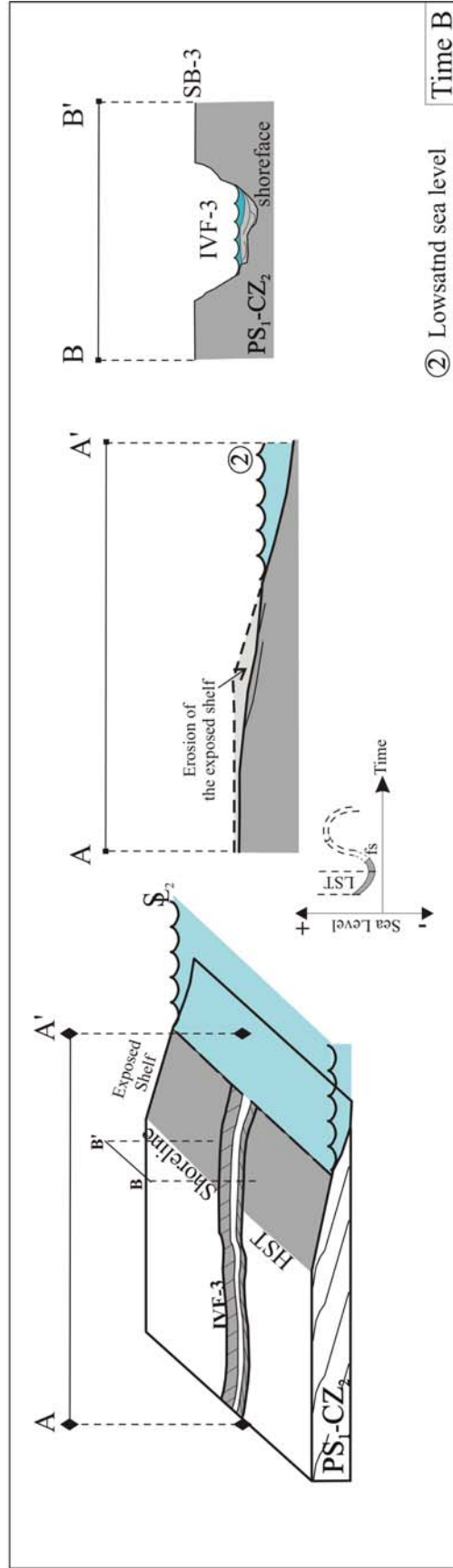
Figure 32. Evolution of sequence CZ_3 is explained through different stages of base level fluctuation. Time A: PS_1-CZ_2 progrades during the highstand phase (HST) of sequence CZ_2. Time B: During early lowstand (LST), the fall in sea level forms the surface (SB-3), and marks the base of depositional sequence CZ_3. Localized incision forms the incised valley (IVF-3). During the early stage of sea-level fall, the incised valley is the site of sediment bypass.
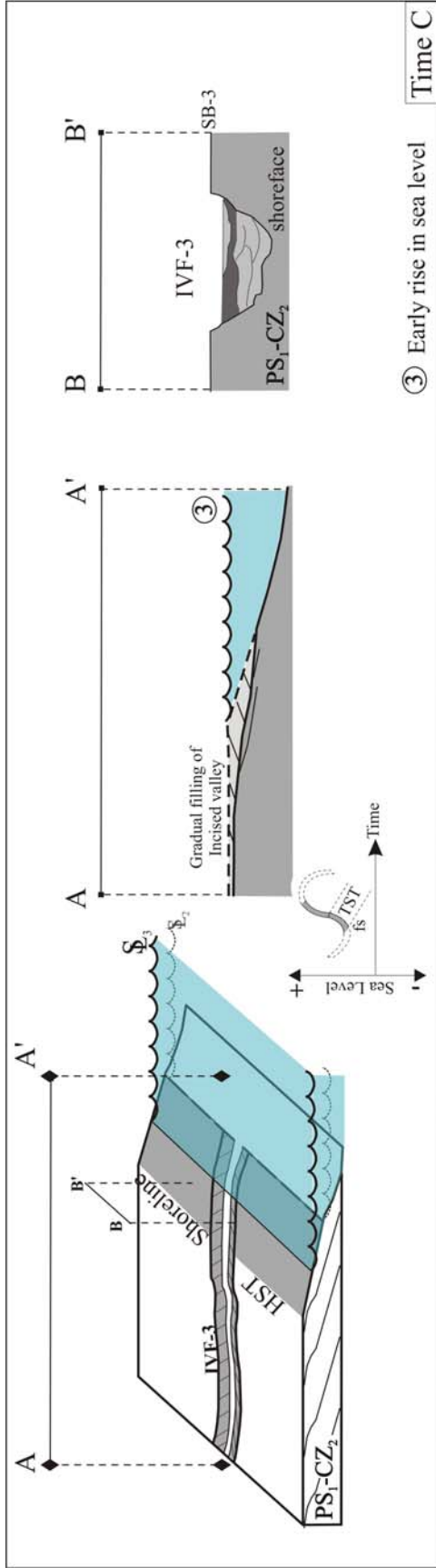
AA': Dip-oriented section, from strandplain extending into shoreface.

BB': Strike-oriented section through the subaerially exposed shoreface deposits of CZ_2, showing the incised-valley fill.

fs: Minor flooding surface that marks the base of the transgressive systems tract. It delineates the late-phase of relative fall in sea level from the above early-phase of relative rise in sea level.
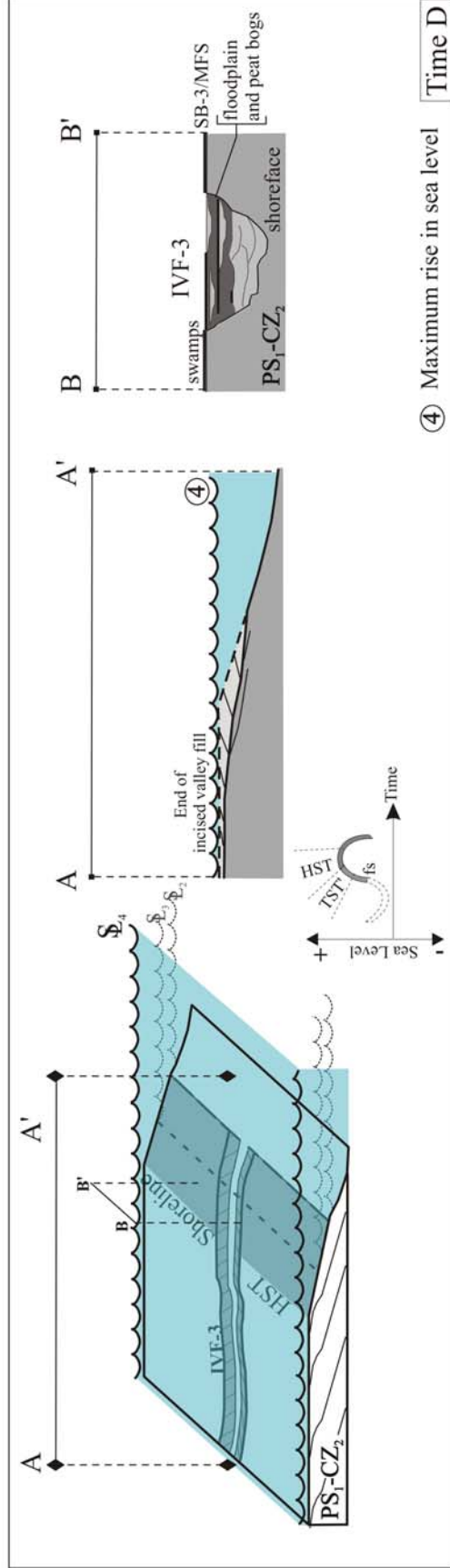
Figure 32 (continued). Time C: During the late lowstand or early transgressive phase (TST), the incised valley is filled with amalgamated channel-fill sands of high energy rivers, which are overlain by isolated sand lenses and floodplain deposits associated with low-energy rivers. Time D: During the late transgressive phase (TST'), the shoreline has migrated landward and floods the top of the incised-valley fill. Isolated thin peat horizons may form within incised-valley fill.

96

Time E

⑤ Highstand sea level

B' shoreface shoreface B
PS₁-CZ₃ PS₁-CZ₂

A' ⑤ A
HST fs
Sea Level + − Time

SB₅
shoreline
IVF-3 HST
River
PS₁-CZ₃
PS₁-CZ₂
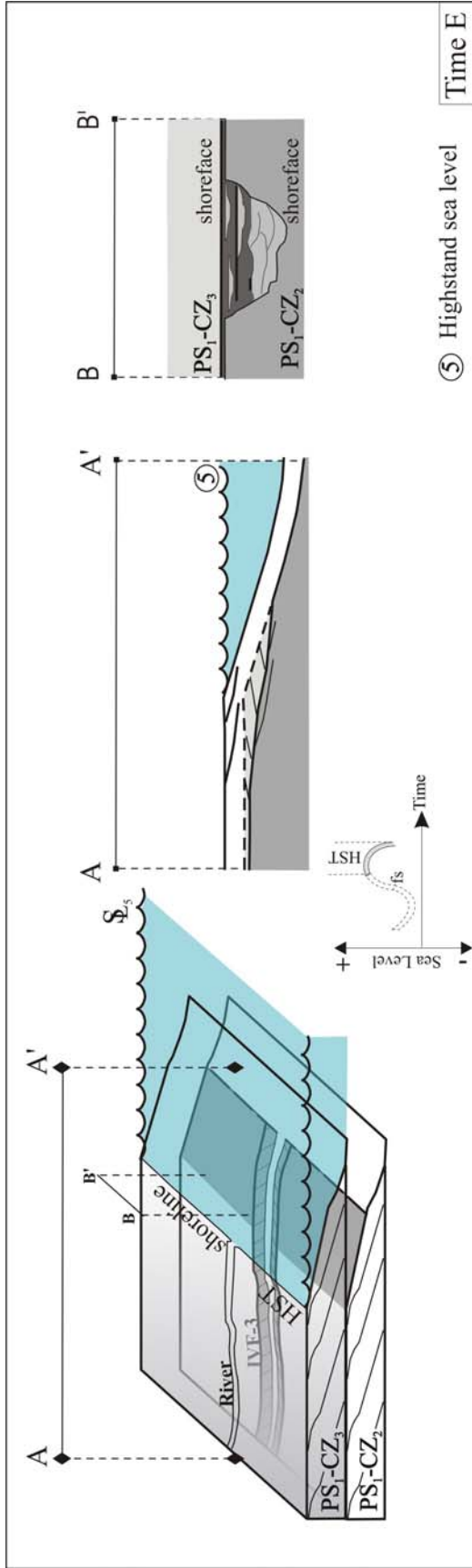
AA': Dip-oriented section, from strandplain to shoreface.

BB': Strike-oriented section, through the subaerially exposed shelf, showing incised-valley fill.

fs: Minor flooding surface that marks the base of the transgressive systems tract. It delineates the late-phase of relative fall in sea level from the above early-phase of relative rise in sea level.

Final

⑥ Lowstand sea level

R₁
SB-4
Sequence 3 (CZ₃)
SB-3
CZ₂

B' IVF-4 shoreface shoreface B
PS₁-CZ₃ PS₁-CZ₂

A' ⑥ A
LST fs
Sea Level + − Time

SB₆
Exposed Shelf
Shoreline
IVF-4 HST
PS₁-CZ₃
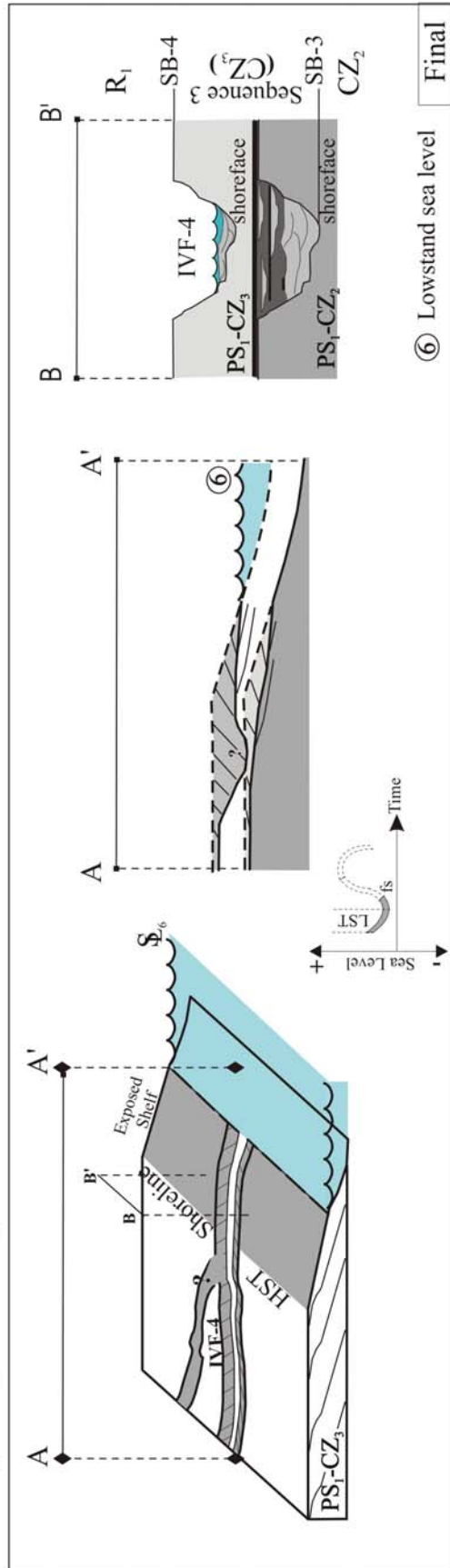
Figure 32 (continued). Time E: During highstand conditions, the shoreline progrades and PS₁-CZ₃ is deposited. A fall in sea level forms the surface SB-4 which marks the upper contact of the depositional sequence 3 (CZ₃). Final: Localized incision forms an incised valley (IVF-4), which locally incises into IVF-3.

97

During the late lowstand or early transgressive phase, the seaward extent of the incised valley is overlain by amalgamated channel-fill sandstones that form a continuous cover over the erosive surface SB-3 (Figure 32-Time C). The electrofacies patterns observed in well logs show that the valley floor during this phase is dominated by channelized sandstones that coalesce to form connected sandstone bodies. These sandstones may be the deposits of a high-energy fluvial system (low-sinuosity). During the late phase of deposition of the transgressive systems tract (TST), the shoreline continues to advance landward. As this occurs, the gradient of fluvial systems decreases and the water table rises to support peat growth (Figure 32-Time Final). The valley fill during this phase is dominated by overbank and flood plain fines and lower energy fluvial channel-fill sandstones. The electrofacies patterns observed in well logs show isolated channel-fill sandstones of probable high-sinuosity fluvial systems.

In the updip extent of the study area, the upper reaches of the incised valleys incise into strandplain and earlier incised-valley-fill deposits (Figure 33). This results in the overlap of incised-valley fills of different age. Incised valleys, which occur in response to a lowering of base level, are influenced by many factors including the shelf gradient (Van Wagoner et al., 1990), and the occurrence of peat beds. The strandplain is interpreted as a horizontal to near-horizontal surface. This interpretation is supported by observations from modern strandplains, and by the consistent thickness between coal beds located at the top of the Corcoran Sandstone Member and the top of the Rollins Sandstone Member. Coal beds form from extensive peat horizons, which would have protected the underlying strandplain from incisions. The trends of fluvial systems and incised valleys may reflect trends established further up dip, partially controlled by peat

horizons. The morphology (including depth) of each incised valley may differ. This further complicates parasequence correlations within nested incised valleys (Figure 33-b). Facies of different incised-valley fills may be juxtaposed, and when that occurs, it is difficult to determine where one valley-fill ends and another starts. Tracing sequence boundaries in succession of incised-valley fills is difficult at best.
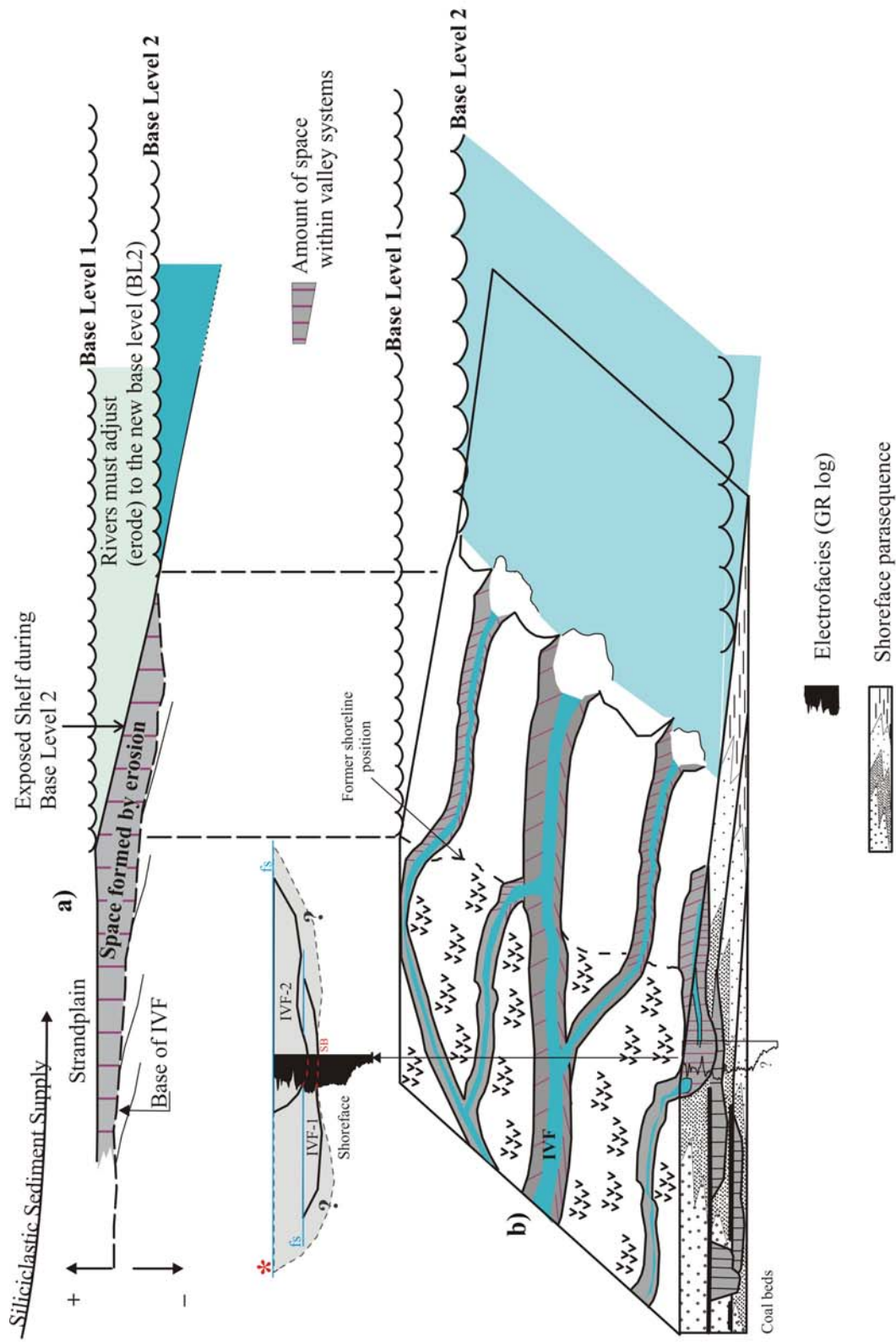
Figure 33. Schematic block diagram showing updip stratigraphic complications within incised-valley fills. a) In low-gradient profile, shallow incised valleys form in response to sea-level fall (BL2) and erode into strandplain deposits. b) Strandplains form following the prograding shoreface; peats form when plants are preserved by a rise in the water table (rise in sea level). Significant peat beds prevent overlying incised valleys from eroding into underlying strandplain deposits and force different age incised valleys to overlap elsewhere. Incised valley interpretation using GR log response may include diachroneous facies (*).

In the last phase of deposition of the transgressive systems tract (TST), the shoreline transgresses landward of the former highstand shoreline position (point X). The rate of landward movement of the shoreline increases dramatically at point "X" (Figure 34) where the gradient of the surface being transgressed decreases significantly (Wehr, 1994).
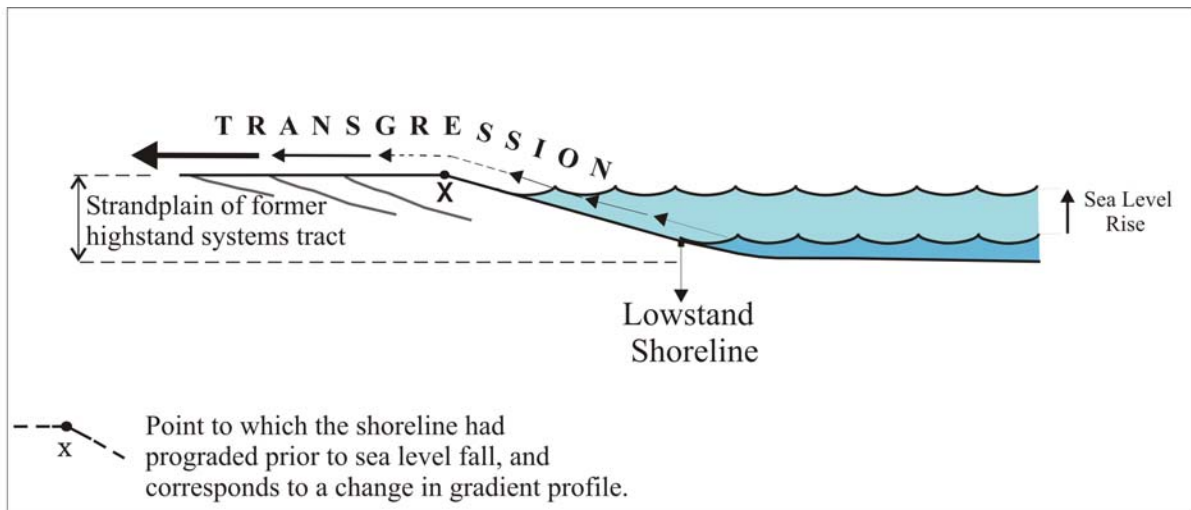
Figure 34. Rate of transgression changes at the deflection point (X). Increasing line-weight of arrows indicates progressive increase in transgression rate as shoreline migrates landward at the point (X).

As this occurs, vast areas of the strandplain (interfluves) are flooded quickly, and a parasequence boundary (flooding surface) is formed at the top of the incised-valley fill and strandplain deposits. The parasequence boundary forms the base of the overlying parasequence PS_1-CZ_3. During the subsequent highstand, the shoreline of this parasequence (PS_1-CZ_3) prograded seaward, throughout the study area (Figure 28-Time E). Following the shoreline progradation of PS_1-CZ_3, another fall in sea level occurs, and river systems incise into the highstand deposits of PS_1-CZ_3, forming yet another incised-

valley fill. This fall in sea level results in the erosive surface SB-4, which terminates the deposition of sequence 3 (CZ_3) (Figure 32-Time Final).

The same processes and sequence of events occurred in all the depositional sequences with slight variations in each. These variations concern facies patterns within the incised-valley fills and continuity of the marine sandstone. The different combination of facies patterns noticed within each fill may be an artifact of the orientation of the cross-section lines. Variation in the continuity of the marine sandstones across the study area is related to the extent to which each shoreline has prograded. Those shorelines with the greatest amount of progradation, i.e., PS1-R1 will have the greatest continuity of sandstone in the downdip direction.

II. Stacking Pattern of Sequences

The vertical architecture of sequences indicates an overall change in stratal pattern from retrogradational to progradational. Sequences CZ_1 through CZ_3 exhibit a retrogradational stacking pattern. The retrogradational stacking pattern changes with the last sequence, R_1, as the marine shoreline of PS_1-R_1 progrades extensively (>100 km) and slightly thickens basinward. The retrogradational phase is identified to overlap the stratigraphic limit between the Cozzette and the Rollins members. Sequence R_2 appears only as incised-valley fills, and is therefore a continuation of the regression noted in sequence R_1. The stacking pattern between sequences R_2 and R_1, however, is difficult to establish because no prograding or retrograding marine strata within the overlying sequence R_2 was established in this current study, and also the extensive coal beds of the

Cameo-Wheeler coal zone throughout the Piceance basin may suggest a significant rise in

sea level prior to the development of the overlying non-marine fluvial systems.

DISCUSSION

NPH-DPH logs are porosity logs that help greatly in preliminary stratigraphic correlations, distinguishing marine from non-marine environments. The analysis of log responses of the current study shows that the NPH-DPH log separation C is not typical of open-marine deposits. It may occur, however, in areas where thin marginal-marine successions inter-tongue with the marine. In these areas, lateral facies change is complicated and the distinction between marine and non-marine to marginal-marine strata remains difficult using well-log data alone.

In heterogeneous strata (shaly sandstone/sandy shale), shale laminae is a facies characteristic of non-marine to marginal-marine deposits. Shale laminae are also the main factor that explains the overall linear relationship of NPH-DPH log separation (C) where a gradual change from silt (shale) to sand, or vice versa, must occur at a millimeter scale (NPH-DPH-laminae chart). This feature prevails in environments of smaller cyclicity, such as fluvial systems and bayhead deltas. For example, the periodicity of rivers provides constantly a sand-shale mixture that is reworked quickly into small sequences with upward-fining or coarsening trend, and in which shale, for example, is scattered throughout the small sand-rich sequences as laminae, ripples or bioturbation linings. The bed resolution of the log tool (2-3 feet) considers the highly heterogeneous sequences as a homogenous sand-shale mixture, where the change from shale to sand (or sand to shale) occurs indistinguishably. The process of a gradual increase of sand results in a loss of hydrogen index and a gain of bulk density. The loss in hydrogen index, which induces the NPH log measurements to decrease, is compensated with an increase

of bulk density, which in turn, induces the DPH log measurements to decrease. The apparent porosity recorded by both NPH and DPH logs, therefore, decrease together gradually. The opposite takes place when the process of a gradual change of shale in detriment of sand occurs. When the shale or silt laminae prevail (abundant draping structures or burrows), both NPH and DPH log values increase. The increase of DPH log reflects a decrease in bulk density and is explained as follows. Shale is less dense than quartz and becomes much lighter when the dispersed shale invades the pore-space network by adsorbing more water content and escaping the process of a maximum compaction.

The strong and simultaneous deflection of the log pattern (C) is a feature that is not likely to occur in marine strata. In marine environments, wave energy is greater and reworks the sand/shale mixture into thicker sequences of either sand-rich intervals (electrofacies 1) or mud-rich intervals (electrofacies 3 and 4). The vertical bed resolution of both NPH-DPH tool (2-3 feet) detects the burrowed offshore deposits, for example, as homogenous shale because the prevailing lithology is mud (>50%). The offshore-shoreface transition deposits are extensively burrowed and are subject to alternating deposition of clay and sand. However, as the sand beds grade upwards, the replacement of shale by sand does not occur at a millimeter scale, which annihilate the main condition for the log pattern (C) to occur. In conclusion, neutron and density logs should be analyzed carefully to better support the distinction between marine and non-marine rocks.

CONCLUSION

An outcrop description of the Rollins Sandstone Member of the Mt. Garfield Formation records a depositional succession that changes from complex marginal-marine deposits at the base to marine wave-dominated shoreface succession at the top. The uppermost parasequence is a wave-dominated shoreface succession that forms a continuous and dominant stratigraphic element. The lower marginal-marine deposits are interpreted to occur within multiple incised-valley fills. The deposional complexity is caused, in part, by multiple sequence boundaries and nested incised-valley fills.

The subsurface analysis for this Cozzette and Rollins Sandstone members distinguishes 5 sequence boundaries, expressed as either erosional surfaces or interfluve expressions. An additional sequence boundary was identified within the Cozzette Sandstone Member in comparison with the results of Madof's outcrop study. Sequence boundaries in this current study delineate 5 depositional sequences of variable thickness and are identified on each of the four cross-sections. The depositional sequences are all similar with proximal incised-valley fill on the west passing to marine shoreface and shelf or offshore deposits to the east. Sequence 1 (CZ_1) is the basal sequence. It presents a nearly constant thickness throughout the study area and contains both marine (distal) and non-marine (proximal) successions. Sequence 2 (CZ_2) and sequence 3 (CZ_3) thin depositionally toward the east. They contain both marine and non-marine successions. Sequence 4 (R_1), which thickens slightly and progressively eastward, is marine dominated. Sequence 5 (R_2) is the youngest and its expression within the Rollins

Sandstone Member is limited to isolated basal incised-valley fills. The incised-valley fills are dominated by marine to marginal-marine strata.

Each depositional sequence is composed of incised-valley fills at the base and proximally and highstand deposits with marine shoreface sandstone at the top and distally. Incised-valley fills within the CZ_1, CZ_2 and CZ_3 (IVF-1, IVF-2, and IVF-3) are nested and form important stratigraphic elements. The incised-valley fill of the uppermost part of the Cozzette Sandstone Member (IVF-3; CZ_3) is the most extensive laterally because it occurs in both western and eastern extents of the study area. The incised-valley fill (IVF-4) of sequence R_1 is thinner, less extensive than that of CZ_1-CZ_3, and is limited to the extreme western extent of the study area where it overlaps with incised-valley fill (IVF-3). The incised-valley fill (IVF-5) is also thinner and crosses sections in separate places, extending to the central part of the study area.

Depositional sequences CZ_1-CZ_3 show a retrogradational stacking pattern. Sequence R_1 does not follow this pattern and builds basinward. The youngest sequence R_2 is incomplete and its stacking relationship with the underlying sequence R_1 is unclear within the study interval. The stratigraphic limit between the Cozzette and the Rollins Sandstone members may lie at the turnaround from the retrogradational sequences (CZ_1 through CZ_3) and the overlying progradational sequence (R_1). The turnaround is a major turning point from retrogradational to progradational staking and coincides with a maximum flooding surface. In outcrop areas, the stratigraphic limit should be located at the top of both incised-valley fill and marine strata that exhibit the most limited lateral extent throughout the Piceance basin (subsurface data) because flooding events (transgressions) trap sediment and prevent it from being transported to the shelf.

The lowstand and transgressive systems tracts occur in the basal incised-valley fill within each sequence. All incised-valley fills present a basinward-thinning wedge. Basinward, the incised-valley fill consists of mainly electrofacies 2, and is overlain by an upward-fining trend associated with rocks of electrofacies 6 and 7. Landward, the incised valleys are nested and show highly variable log patterns that reflect complex marginal marine deposits. The complexity inhibits differentiation into systems tracts. The highstand systems tract occurs in the upper part of each depositional sequence and is the most prevalent basinward. The stratigraphic signature of highstand systems tract is presented by the funnel-shaped pattern on well logs (electrofacies 1, 3 and 4), which indicates a progradational, upward-coarsening succession.

REFERENCES

Asquith, G. B., 1990, Log evaluation of shaly sandstones--a practical guide: American Association of Petroleum Geologists, Continuing Education Course Note Series 31, 59 p.

Asquith, G. B. and C. R. Gibson, 1982, Basic well log analysis for geologists: American Association of Petroleum Geologists, Methods in Exploration Series 3, 216 p.

Armstrong, R. L., 1968, Sevier orogenic belt in Nevada and Utah: Geological Society of America Bulletin, v. 79, no. 4, p. 429-458.

Blum, M. D., 1993, Genesis and architecture of incised valley fill sequences: A Late Quaternary example from the Colorado River, Gulf Coastal Plain of Texas, *in* P. Weimer, and H. W. Posamentier, eds., Siliciclastic sequence stratigraphy: recent developments and applications: American Association of Petroleum Geologists Memoir 58, p. 259-283.

Bourgeois, J., 1980, A transgressive shelf sequence exhibiting hummocky stratification: the Cape Sebastian Sandstone (Upper Cretaceous), southwestern Oregon: Journal of Sedimentary Petrology, v. 50, p. 681-702.

Bourgeois, J., and E. L. Leithold, 1984, Waved-worked conglomerates--depositional processes and criteria for recognition, *in* E. H. Koster, and R. J. Steel, eds., Sedimentology of gravel and conglomerates: Calgary, Canadian Society of Petroleum Geologist Memoir 10, p. 331-343.

Brown, A. C., T. M. Smagala, and G. R. Haefele, 1986, Southern Piceance basin models-Cozzette, Corcoran, and Rollins sandstones, *in* C. W. Spencer, and R.F Mast, eds., Geology of tight gas reservoirs: American Association of Petroleum Geologists Studies in Geology 24, p. 207-219.

Cant, D. J., 1992, Subsurface facies analysis, *in* R. G. Walker, and N. P. James, eds., Facies models-response to sea level change: Geological Association of Canada, p. 27-45.

Carter, C. H., 1978, A regressive barrier and barrier-protected deposit: depositional environment and geographic setting of the Late Tertiary Cohansey Sand: Journal of Sedimentary Petrology, v. 48, 933-950.

Cobban, W. A. and J. B. Reeside, 1952, Correlation of the Cretaceous formations of the Western Interior of the United States: Geological Society of America, v. 63, p. 1011-1044.

Cole, R., and S. P. Cumella, 2003, Stratigraphic architecture and reservoir characteristics of the Mesaverde Group, southern Piceance basin, Colorado, field trip guidebook, *in* S. P. Cumella et al., eds., Piceance basin guidebook: Rocky Mountain Association of Geologists and American Institute of Professional Geologists, p. 392-432.

Collins, B. A., 1977, Coal deposits of eastern Piceance basin, *in* D. K. Murray, ed., Resource series Colorado Geological Survey, Department of Natural Resources, Colorado: proceeding of the 1976 Symposium of the Geology of Rocky Mountain Coal, p. 29-43.

Collinson, J. D., and D. B. Thompson, 1982, Sedimentary structures, Allen and Unwin, London, 194 p.

Cross, T. A., 1988, Controls on Coal distribution in transgressive-regressive cycles, Upper Cretaceous, Western Interior, U.S.A., *in* C. K. Wilgus, B.S. Hastings, C. G. St. C. Kendall, H. W. Posamentier, C. A. Ross, and J. C. Van Wagoner, eds., Sea-level changes-an integrated approach: Society of Economic Paleontologists and Mineralogists Special Publication 42, p. 371-380.

Dalrymple, R. W., B. A. Zaitlin, and R. Boyd, 1992, Estuarine facies models: conceptual basis and stratigraphic implications: Journal of Sedimentary Petrology, v. 62, p. 1130-1146

Davidson-Arnott, R. G. D., and B., Greenwood, 1974, Bedforms and structures associated with bar topography in the shallow water wave environment, Kouchibouguac Bay, New Brunswick, Canada: Journal of Sedimentary Petrology, 44, p. 698-704.

Dewan, J. T., 1983, Essentials of modern open-hole log interpretation, Penn Well, Tulsa

Dickinson, W. R., 1978, Plate tectonics of the Laramide orogeny, in Laramide folding associated with basement block faulting in the western United States: Geological Society of America Memoir 151, p. 355-366.

Dickinson, W. R., 1987, Laramide tectonics and paleogeography inferred from sedimentary record in Laramide basins of central Rocky Mountain region: Abstracts with Programs, Rocky Mountain Section, 40th Annual Meeting: Geological Society of America, v. 19; no. 5, 271 p.

Dott, R. H, Jr., 1963, Dynamics of subaqueous gravity depositional processes: American Association of Petroleum Geologists Bulletin, v. 47, p. 104-128.

Dott, R. H., and J. Bourgeois, 1982, Hummocky stratification: significance of its variable bedding sequences: Geological Society of America Bulletin, v. 93, p. 663-680.

Doveton, J. H., and S. E Prensky, 1992, Geological applications of Wirelogs: a synopsis of developments and trends: The Log Analyst, v. 33, no. 3, p. 286-303.

Doveton, J. H., 1994, Geological log interpretation: reading the rocks from wireline logs, 169 p.

Dresser Atlas, 1974, log review 1: Houston, Texas, Dresser Industries, Inc, Ill.

Einsele, G., 1992, Sedimentary basin: evolution, facies, and sediment budget, Springer-Verlag, Berlin, 628 p.

Elliott, T., 1986, Siliciclastic shoreline, *in* H. G. Reading, ed., Sedimentary environments and facies, 2nd edition: Blackwell Scientific Publications, p.155-188.

Ellis, D. V., 1987, Well logging for earth scientists: Elsevier, New York, 532 p.

Emery, D. and Myers, K. J., eds., 1996, Sequence stratigraphy: Great Britain, Blackwell Science, 269 p.

Erslev, E. A., 1993, Thrust, back-thrust, and detachment Rocky Mountain foreland arches, *in* C. J. Schmidt, R. B. Chase, and E. A. Erslev, eds., Laramide basement deformations in the Rocky Mountain Foreland of the western United States: Geological Society of America Special Paper 280, p. 339-358.

Fassett, J. E., and J. S. Hinds, 1971, Geology and fuel resources of the Fruitland Formation and Kirtland Shale of the San Juan Basin, New Mexico and Colorado: U.S. Geological Survey Professional Paper 676, 76 p.

Flores, R. M., 1981, Coal deposition in fluvial paleoenvironments of the Paleocene Tongue River Member of the Fort Union Formation, Powder River area, Powder River Basin, Wyoming and Montana, *in* F. G. Ethridge, and R. M. Flores, eds., Recent and ancient nonmarine depositional environments: models for exploration: Spec. Publ. Soc. Econ. Paleont. Miner., 31, Tulsa, p. 169-190.

Fouch, T. D., T. F. Lawton, D. J. Nichols, W. B. Cashion, W. A. Cobban, 1983, Patterns and timing of synoregenic sedimentation in Upper Cretaceous rocks of central and northeast Utah, in Mesozoic paleogeography of the west-central United State: Rocky Mountain Paleogeography, Symposium 2, p. 305-336.

Franczyk, K. J., L. K. Pitman, W. B. Cashion, J. R. Dyni, T. D. Fouch, R. C. Johnson., M. A. Can, J. R. Donnell, T. F. Lawton, and R. R. Remy, 1989, Evolution resource-rich foreland and intermontane basins in eastern Utah and western Colorado, Salt Lake City, Utah, to Grand Junction, Colorado: Field Trip For The 28th International Geological Congress, Guidebook T324, p. 1-49.

Frey, R. W., and S. G. Pemberton, 1984, Trace fossil facies models, *in* R. G. Walker, ed., Facies models, 2nd edition, Geoscience Canada, p. 189-207

Frey, R. W., and S. G. Pemberton, 1985, Biogenic structures in outcrops and cores: I: approaches to ichnology: Bulletin of Canadian Petroleum Geologists, 33, p. 72-115.

Gani, M. R., and J. P. B. Bhattacharya, 2005, Lithostratigraphy versus chronostratigraphy in facies correlations of Quaternary deltas: application of bedding correlation: SEPM Special Publication, p. 1-43.

Gill, J. R., and W. J. Jr. Hail, 1975, Stratigraphic sections across Upper Cretaceous Mancos Shale-Mesaverde Group boundary, eastern Utah and western Colorado: U.S Geological Survey Oil and Gas Investigations Chart OC-68, 1 sheet.

Greenwood, B., and D. J. Sherman, 1986, Hummocky cross-stratification in the surf zone: flow parameters and bedding genesis: Sedimentology, v. 33, p. 33-45.

Harms, J. C., J. B. Southard, D. R., Spearing, and R. G., Walker, 1975, Depositional environments as interpreted from primary sedimentary structures and stratification sequences: Society of Economic Paleontologists and Mineralogists Short Course. no. 2, 161 p.

Hettinger, R. D., and M. A. Kirschbaum, 2002, Stratigraphy of the Upper Cretaceous Mancos Shale (upper part) and Mesaverde Group in the southern part of the Uinta and Piceance basins, Utah and Colorado: U. S. Geological Survey, Geologic Investigations Series I-2764, 21 p., 2 sheets. <http://greenwood.cr.usgs.gov/pub/i-maps/i-2764/>.

Howard, J. D., and H. E. Reineck, 1981, Depositional facies of high-energy beach to offshore sequence: comparison with low-energy sequence: American Association of Petroleum Geologists Bulletin, v. 65, p. 807-830.

Hubbard S. M., S. G. Pemberton, M. K. Gingras, M. B. Thomas, 2002, Variability in wave-dominated estuary sandstone: implications on subsurface reservoir development: Bulletin of Canadian Petroleum Geology, v. 50, 31, p. 118-137.

Johnson, R. C., 1988, Geologic history and hydrocarbon potential of Late Cretaceous-age, low permeability reservoirs, Piceance basin, western Colorado: evolution of sedimentary basins, Uinta and Piceance basin: U.S. Geologic Survey Bulletin 1787, p. 1-51.

Johnson, J. D. and C. T. Baldwin, 1996, Shallow clastic seas, *in* H. G. Reading, ed., Sedimentary environments: processes, facies and stratigraphy: Oxford, Blackwell Science Ltd., p. 232-280.

Jordan, T. E., 1981, Thrust loads and Foreland basin evolution, Cretaceous western United States: American Association of Petroleum Geological Bulletin, v. 65, no. 12, p. 2506-2520.

Jordan, T. E., 1995, Retroarc foreland and related basins, *in* C. J. Busby, and R. V. Ingersoll, eds., Tectonics of sedimentary basins, p. 331-362.

Kamola, D. L., and J. C. Van Wagoner, 1995, Stratigraphy and facies architecture of parasequences with examples from the Spring Canyon Member, Blackhawk Formation, Utah, *in* J. C. Van Wagoner, and G. T. Bertram, eds., Sequence stratigraphy of Foreland Basin deposits: outcrop and subsurface examples from the Cretaceous of North America: American Association of Petroleum Geologists, Memoir 64, p. 27-54.

Kamola D. L, and J. A. Howell, An online guide in sequence stratigraphy, University of Virginia, http://www.uga.edu/~strat/sequence/accommodation.html

Kirschbaum, M. A., and R. D. Hettinger, 2002, Variation in systems tract architecture and accommodation space in Upper Campanian strata in eastern Book Cliffs, Colorado and Utah: AAPG Abstracts Annual Meeting, Houston, Texas, A95 p.

Koczy, F. F., 1956, Geochemistry of the radioactive elements in the ocean: Deep Sea Research, v. 3, p. 93-103.

Laird, M. G., 1968, Rotational slumps and slump scars in Silurian rocks, western Ireland. Sedimentology 10, p. 111-120.

Lawrence, D. T., 1994, Evaluation of eustasy, subsidence, and sediment input as controls on depositional sequence geometries and the synchroneity of sequence boundaries, *in* P. Weimer, and H. W Posamentier, eds., Siliciclastic sequence stratigraphy: recent developments and applications: American Association of Petroleum Geologist Memoir 58, p. 337-367.

Lorenz, J. C., 1982, Sedimentology of the Mesaverde Formation at Rifle Gap, Colorado, and implications for gas-bearing intervals in the subsurface: Sandia Report, SAND 82-0604, March 1982.

Madden, D. J., 1985, Description and origin of the lower part of the Mesaverde Group in Rifle Gap, Garfield County, Colorado: The Mountain Geologist, v. 22, no. 3, p. 128-138.

Madden, D. J., 1989, Stratigraphy, Depositional environments, and paleogeography of coal-bearing strata in the Upper Cretaceous Mesaverde Group, Central Grand Hogback, Garfield County, Colorado: New correlations of the Trout Creek Sandstone Member: U. S. Geological Survey Professional Papers 1485, p.1-45.

Madof, A., 2006, Sequence stratigraphic analysis of high frequency sequences: Cozzette Sandstone Member, Mount Garfield Formation, Book Cliffs, Colorado, U.S.A.: Master's Thesis, Department of Geology, University of Kansas, Lawrence, Kansas 153 p.

Master, C. D., 1967, Use of sedimentary structures in determination of depositional environments, Mesaverde Formation, Williams Fork Mountains, Colorado: American Association of Petroleum Geologists Bulletin, v. 51, p. 2033–2043: Facies Reconstruction of Environments: American Association of Petroleum Geologists Reprint Series No. 10, p. 190-200, Tulsa.

McCubin, D. G., 1982, Barrier island and strand-plain facies, *in* P. A. Scholle, and D. Spearing, eds., Sandstone depositional environments: American Association of Petroleum Geologists Memoir 31, p. 247-279.

McCabe, P. J., 1984, Depositional environments of coal and coal bearing strata, *in* R. A. Rahmani, and R. M. Flores, eds., Sedimentology of coal and coal bearing sequence: International Association of Sedimentologists Special Publication, v. 7. p. 13-42.

McLlroy, D., 2004, Application of ichnofacies to palaeoenviromments and stratigraphic analysis: Geological Society of London, Special Publication 228, p. 45-53.

Miller, W. C., 2007, Trace fossils: concepts, problems, prospect, 3rd edition, p. 113-119.

Mitchum, R. M., P. R., Vail, and S. Thompson, 1977, Seismic stratigraphy and global changes of sea level, Part 2: the depositional sequence as the basic unit for stratigraphic analysis, *in* C. E. Payton, ed., Seismic stratigraphy-applications to hydrocarbon exploration: American Association of Petroleum Geologists Memoir 26, p. 53-62.

Mitchum, R. M., and J. C. Van Wagoner, 1991, High frequency sequences and their stacking patterns: sequence-stratigraphic evidence of high-frequency eustatic cycles: Sedimentary Geology, v. 70, p. 131-160.

Mitchum, Jr. R. M., J. B., Sangree, P. R. Vail, and W. Wornardt, 1994, Well-log and seismic criteria for recognizing sequences and systems tracts in late Cenozoic expanded sections, Gulf of Mexico, *in* P. Weimer, and H. W. Posamentier, eds., Siliciclastic sequence stratigraphy: recent developments and applications: American Association of Petroleum Geologists Memoir 58, p. 163-198.

Newman, K. R., 1982, Stratigraphic framework of Upper Cretaceous (Campanian) coal in western Colorado, field trip, southeastern Piceance basin: Grand Junction Geological Society, p. 61-67.

Nichols, M. M., and R. B. Biggs, 1985, Estuaries, *in* R. A. Jr. Davis, ed., Coastal

sedimentary environments, 2nd edition: New York, Spinger-Verlag, p. 77-186.

Nio, S. D., and C. Yang, 1991, Diagnostic criteria of clastic tidal deposits: A review, *in* D. G. Smith, G. E. Reinson, B. A. Zaitlin, and R. A. Rahmani, eds., Clastic tidal sedimentology: Calgary, Canadian Society of Petroleum Geologist Memoir 16., p. 3-28.

Nowak, H. C., 1991, Depositional environments and stratigraphy of Mesaverde Formation, southeastern Piceance Basin, Colorado-implications for coalbed methane exploration: Coalbed Methane, Rocky Mountains Association of Geologists, p. 1-20.

Nummedal, D., and C.M. Molenaar, 1995, Sequence stratigraphy of a ramp-setting strand plain successions: the Gallup Sandstone, New Mexico, *in* J C. Van Wagoner, and G. B. Bertram, eds., Sequence stratigraphy of Foreland Basins deposits-outcrop and subsurface examples from the Cretaceous of North America: American Association of Petroleum Geologists Memoir 64, p. 277-310.

Pemberton, S. G., J. C. Van Wagoner, and G. D. Wach, and S. G. Pemberton, 1992, Applications of ichnology to petroleum exploration: Society of Economic Petrologists Core Workshop 17, p. 339-382.

Pemberton, S. G., and J. A. Maceachern, 2002, Significance of ichnofossils to genetic stratigraphy in applied stratigraphy, *in* E. A. Koutsoukos, ed., Applied stratigraphy, p. 279-300.

Pemberton, S. G. et al., 2004, Stratigraphic applications of substrate-specific ichnofacies: delineating discontinuities in the rock record, *in* D. McIlroy, and A. Taylor, eds., The application of ichnology to stratigraphic analysis, Lyell Meeting, 2003: The Geological Society of London, Special Publication v. 228, p. 29-62.

Posamentier H. W, M. T. Jervey, and P. R Vail, 1988, Eustatic controls on clastic deposition. I. Conceptual framework, *in* C. K. Wilgus, B. S Hastings, C. G. St. C Kendall, H. W. Posamentier, C.A. Ross, J. C. Van Wagoner, eds., Sea level changes-an integrated approach, v. 42: SEPM Special Publication, p. 110– 124.

Posamentier H. W., G. P. D. Allen James, and M. Tesson 1992, Forced Regression in a Sequence Stratigraphic Framework: concepts, examples and exploration significance: The American Association of Petroleum Geologists Bulletin, v. 76, n. 11, p. 1687-1709.

Posamentier H.W., G. P. Allen, 1993a, Variability of the sequence stratigraphic model: effect of local basin factors: Sedimentary Geology, v. 86, p. 91-109.

Prothero, D. R., and F. Schwab, 2004, Sedimentary geology: an introduction to sedimentary rocks and stratigraphy: New York, W. H. Freeman and company, second edition, 557 p.

Reading, H. G., and J. D. Collinson, 1996, Clastic coasts, *in* H. G. Reading, ed., Sedimentary environments: processes, facies and stratigraphy: Oxford, Blackwell Science Ltd., p. 154-231.

Reinson, G. E., 1984, Barrier-island and associated strand-plain systems, *in* R. G. Walker, eds., Facies models, 2nd edition: Geoscience Canada Reprint series 1, p. 119-140.

Rider, M., 1986, The geological interpretation of well logs: London, Blackie, 175 p.

Ryer, T. A., and M. McPhillips, 1983, Early Late Cretaceous paleogeography of eastcentral Utah, *in* M. W. Reynolds, and E. D., Dolly, eds., Mesozoic paleogeography of West-Central United State: SEPM, Rocky Mountain Section, Rocky Mountain Paleogeography Symposium 2, p. 253-271.

Schlumberger, 1972, Log interpretation, I, Principles: Schlumberger Limited, New York, USA, 113 p.

Schlumberger, 1974, Log interpretation, II, Applications: Schlumberger Limited, New York , USA , 116 p

Schmoker, J. W., and T. C. Hester, 1983; Organic carbon in Bakken formation, United State portion of Williston Basin: Bulletin of American Association of Petroleum Geology, v. 67, p. 184-195.

Selley, R. C., 1974, Environmental analysis of subsurface sediments: Paper J, 3rd European Formation Evaluation Symposium Transactions: Society of Professional Well Log Analysts, London Chapter, 15 p, later published in 1976, Subsurface environmental analysis of North Sea sediments: AAPG Bulletin, v. 60, no. 2, p. 184-195, also published in 1976, The Log Analyst, v. 17, no. 1, January-February, p. 3-11.

Selley, R. C., 1978, Concepts and methods of subsurface facies analysis: AAPG Continuing Education Course Note Series -- no. 9, AAPG Dept. of Educational Activities in Tulsa, OK, 82 p.

Serra, O., 1984, Fundamentals of well-log interpretation. 1: the acquisition of data: Developments in Petroleum Science, 15A, Elsevier Science Ltd, 435 p.

Serra, O., 1984, Fundamentals of well-log interpretation. 2: the interpretation of logging data: Developments in Petroleum Science, 15B, Elsevier Science Ltd, 684 p.

Swift, D. J. D., and J. A. Thorne, 1991, Sedimentation on continental margins, I: a general model for shelf sedimentation, *in* D. J. P. swift, G. F, Oertel, R. W. Tillman, and J. A. Thorne, eds., Shelf sand and sandstone bodies: International Association of Sedimentologists Special Publication, No. 14, p. 3-31.

Taylor, R. B., 1975, Neogene tectonism in south central Colorado, Cenozoic history of the southern Rocky Mountains, Boulder County, Colorado: Geological Society of America Memoir 144, p. 211-226.

Tucker., M. E., 2001, Sedimentary petrology: an introduction to the origin of sedimentary rocks, 3rd edition: Blackwell Scientific Publications, 272 p.

Tweto, O., 1973, Laramide (Late Cretaceous-early Tertiary) orogeny in the southern Rocky Mountains: Geological Society of America Memoir 144, p. 1-43.

Tweto, O., and P. K Sims, 1963, Precambrian ancestry of the Colorado mineral belt: Geological Society of America Bulletin, v. 74, p. 991-1014.

Vail, P. R., R. G. Todd, and J. B. Sangree, 1977, Seismic stratigraphy and global changes of sea level: part 5. chronostratigraphic Significance of Seismic Reflections: Section 2, Application of Seismic Reflection Configuration to Stratigraphic Interpretation Memoir 26, p. 99 -116.

Walker, R. G., 1984, Shelf and shallow-marine sands, in Walker, R. G. ed., Facies models (second edition): Geoscience Canada Reprint Series 1, p. 141-170.

Walker, R. G., 1985, Comparison of shelf environments and deep-basin turbidities systems, *in* R. W. Tillman, D. J. P. Swift, and R. G. Walker, eds., Shelf sands and sandstone reservoirs: Society of Economic Paleontolgist and Mineralogists Short Course Notes 13, p. 465-502.

Van Wagoner, J. C., H. W. Posamentier, R. M. Mithchum, P. R. Vail, J. F. Sarg, T. S. Loutit, and J. C. Hardenbol, 1988, An overview of the fundamentals of sequence stratigraphy and key definitions: sea level changes-an integrated approach: SEPM Special Publication No. 42, 1988: The Society of Economic Paleontologists and Mineralogists, p. 39-45.

Van Wagoner, J. C., H. W. Posamentier, R. M. Mitchum, K. M. Campton, and V. D. Rahmanian, 1990, Silicoclastic sequence stratigraphy in well-logs, cores, and outcrop: concepts for high Resolution correlation of time and facies: American Association of Petroleum Geologists, Methods in Exploration Series 7, 55 p.

Van Wagoner, J. C., 1995, Sequence stratigraphic and marine to non-marine facies architecture of foreland basin strata, Book Cliffs, Utah, USA, *in* J. C. Van Wagoner, and G. T. Bertram, eds., Sequence stratigraphy of foreland basin

deposits, outcrop and subsurface examples from the Cretaceous of North America: American Association of Petroleum Geologists, Memoirs 64, p. 137-223.

Wanless, H. D., 2011, http://mgg.rsmas.miami.edu/rnggsa/wanlessfinal.pdf

Warner, D., 1964, Mancos-Mesaverde (Upper Cretaceous) intertonguing relations southeast Piceance basin, Colorado: American Association of Petroleum Geological Bulletin, v. 48, no. 7, p. 1091-1107.

Wehr, F. L., 1994, Effect of variation in subsidence and sediment supply on parasequence stacking patterns, *in* P. Weimer, and H. W. Posamentier, eds., Recent advances in and applications of siliciclastic sequence stratigraphy: American Association of Petroleum Geologists Memoir No. 58, p. 369-379.

Wood, L. J., F. G. Ethridge, and S. A. Schumm, 1994, An experimental study of the influence of subaqueous shelf angle on coastal-plain and shelf deposits, *in* P. Weimer, and H. W. Posamentier, eds., Recent advances in and applications of siliciclastic sequence stratigraphy: American Association of Petroleum Geologists Memoir No. 58, p. 381-391.

Yang, B. C., R.W. Dalrymple, and S. S. Chun, 2005, Sedimentation on a wave-dominated, open-coast tidal flat, southwestern Korea: summer tidal flat-winter shoreface: Sedimentology, v. 52, p. 235-252.

Young, R. G., 1955, stratigraphy and petroleum geology of the Mesaverde Group, southeastern Piceance Creek basin, Colorado, field trip, southeastern Piceance basin: Grand Junction Geological Society, p. 45-54.

Young, R. G., 1983, Book Cliffs coal field, western Colorado, field trip: Grand Junction Geological Society, p. 9-15.

Zapp, A. D., and W. A. Cobban, 1960, Some Late Cretaceous strand lines in northwestern Colorado and northeastern Utah: Geological Society Research, Short papers in the Geological Sciences, p. 246-249.

Zater, M., 2005, High-frequency sequence stratigraphy of nearshore strata: Corcoran Sandstone Member, Mount Garfield Formation, Book Cliffs, Colorado, U.S.A.: Master's Thesis, Department of Geology, University of Kansas, Lawrence, Kansas 108 p.

APPENDIX